Activation and Reduction of Carbon Dioxide Using Bis-Mesityl Imidazole Ylidene

by

Solita Wilson

Submitted in Partial Fulfillment of the Requirements

for the Degree of

Master of Science

in the

Chemistry

Program

YOUNGSTOWN STATE UNIVERSITY

May, 2019

Activation and Reduction of Carbon Dioxide Using Bis Mesityl Imidazole Ylidene

Solita Wilson

I hereby release this thesis to the public. I understand that this thesis will be made available from the OhioLINK ETD Center and the Maag Library Circulation Desk for public access. I also authorize the University or other individuals to make copies of this thesis as needed for scholarly research.

Signature:

_____

Solita Wilson, Student Date

Approvals:

_____

Dr. Clovis A. Linkous, Thesis Advisor Date

_____

Dr. Brian D. Leskiw, Committee Member Date

_____

Dr. Douglas T. Genna, Committee Member Date

_____

Dr. Salvatore A. Sanders, Dean of Graduate Studies Date

Abstract:

N-Heterocyclic carbenes have been recognized for their ability to capture CO_2 at standard temperature and pressure. This makes them a molecule that could be used for renewable energy synthetic methods. Synthesis and characterization of an $IMesCO_2$ derivative based on bis-mesityl imidazolium chloride was performed, followed by one of four commonly used reduction methods. Methanol is a possible product from a successful reduction through hydrogenation. Efficient production of this species could establish CO_2 as a viable renewable energy source. A high pressure hydrogen gas experiment as well as three possible hydride reduction pathways were investigated. Hydrogen gas was used to beak the C2-carbon dioxide bond. This technique explores the results of introducing the $IMesCO_2$ to a neutral hydrogen, which resulted in the formation of formic acid. Hydride reductions were done with lithium aluminum hydride, lithium borohydride and sodium borohydride. They were introduced to the $IMesCO_2$ to donate a hydride to the C2-carbon dioxide bond. The different hydrides varied in selectivity toward $IMesCO_2$ reduction. $IMesCO_2$, possessing a carbonyl group, was subjected to all the hydrides in appropriate solvents. Therefore, the reaction showed the formation of formate for several scenarios. The key to these reductions was the solvent: tetrahydrofuran in conjunction with lithium aluminum hydride; tetrahydrofuran, acetonitrile, and dimethyl sulfoxide used with lithium borohydride; and tetrahydrofuran, acetonitrile, and dimethyl sulfoxide with sodium borohydride. However, there seemed to be a need for a balance between reducing strength of the hydride and selectivity for the carbonyl. To further expand on the idea of using appropriate solvents, sodium tetraphenyl borate was included as an additive to promote reduction via increased solubility, but reactivity with the sodium borohydride did not generally increase. Furthermore, several reaction spectra show evidence of the imidazole ring opening to form unanticipated products. The ring opening may produce some of the reagents that were originally used to make the bis-mesityl imidazolium chloride.

Acknowledgements:

I am a religious person and I have to be thankful first and foremost to my Lord and Savior Jesus Christ. I always felt I was on a pathway, and it is through him that I am where I am at today. I am very thankful to my mom. She is the source and of the strength that I yield today. I take after my mother in the way that I have faced and overcome the many challenges life has thrown at me single handedly.

Before I started the program, I had went through some traumatic losses in my life, but I kept moving forward and moved on to other things. I started in the department of English working toward a graduate certificate, but when I completed that, I wanted to return to chemistry. I asked admissions if funding was available and they told me to apply and find out, but before applying I asked the grad school coordinator of the chemistry department if there was any funding for me and I heard again to apply and find out. After applying I was awarded a partial assistantship, then because of my excellent job I received funding for the entire year. I am very thankful for the help of Dr. Sherri Lovelace-Cameron for the help and support, and the department for funding me, my first year in the department. Looking back on these this helps me realize how lucky I was, they changed my life. I was later funded by the Cushwa Commercial Shearing Fellowship. I am eternally grateful to them for funding my second year.

Each day began to feel longer than the last at some point, and I have to thank my friends and lab mates for their support. There was nothing more therapeutic than talk to another grad student who was able to completely relate to my situation. I appreciate their faith in me and their understanding.

I am very thankful to my advisor, Dr. Clovis Linkous for allowing me to work in his lab and helping me to get to this point. My advisor showed me patience and persistence. He helped me every step of the way and I am fortunate to have been a part of this research.

As for my committee, Dr. Genna and Dr. Leskiw, I appreciate their time and effort they gave to me to finish my thesis. They read my drafts, showed up to my meetings, and answered my many emails. Their patience and guidance helped me mold in to a better student and therefore chemist. I am also grateful to all the faculty and staff, through a collaborative effort I was able to make progress.

TABLE OF CONTENTS

LIST OF FIGURES, TABLES, DIAGRAMS, AND SCHEMES

LIST OF FIGURES

LIST OF TABLES

LIST OF DIAGRAMS

APPENDIX FIGURES

CHAPTER 1 INTRODUCTION TO PROBLEM:

CO_2 is a major concern for individuals all over the world. Its production is continuously increasing, which is causing a build-up because it is not being consumed as quickly as it is being produced. During preindustrial time its concentration was around 270 ppm and now has reached about 400 ppm [1]. CO_2 is normally consumed by autotrophs for photosynthesis, which recycles the molecule since oxygen gas is released which is later consumed by heterotrophs. Autotrophs being the main source of the world's oxygen, are being destroyed, and fewer autotrophs means less consumption of CO_2 to be replaced with oxygen. Although some of these reasons for destroying autotrophs are for human survival, the environmental effects are still happening.

World population has reached over seven billion people and is still growing. Each individual person leaves a carbon foot print which is the amount of CO_2 a single person has produced in their lifetime. Animal livestock contributes to this process as well. These animals are being raised to an unnaturally high population for food production, so they massively contribute to CO_2 emission. They produce around six billion tons of gases which contribute up to18% of global emissions [2]. With such a high human and animal population on the planet, it is easy to imagine why CO_2 is building up and is such an issue.

CO_2 is a greenhouse gas; this means that the gas can cause the greenhouse effect. Infrared radiation from the earth's surface, originating from the sun, enters the atmosphere and is absorbed by CO_2 molecules and is then converted to heat energy and released into the atmosphere as displayed in Figure 1. Climate change is the result of

more heat gain by the atmosphere. Most weather activity is dependent on temperature, and so CO_2 is responsible for atmospheric temperature change and the climate changes that will result.

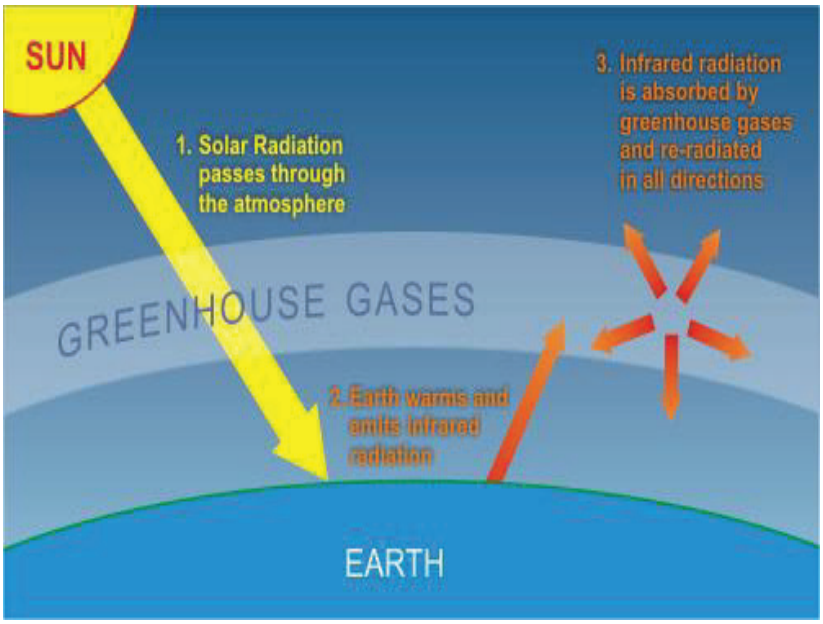

Figure 1: Retrieved from https://skepticalscience.com. Illustration of the greenhouse effect. Reproduced with permission.

CO_2 is also the byproduct of combustion reactions. Most of our cars run on combustion engines that are fueled through gasoline distilled from fossil fuel oil. Fossil fuels play a major part in the sources of energy for all the countries of the world. They are burned to power engines, used as a heating source for homes and buildings, and to even generate electricity. Whatever their current use may be, these fossil fuels are burned to harvest the energy from them. When burned they release CO_2, and if the combustion is happening in the engine of a car, CO_2 is released out of the exhaust pipe and into the atmosphere.

Capturing CO_2 and using it for a practical purpose is of interest. A practical solution to the CO_2 build up includes capturing CO_2 and recycling it so that it may be a

reagent source for another reaction of a conversion into a fuel for a vehicle. This can perhaps be done by CO_2 reduction. There are many ways to reduce CO_2 but doing this using a mild CO_2 capture and common reduction techniques is not clear. Using hydrogen to reduce CO_2 at temperatures below 80 °C could be an interesting lead to renewable energy resources.

N-Heterocyclic carbenes (NHC) have an affinity toward CO_2 at room temperature [3]. Carbenes are a well-known organic catalyst, and they have been used to capture CO_2 before. They are great alternatives to other catalysts because they can be generated from a stable salt form, are controllably reactive, and have a high affinity for bonding with CO_2. When bonding to CO_2, the carbene changes the linear shape of the CO_2 molecule to a bent geometry [4]. The CO_2 will turn perpendicular to the nitrogen groups, as displayed in Diagram 1 [5]. Once the carbene captures the CO_2 the new bis-mesityl imidazole carboxylate ($IMesCO_2$) can be characterized and then used as a starting material for a reduction. Formate is a possible product of a reduction reaction with CO_2. This ion can possibly be further reduced to formaldehyde. Formaldehyde has many possibilities to become another reagent. Methanol is another possibility and perhaps the most desired product because it is a fuel source for heat engines and direct methanol fuel cells [6].

This idea has potential, especially if the reduction products can be formed. It can help contribute to the answer to the CO_2 problem. Perchance the products could be consumed, CO_2 would be produced. Then the CO_2 can be collected and reduced again to reform products that can be reacted again to become the fuel for the vehicle.

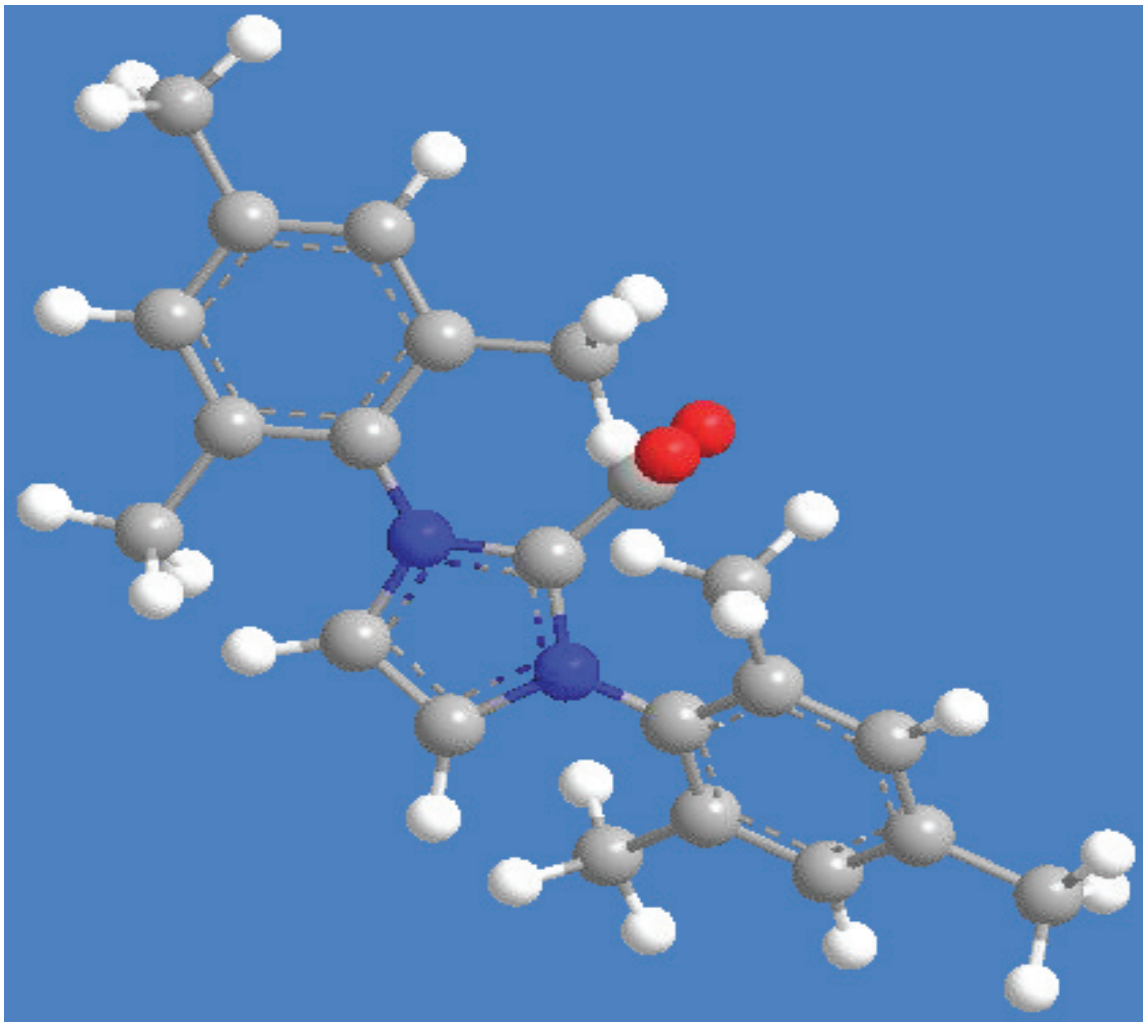

Diagram 1: 3D Chemical structure of captured CO_2 with a bent geometry.

Introduction to Carbenes:

Imidazole is a nitrogen containing heterocycle. It has three carbon, two nitrogen, and four hydrogen atoms. It is named as such because it has a carbon-nitrogen double bond, making the compound an imine and an example of a diazole. Found in the amino

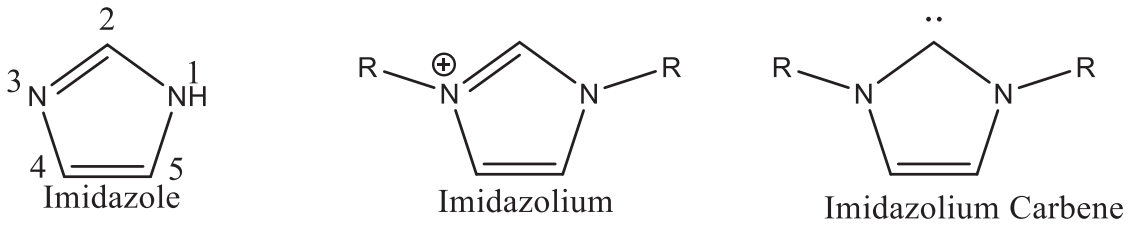

Diagram 2: Depiction of imidazole, Imidazolium and imidazolium carbene.

acid histidine, it has major biological functions, pharmaceutical applications, industrial uses, and is a white solid at room temperature [7, 8, 9]. Imidazolium is the cation of imidazole and has the potential to be deprotonated on carbon 2 (C2), between the nitrogen atoms, within its diazole ring, and the valence electrons on the carbon will still be stable. Diagram 2 shown above indicates the difference between the imidazole, imidazolium and the carbene. There is a family of these molecules called *N*-heterocyclic carbenes (NHC's) that are both a carbene with two valence electrons and heterocyclic in structure [10]. These heterocyclic structures must contain at least one nitrogen atom at the 1 or 3 positions. The other position can be either another nitrogen, sulfur, carbon, or oxygen atom. Electronegativity of these other atoms is able to stabilize the unbonded electrons on the C2 carbon. Adjacent atoms to the carbon have an effect on the carbene electrons with sigma bond withdrawing and pi bond donating [11]. The two electrons are in the same orbital, which helps prevent dimerization. Atoms at the one and three positions normally have an alkyl or aromatic group bonded to it. This bonding creates a steric effect that protects the C2 carbene.

History of Carbenes Use and Formation:

N-Heterocyclic carbenes were first classified in 1958 by Ronald Breslow, who suggested "anions on a stable triply-bonded carbon". He referred to the molecule as a carbene, with a resonance structure of two neutral valence electrons on the carbon. Breslow looked at a reaction with thiazolium zwitterion that are stabilized through resonance as shown in Diagram 3. He speculated on the carbene's formation and its catalytic role in benzoin condensation [12].

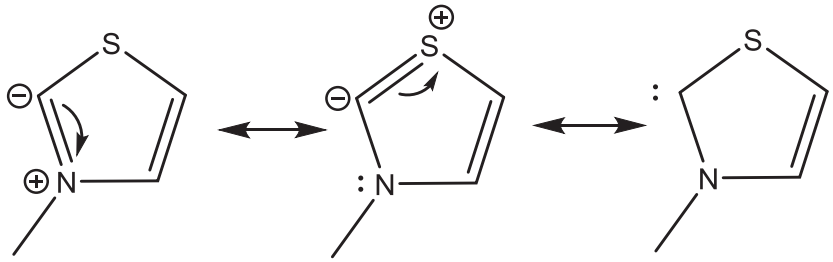

Diagram 3: Thiazolium resonance structures.

In the 1960's Wanzlick took NHC's and used them as ligands for metal complexes [13]. His results were not successful he would dimerize the carbene, but further products would not form because the dimers were not reactive. In 1991, Arduengo did a study that led to the synthesis of stable carbenes [11]. Arduengo used a variety of imidazole derivatives for his study. He used molecules with different substituent groups bonded to the nitrogen atoms to make his carbenes. He claimed that the carbenes he worked with were both kinetically and thermodynamically stable [14]. It seems that the bulkier the *N*-groups, the more stable the carbene. Now that carbenes have stable forms, they may have other functions [15].

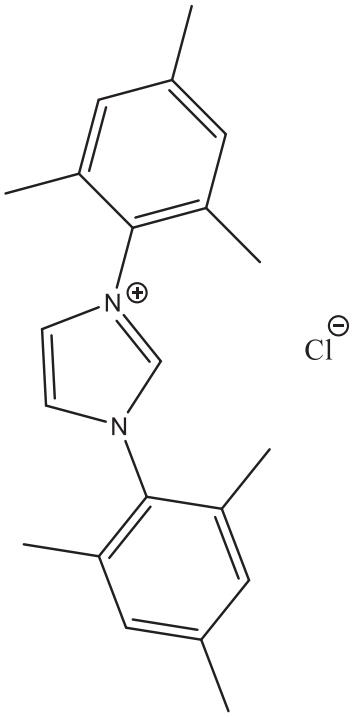

Diagram 4: Bis-mesityl-imidazolium chloride.

The NHC of principal interest is derived from an imidazolium salt, bis-mesityl-imidazolium chloride (IMesCl) shown in Diagram 4. The chemistry performed in this thesis does not focus on the ligand behavior of the resulting carbene, but rather its reaction with CO_2. However, the CO_2 capture produces a bis-mesityl imidazole carboxylate ($IMesCO_2$) that is not very stable. CO_2 can easily be pulled off of the carbene molecule and limits the possibilities of follow-up reactions with the $IMesCO_2$ [5]. However, a weaker bond can lead to better interactions with other molecules because less energy is needed to break the bond. NHC's could have the potential to help reduce CO_2 depending on the substituents and conditions. The mesityl group is a very bulky group. Synthesis with this molecule may be difficult because of the steric effects of the

mesityl groups in the imidazole ring, but these mesityl groups may provide the right balance of protecting and weakening the bond for a reduction.

Reaction with Carbon Dioxide:

In 2002, Holbrey and his colleagues set out to react CO_2 with a 1,3-dimethylimidazole carbene complex [4]. They wanted to synthesize methyl carbonate from dimethyl carbonate and 1-ethylimidazole followed by a hydrolysis. Holbrey *et al.* wanted to make an ionic liquid with a methyl carbonate salt. However, they ended up synthesizing a carbene-carbon dioxide adduct [4]. CO_2 was not expected to bond to the carbene. This discovery contributed to the green chemistry discipline. The carbene molecule was able to capture CO_2 and introduce the possible green chemistry that these carbene molecules have.

Synthesis of the Carbene and IMesCO_2:

Synthesis of the carbene can be accomplished by deprotonating an imidazolium salt at the C2 with a pKa of ~23 with potassium hexamethyldisilylazide (KHMDS), which has a pKa of 26 in toluene [16,17]. The reaction was also attempted with potassium t-butoxide with sodium hydride, but the reaction produced carboxylate contaminated with *tert*-butanol. KHMDS is a strong base and will break the C-H bond on the C2 carbon to form the carbene [17]. Van Ausdall did work on several carbene to carboxylate syntheses. Starting with the carbene in tetrahydrofuran at room temperature one atmosphere of CO_2 gas is added to form a carboxylate including IMesCO_2. He was able to try different imidazole salts for his reaction and characterize his products. The NHC's varied from having a simple methyl group on the nitrogens to a complex 2, 6-diisopropylphenyl group on the nitrogen heteroatoms as described in Diagram 5.

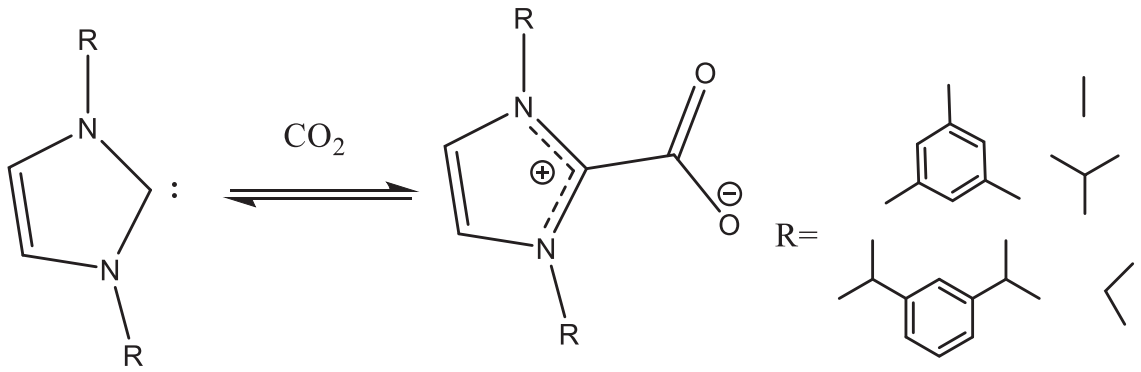

Diagram 5: General reaction of NHC with CO_2.

Van Ausdall produced nuclear magnetic resonance spectroscopy (NMR), infrared spectroscopy (IR), X-ray diffraction (XRD) analysis data and thermogravimetric analysis (TGA) on these molecules. Van Ausdall found that $IMesCO_2$ is synthesized with a high yield >70% and little by-product. An interesting part of Van Ausdall's thesis was a study of $IMesCO_2$ reaction with water. If a NHC is exposed to water the C2 carbon may protonate regenerating the IMesCl. Knowing how the $IMesCO_2$ is affected by water will help with the understanding of its stability in a moist atmosphere. When water was introduced to some of the carboxylates, protonation immediately occurred, forming the imidazolium ion and bicarbonate. Van Ausdall dissolved the $IMesCO_2$ in dichloromethane (DCM) and added water as shown in Diagram 6.

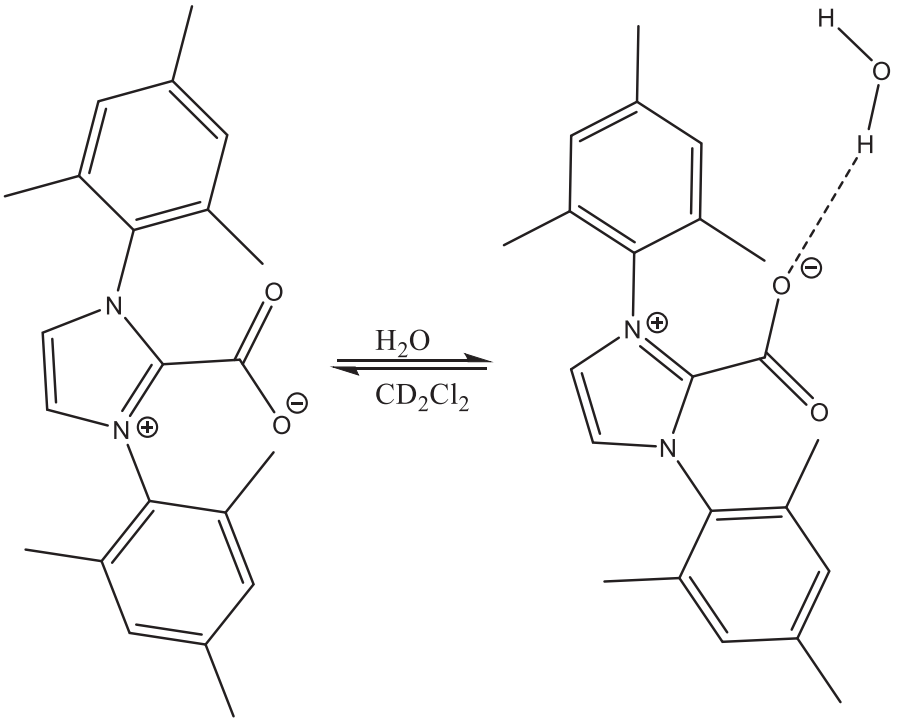

Diagram 6: Bis-mesityl imidazolium $IMesCO_2$ interaction with water.

^{1}H-NMR spectra of the solutions were taken and examined for the appearance of a peak that would correspond to a protonated NHC. The H2 hydrogen, which is bonded to the C2, can be found in the range of 8-11 δ depending on the groups bonded to the nitrogen. Van Ausdall did use an imidazole complex with mesitylene subgroups bonded to the nitrogen, known as IMes, for his study. When he tried a reaction with water, the results were different than what was observed for NHCs with smaller groups on the nitrogen atoms. He did not see a disappearance of the carbene signal. Instead he saw the mesityl protons shifting downfield on the NMR spectrum. This change was attributed to a species that was hydrogen bonding with water at the carboxylate position. Another trend uncovered by Van Ausdall was during thermogravimetric analysis. Van Ausdall wanted to determine the temperature at which these carboxylates would start to

decompose. The bond between C2 and the CO_2 carbon would break, and the molecule would decarboxylate at a certain temperature. It was found that as the nitrogen substituent size increased, the decarboxylation temperature decreased. The bigger substituents must have caused a weaker carboxylate bond because of steric hindrance. The carbon-carbon bond is longer for these molecules and therefore weaker. IMesCO_2 was reported to decarboxylate at 155 ºC, and Van Ausdall's XRD data shows this trend was verified [17]. Conversely, the decomposition temperature for a mesityl substituent is higher than the temperature for an isopropyl phenyl group. This may be due to the stabilizing effect of the aromatic rings of the mesityl groups. Adding to the interest of the reactions with water, early work done with carbenes in water showed that and these reactions proceeded without protonation of the carbene. The stability of the carbene should prevent protonation.

The Activation of CO_2:

As far as the mechanism for this organic synthesis, it seems to be a simple nucleophilic addition as shown in Diagram 7. Carbenes have a nucleophilic reactivity, and with CO_2 being an electrophile, this reaction is just a nucleophilic addition. According to Arduengo, electron donation into the carbene out of the p orbital by an electron rich system leads to the electrophilic reactivity [14].

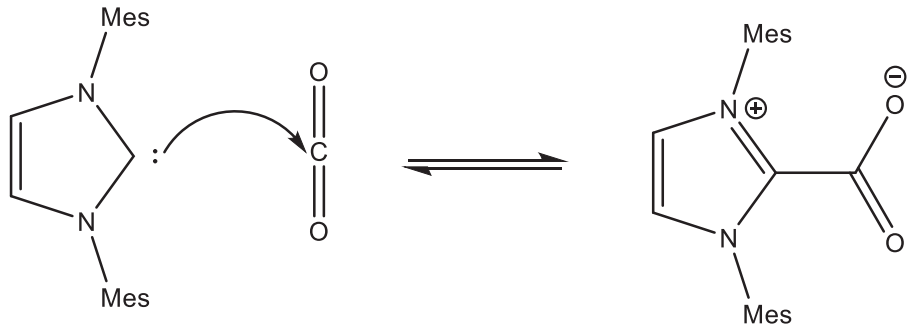

Diagram 7: NHC nucleophilically capturing CO_2.

Reduction of Carbon Dioxide:

When considering the electro-reduction of CO_2, most people think of the standard reduction reaction:

$$CO_2 + 2H^+ + 2e^- \rightleftharpoons CO + H_2O$$

CO_2 gains electrons and water and carbon monoxide are produced. However, this is not the goal of this research. The $IMesCO_2$ is the molecule that will be reduced, and in reacting with a hydrogen atom or hydride, reduction products should be synthesized. However, there are some things to consider with redox chemistry. The carbon-carbon bond between the imidazole ring and CO_2 is the target bond for the redox chemistry to occur, but imidazole is a large molecule and may have bonds that would be easier to reduce than the target bond.

A possible redox reaction is the following:

$$ImesCO_2 + 2H^+ + 2e^- \rightleftharpoons ImesH^+ + HCOO^-$$

The chemistry can change depending on how many equivalents of hydrogen is added to the system. In theory this chemistry seems reasonable, but in the past scientists struggled with the high over potentials for starting the reaction and poor selectivity. A catalyst for this reduction seems like a necessity. The catalyst that may be used can help aid the reaction in lowering the over potential, so that products can be formed [18].

Hydrogenation:

The reduction of CO_2 into methanol using hydrogen gas is a reversible exothermic reaction.

$$CO_2 + 3H_2 \rightleftharpoons CH_3OH + H_2O$$

CO_2 is thermodynamically stable and requires high energy to be reduced [19]. Similarly, hydrogen gas or molecular hydrogen demands activation and can be activated through harsh and mild conditions. Whatever conditions are used the H-H bond needs to be cleaved to produce a chemically reactive species. To reduce the IMesCO_2, it will be treated with hydrogen, this process is called hydrogenation. For this hydrogenation the mole ratio of hydrogen that can be added to the IMesCO_2 is not certain. The more hydrogen equivalence added the more C-H bonds will form to create different products. All the proposed reactions are possibilities of product formation are presented in Diagram 8. When the hydrogen donor is water, oxygen will bond with the CO_2 to form bicarbonate, but this chemistry would be counterproductive because bicarbonate can dissociate to CO_2. A hydrolysis of the product with water is not the ideal path. Bicarbonate is the same oxidation state as CO_2 when it is bonded to IMes, so reduction did not occur, and the imidazolium salt is also regenerated. Although regenerating the

imidazolium salt is not a negative consequence of this reaction, the bicarbonate is. The main purpose of this reaction is to manipulate the CO_2 into another product.

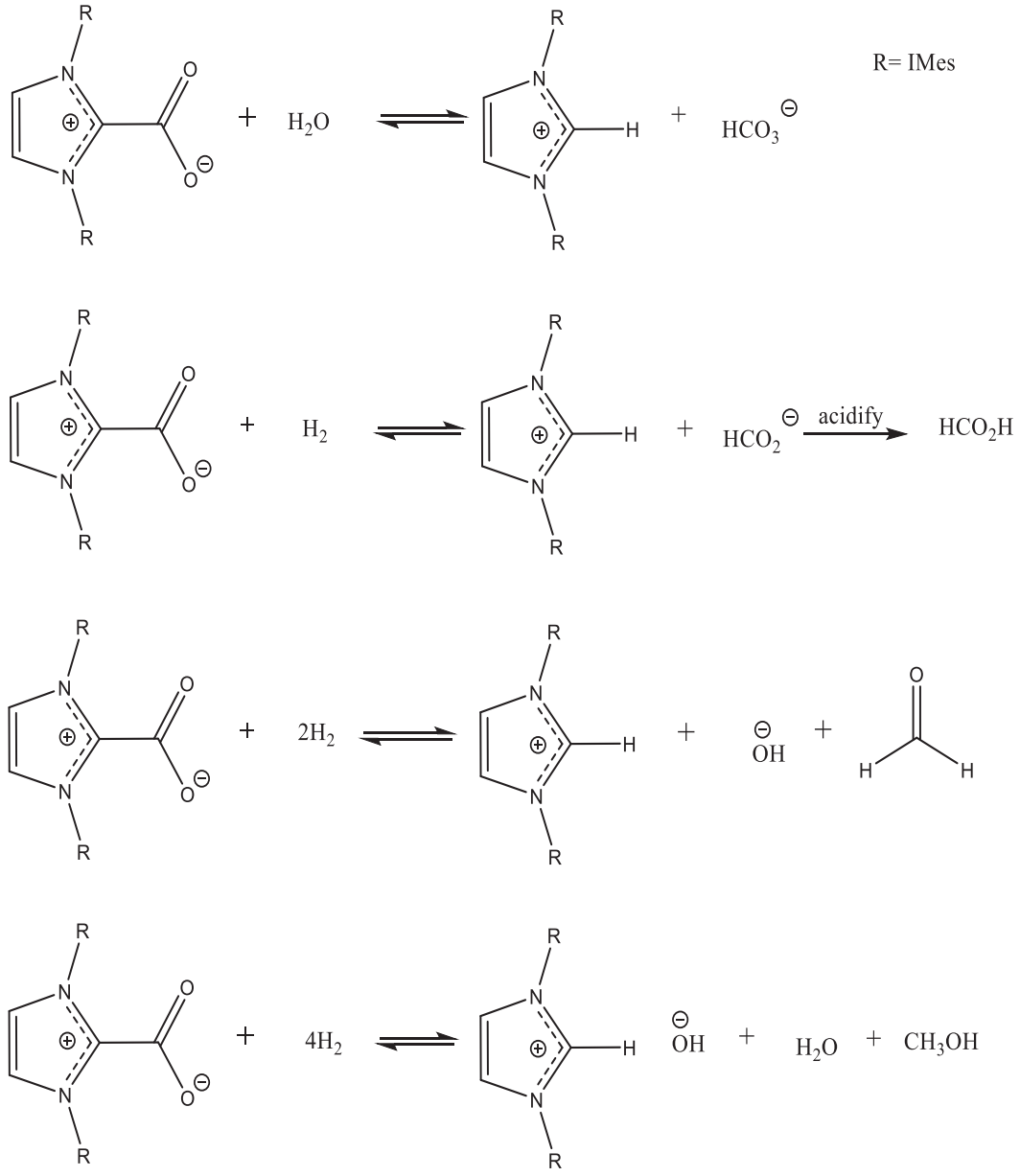

Diagram 8: Possible reduction pathways of $IMesCO_2$ with hydrogen.

A more specific reaction term for the synthesis proposed is a hydrogenolysis. The product carbon-carbon bond will be cleaved with hydrogen molecules added to the products. This is what is hoped to be accomplished. If the C2 carbon and the CO_2 bond is cleaved, the possible products are outlined in Diagram 8. The second reaction shows the reduction into a formate that is acidified to formic acid. The third reaction shows the reduction to formaldehyde, and fourth reaction shows the formation of methanol.

A task to be explored by this research would be the discovery of a possible process of reducing the bis-mesityl imidazolium carboxylate. The goal is to use hydrogen gas as a reducing agent or a hydride reducing agent. This new carbon-carbon bond formed when the carbene is carboxylated is not strong, and the captured CO_2 can be easily rereleased into the atmosphere. If this occurred, nothing of significance was accomplished. This IMesCO_2 is known to release CO_2 at the approximately 150 °C, so it seems the bond can be reduced. Ying and company successfully reduced CO_2 via NHCs into methanol with silanes [20]. Therefore, other reduction techniques should be possible.

Hydrogen gas will be added to the IMesCO_2 in solution. There is a need for a catalyst for a pressurized hydrogen reaction, but essentially it is hypothesized that the hydrogen molecule will break the carbon-carbon bond between the NHC and CO_2. The carbene will be protonated as will the CO_2. A catalyst will bond with the hydrogen gas molecule and break the H-H bond activating the hydrogen. The energy needed to break a hydrogen break on the catalyst surface is only 2 kcal/mol, while the energy need for bonding is 60 kcal/mol. One of the best hydrogen adsorption catalysts is platinum as

shown in Figure 2 of the plot of hydrogen bond strength with certain metals. So,

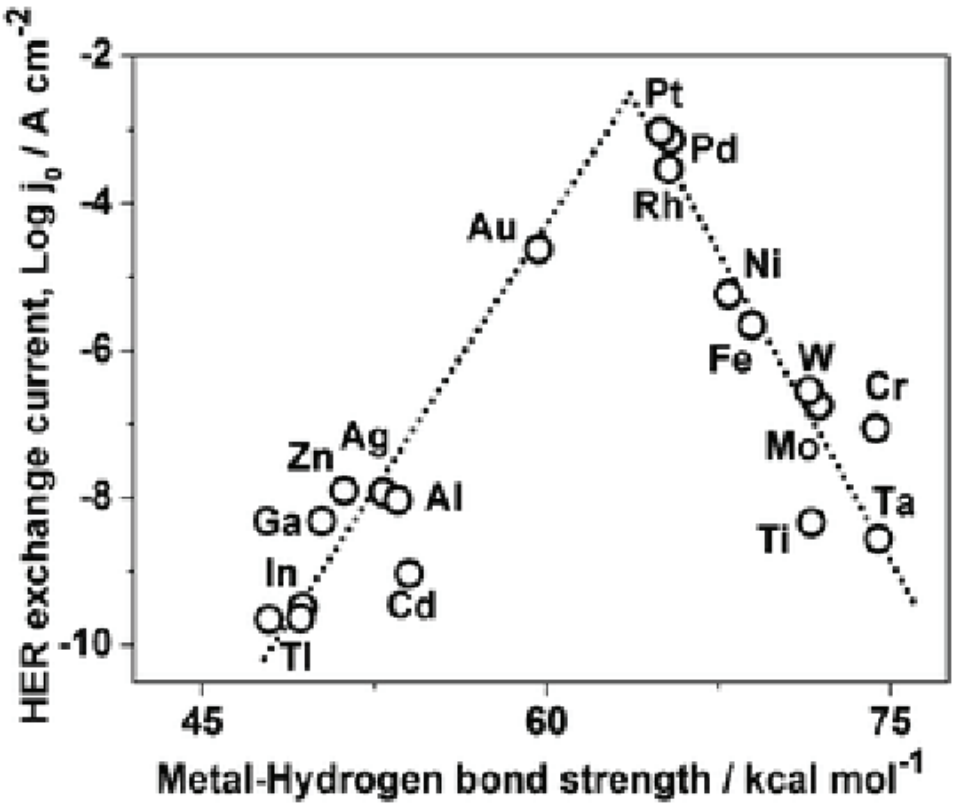

Figure 2: Trassati's volcano plot for the hydrogen evolution reaction [21].

platinum would be a great catalyst to start with, but palladium can be used as well. In addition, the conditions for the hydrogenation need to be tested as well. The reaction can be optimized through specified hydrogen, pressure, temperature, and duration.

Other possible reducing agents are also considered. Lithium aluminum hydride ($LiAlH_4$) is a strong reducing agent that can donate multiple hydrides to a reaction. It is a common organic synthesis reagent formally used to reduce aldehydes and ketones. The hydride ions are bonded to the aluminum metal, and these hydrides can nucleophilically attacks an electrophilic carbonyl carbon [22]. The resulting alkoxide goes through an aqueous work up to form the resulting alcohol. The $IMesCO_2$ product will hopefully act as the electrophilic carbonyl and be reduced via this chemical reaction.

The mentioned qualities are like other more selective reducing agents. Lithium borohydride ($LiBH_4$) and sodium borohydride ($NaBH_4$) also reduce by releasing a hydride ion, but they are more selective for aldehydes and ketones. [22] The selectivity comes from the boron center for the hydrogens, compared to a metal center the reactivity of a boron center is not as potent. Also, the counter ion contributes to the strength or reactivity of the reducing agent. Lithium is more reactive than sodium because it is a smaller cation and better Lewis acid. Because of the differences of the reactivity, this contributes to a more selective reagent on what $IMesCO_2$ will react with [23]. This is important to note because $LiAlH_4$ reacts with many organic solvents [24]. The solvent is always in larger portions to the reactant, and if the reducing agent is reactive with the solvent, the reactant will never have an opportunity to react with the reducing agent. With this in mind, the reaction solvents with $LiAlH_4$ will be more restricted than $LiBH_4$ and $NaBH_4$.

CHAPTER 2 EXPERIMENTAL SECTION:

Preparation of the $IMesCO_2$:

A bottle of 1,3-bis-2,4,6-trimethylphenyl-1,3 dihydro-2H-imidazol-2-ylidene (IMes) was purchased from Sigma Aldrich, so the carboxylation could be directly performed on the carbene. The carbene was first verified with NMR experiments via a Bruker Avance 400 spectrometer; proton, carbon 13, COSY, and HETCOR NMR experiments were done on the IMes. The solvent used for these experiments was deuterated chloroform. Then the carbenes were properly stored in an oxygen-free and moisture-free environment. Long-term storage in a glovebox is ideal for these compounds.

To synthesize $IMesCO_2$, the IMes was weighed out and placed in a dry round bottom flask with a stir bar. The starting material was kept dry and secluded by sealing the flask with a rubber-septum. Dry tetrahydrofuran was placed in a separate round bottom flask. The THF flask was purged with argon to clear out any oxygen and moisture. A 99.998% purity CO_2 tank was hooked up to a hose that was connected to a small column containing a layer of indicator Dri-rite and a layer of calcium chloride followed by another layer of Dri-rite. This column was used to purify the CO_2 from any water that may be trapped in the tubing or other places.

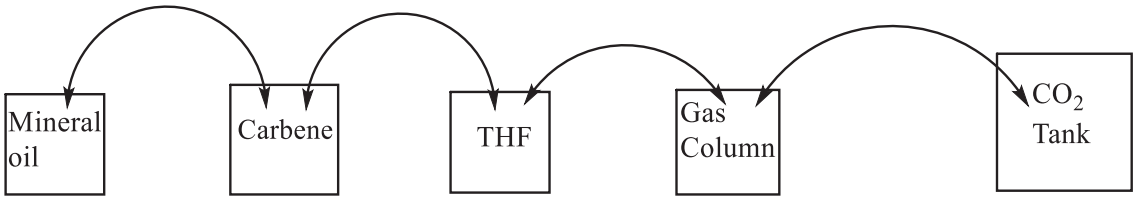

Diagram 9: Scheme of apparatus for $IMesCO_2$ product formation.

This column was connected to a cannula that fed into the THF solvent. The CO_2 was allowed to build up pressure into the THF flask. This helped push the solvent into another cannula that was fed into the flask with the carbene. One end of the cannula that was in the THF flask was submerged in the solvent. Solvent flowed from the THF flask to the flask with IMes. Once IMes was completely in solution, the submerged end of the cannula was pulled out of the solvent, but CO_2 was allowed to continue to flow. Once the system was completely purged with CO_2 and verified through a cannula at the end of the system that fed from the carbene's reaction flask to a small beaker of mineral oil, carboxylation could now occur. A visual of the setup is shown in Diagram 9.

The solution was thoroughly stirred and all the IMes was dissolved when the end of the cannula that was releasing CO_2 was submerged into the mixture. The excess CO_2 caused the solution to bubble, and was allowed to continue for two hours. Within minutes the IMesCO_2 precipitate could be observed coming out of the solution. Once the reaction had reached completion, the IMesCO_2 was then gravity filtered out of the solution using a Buchner funnel and filter paper. The IMesCO_2 was washed with diethyl ether to remove impurities.

IMesCO_2 was also synthesized from the imidazolium salt. The IMesCl was dissolved in anhydrous toluene in a round bottom flask. The system was set up identical to the system used for the carbene. However, a solution of potassium bis(trimethylsilyl)amide (HMDS) is added via an oven-dried syringe to the IMesCl solution to generate the carbene. The solution was then stirred for one hour and then pulled with vacuum through a frit with Celite for filtration. Once the solution came through the filter it entered a clean round bottom flask where CO_2 was then bubbled

through. The reaction was stirred for 2 hours, then washed with diethyl ether. The product was then dried under vacuum overnight and the weighed. Storage was in a small glass vial that was kept in a desiccator with calcium chloride and Dri-rite. Once the $IMesCO_2$ was dried, a ^{1}H and ^{13}C NMR was taken by dissolving 5 mg in 2 mL of deuterated dichloromethane or chloroform. An IR pellet was formed by grinding 7 mg of $IMesCO_2$ and 70 mg of potassium bromide.

Experimental Data:

Infrared Spectroscopy:

Infrared spectroscopic analysis was performed with a Thermo Nicolet NEXUS 670 FT-IR spectrometer. Using infrared light, functional groups are identified based on their absorbance and frequencies. These data are plotted to show the stretching of the functional groups of the sample. The literature lists a range of 1400-1600 cm^{-1} for bonded COO^- in methanol and water solution [25]. This information can help determine if the CO_2 was captured by the carbene to form the $IMesCO_2$.

The IR spectrum of the $IMesCO_2$ product is shown in Figure 3. These data were collected when the $IMesCO_2$ product was dissolved in dichloromethane (DCM) and placed between salt plates to be measured. There is a peak at 1725.86 cm^{-1}, which is outside of the literature range. Dissolving the $IMesCO_2$ in water or methanol is not ideal. Most IR experiments of IMesCO2 were done with pellets, so that would be a better approach to verify the CO_2 capture.

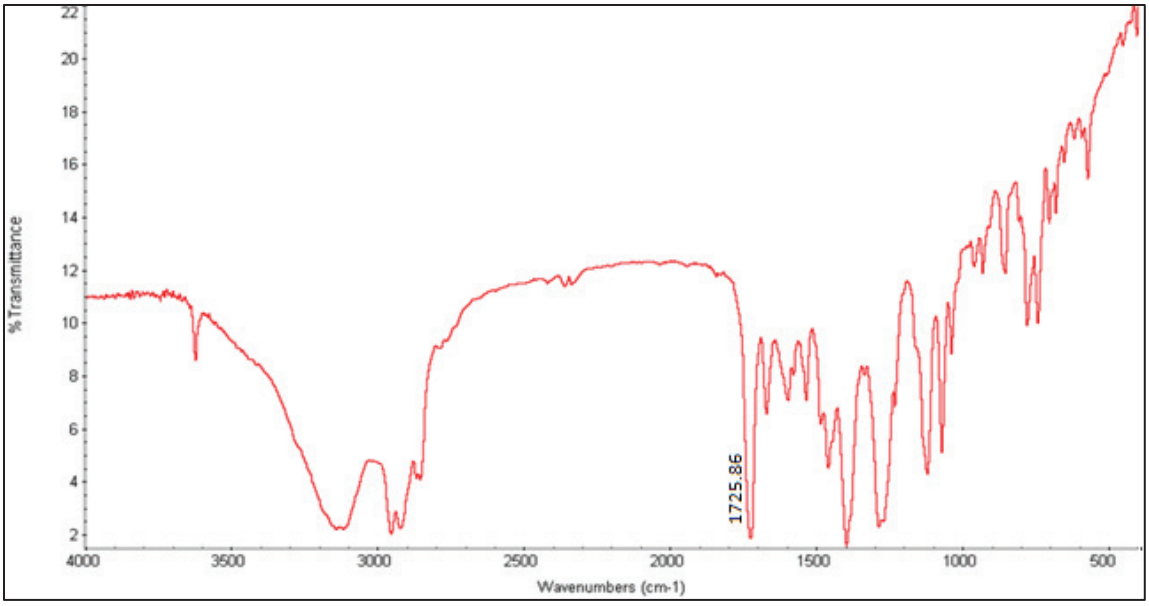

Figure 3: Infrared spectrum of $IMesCO_2$ dissolved in DCM on a salt plate.

The IR spectrum of the IMesCl is shown in Figure 4. Having a spectrum of the starting material will help decipher differences in the spectrum of the product and reactant. This reference is informative in a way that will help further identify the CO_2 peak. Keeping in mind the range of a COO^- peak, there is a peak in the spectrum that is at 1605.25 cm^{-1}, but it is slightly outside of the range and not pronounced, meaning it is not a strong absorption. If there is CO_2 in the starting material, there is more now in the product.

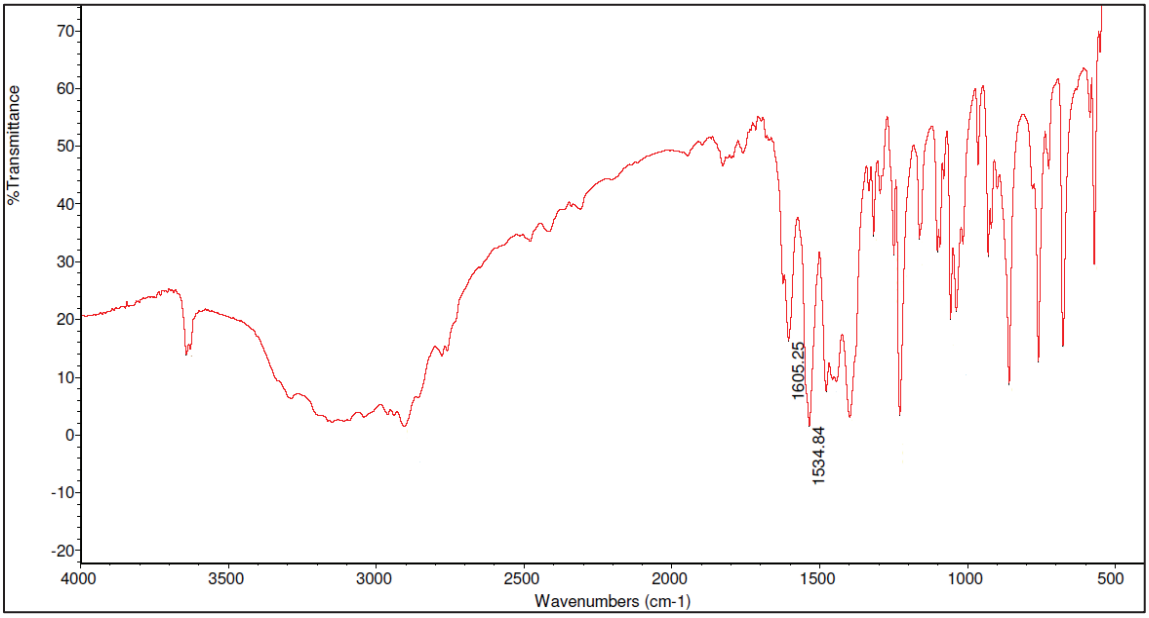

Figure 4: Infrared spectrum of IMesCl starting material dissolved in DCM on a salt plate.

An IR spectrum of the $IMesCO_2$ was taken as a potassium bromide (KBr) pellet to clarify the presence of CO_2 as shown in Figure 5. There is a peak found at 1668.61 cm^{-1}. The product is a solid and the technique of forming a pellet helped minimize contaminate errors. This helps to make sure the sample does have an intrinsic CO_2 peak. Comparing with Tudose *et al.* who generated the same molecule, their CO_2 values from a KBr pellet was 1675 cm^{-1} [26]. Other peaks mentioned were 3160, 3084, 2954, 2921, 2861, 1489, 1298, and 1077 (cm^{-1}). These peaks are also found in the spectrum.

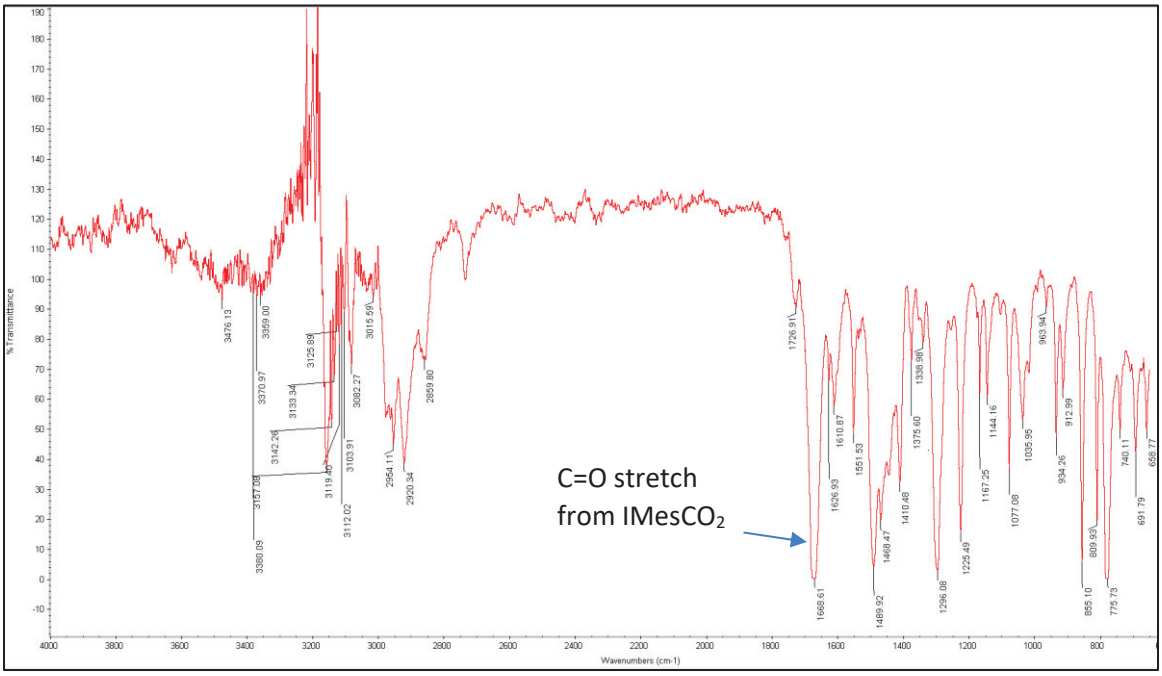

Figure 5: KBr pellet of $IMesCO_2$.

For comparison, Figure 6 shows a KBr pellet of the IMesCl that lacks the peak near 1668.61 cm^{-1}. The $IMesCO_2$ that was synthesized from this IMesCl showed a strong peak at 1668.61 cm^{-1} that indicates the addition of CO_2.

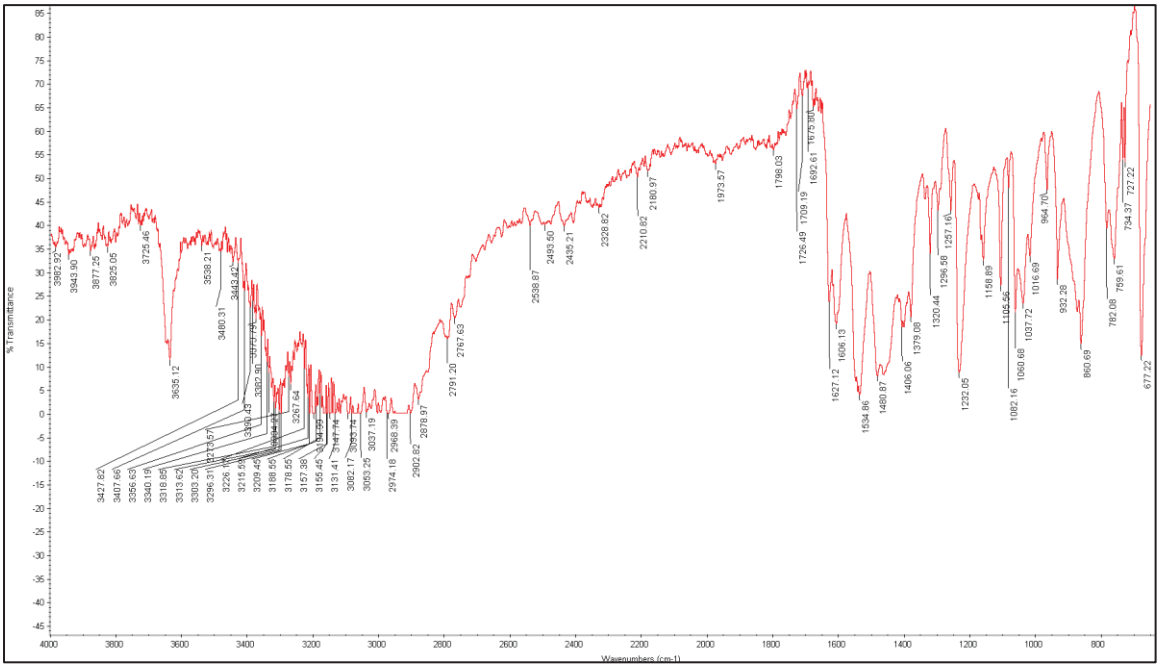

Figure 6: KBr pellet of IMesCl.

Thermogravimetric analysis:

Thermogravimetric analysis displays the weight change of a material as a function of time. The instrument, a TGA Q50 from TA instruments, will take an initial mass of a sample provided and continue to weigh the sample as it is heated until a set maximum time or temperature is reached. The data reveals how the compound will fragment into parts. This can help contribute to identification through knowing the possible fragments of the molecule tested and the percentage that fragment will be relative to the total mass. Those percentages should be close to the percentages measured and calculated by the TGA. For this experiment the TGA was set to stop measuring when it reached a temperature of 600 ℃. The instrument ramped temperature at a rate of 10 ℃ per minute. A 1-5 mg sample is loaded on to an aluminum pan and analyzed by the Q50 TGA. The molecules being tested through thermogravimetric analysis are the $IMesCO_2$ product and the IMesCl starting material. Table 5 below lists possible fragmentations, their molar masses, and mass percentage of the total molecule.

Table 1: Fragments, Molar mass, and Mass percentage of the total molecule.

$IMesCO_2$		
Fragment	Molar Mass	Mass Percentage
CO_2	44.01	12.64%
Mesitylene	120.20	(1)34.54% (2)69.08%
Imidazole	68.08	19.56%

The weakest bond on the $IMesCO_2$ is the C2 carbon and the CO_2 as shown in Diagram 13. This bond is strained because of the large mesitylene groups; they are causing the bond to stretch and rotate, becoming a non-planar molecule. Knowing the nature of this bond, it is easy to imagine that this bond would be broken first if the temperature were to increase. CO_2 is responsible for 12.64% of the total mass of the $IMesCO_2$. Thus, a TGA a value close to 12.64% could very well correspond to CO_2.

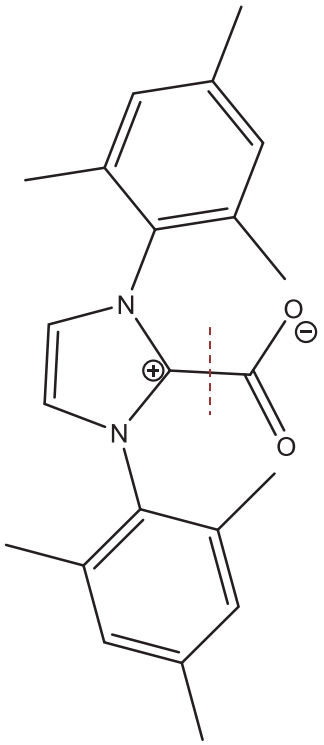

Diagram 10: Depiction of CO_2 decomposition from IMes.

The mesitylenes of the $IMesCO_2$ are subject to decomposition. They are bonded to the nitrogens of the imidazole ring, and this bond can be broken for one or both mesitylenes as shown in Diagram 14. If this were to happen, the mass percentage of one mesitylene would be 34.54% and 69.08% for both. The corresponding mass percentages are listed in the Table 5.

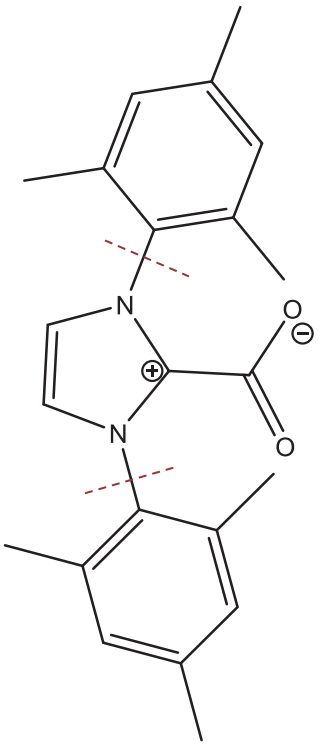

Diagram 11: Depiction of possible mesitylene decomposition.

The imidazole itself is responsible for 19.65% of the total mass of the molecule, but it could fragment into smaller pieces as described in Diagram 15.

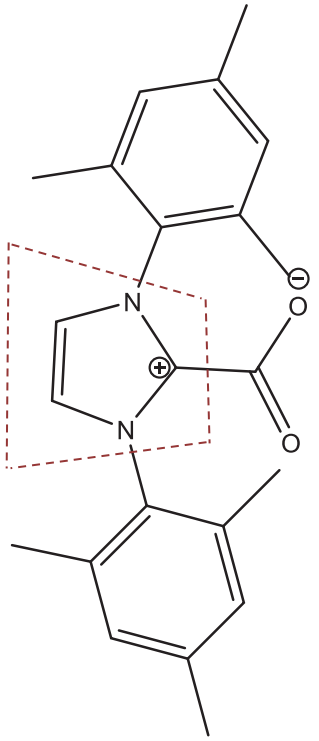

Diagram 12: Depiction of possible Imidazole decomposition.

The temperatures and masses associated with the various transition were found using the derivative of weight change versus time. The transitions are better identified by viewing the peaks of the derivative curve. These data shown in Figure 7 demonstrates that there is a weight change at 141.10 °C. The mass of 0.1365 mg, which is 13.41% of the total mass, is the first fragment to be released. Knowing the proportion of the molecule, this is most likely related to CO_2. Literature values show similar molecules releasing the CO_2 at 155 °C [17]. The next values of 10.47% (0.1066 mg) at 172.55 °C and 24.17% (0.2460 mg) at 197.09 °C. It is not clear what these values may be. The residue is a single mesitylene, with a measured value of 34.03% (0.3464 mg) and a

calculated value of 34.54%.

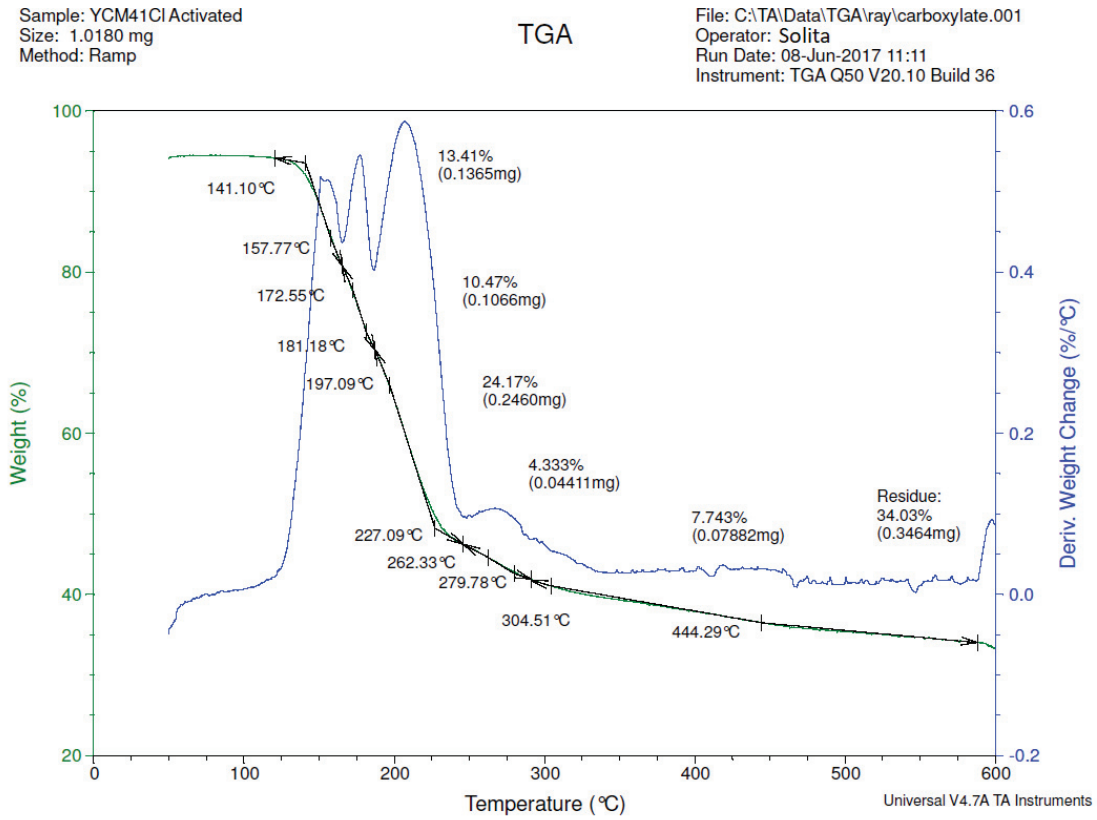

Figure 7: TGA spectrum of IMesCO$_2$.

It is easy to interpret the TGA data of the IMesCl displayed in Figure 8. It has a measured weight loss of 78.08% (0.9931 mg). These values were consistent with the mesityl groups, which account for 78.82% of the total molecule.

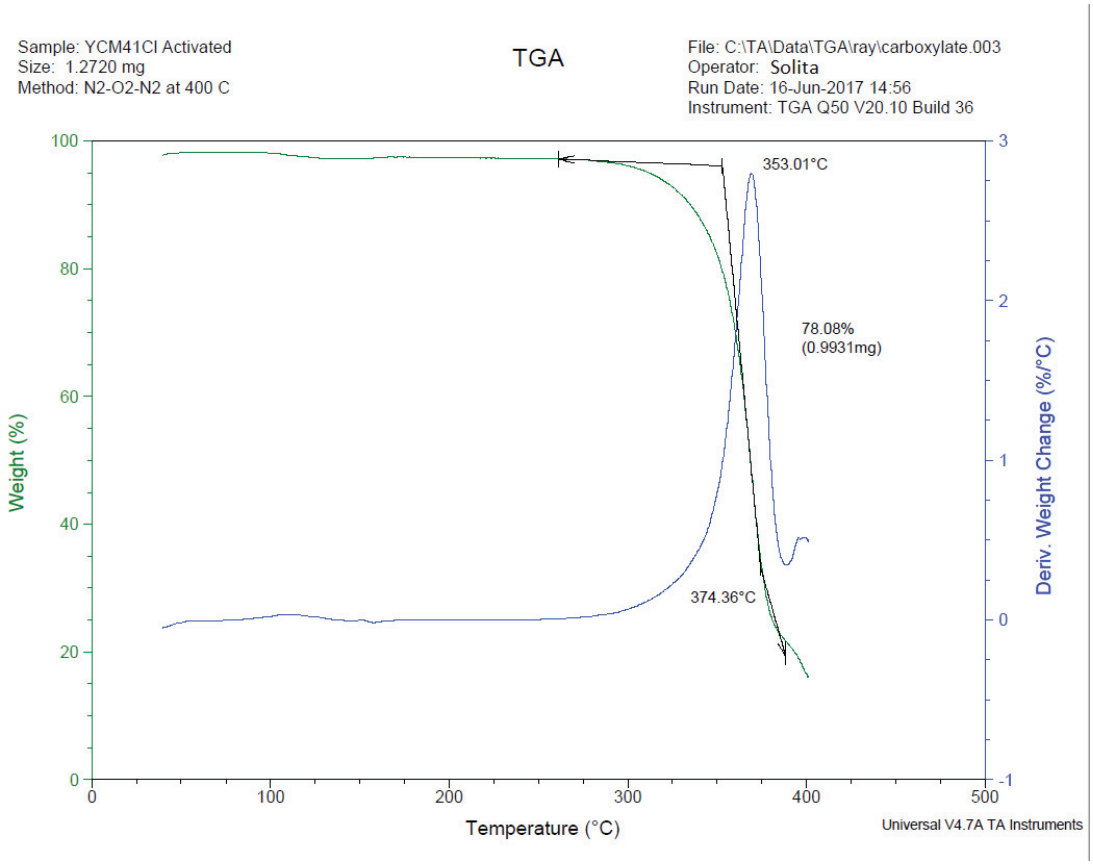

Figure 8: TGA spectrum of IMesCl.

Nuclear Magnetic Resonance Spectroscopy:

NMR spectra of bis-mesityl imidazole chloride

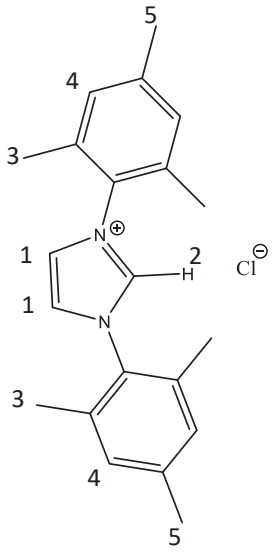

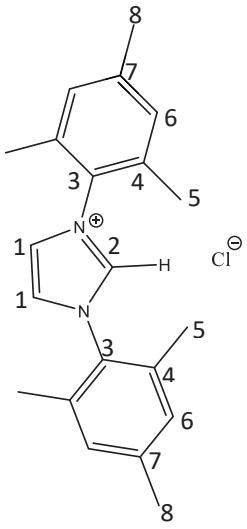

Bis-Mesityl imidazole chloride H^1 NMR Spin	Bis-Mesityl imidazole chloride C^{13} NMR Spin

Bis-Mesityl imidazole chloride was obtained from Sigma Aldrich. A 5 mg quantity was dissolved in 2 mL of chloroform-d for NMR analysis.

Literature values:

^{1}H NMR: δ (400 MHz, $CDCl_3$): δ = 10.48 (singlet (s), 1 H, CH), 7.76 (s, 2 H, olefin), 6.99 (s, 4 H, aromatic), 2.32 (s, 6 H, *para*-Me), 2.13 (s, 12 H, *ortho*-Me) ppm [27].

^{13}C NMR (100 MHz, $CDCl_3$): δ = 141.0 (p-C Mes), 138.8 (CH_2 Im), 134.0 (o-C Mes), 130.6 (i-C Mes), 129.7 (m-CH Mes), 124.9 (CH 4, 5 Im), 21.0 (p-CH_3), 17.5 (o-CH_3) ppm [27].

Measured values:

^{1}H NMR (400 MHz DCM-d_2) δ, 11.1 (s, 1H, CH), 7.6 (s, 2H olefin), 7.2 (s, 2H, aromatic), 2.4 (s, 6H, *para*-Me), 2.2 (s, 12H, *ortho*-Me) ppm. Shown in Figure 9.

^{13}C NMR (100 MHz $CDCl_3$) δ 141.3 (p-C Mes), 139.6 (CH_2 Im), 134.1 (o-C Mes), 131.1 (i-C Mes), 130.7 (m-CH Mes), 124.6 (CH 4, 5 Im), 21.1 (p-CH_3), 17.6 (o-CH_3) ppm.

Shown in Figure 10. The measured eight peak values match the literature for the IMesCl starting material.

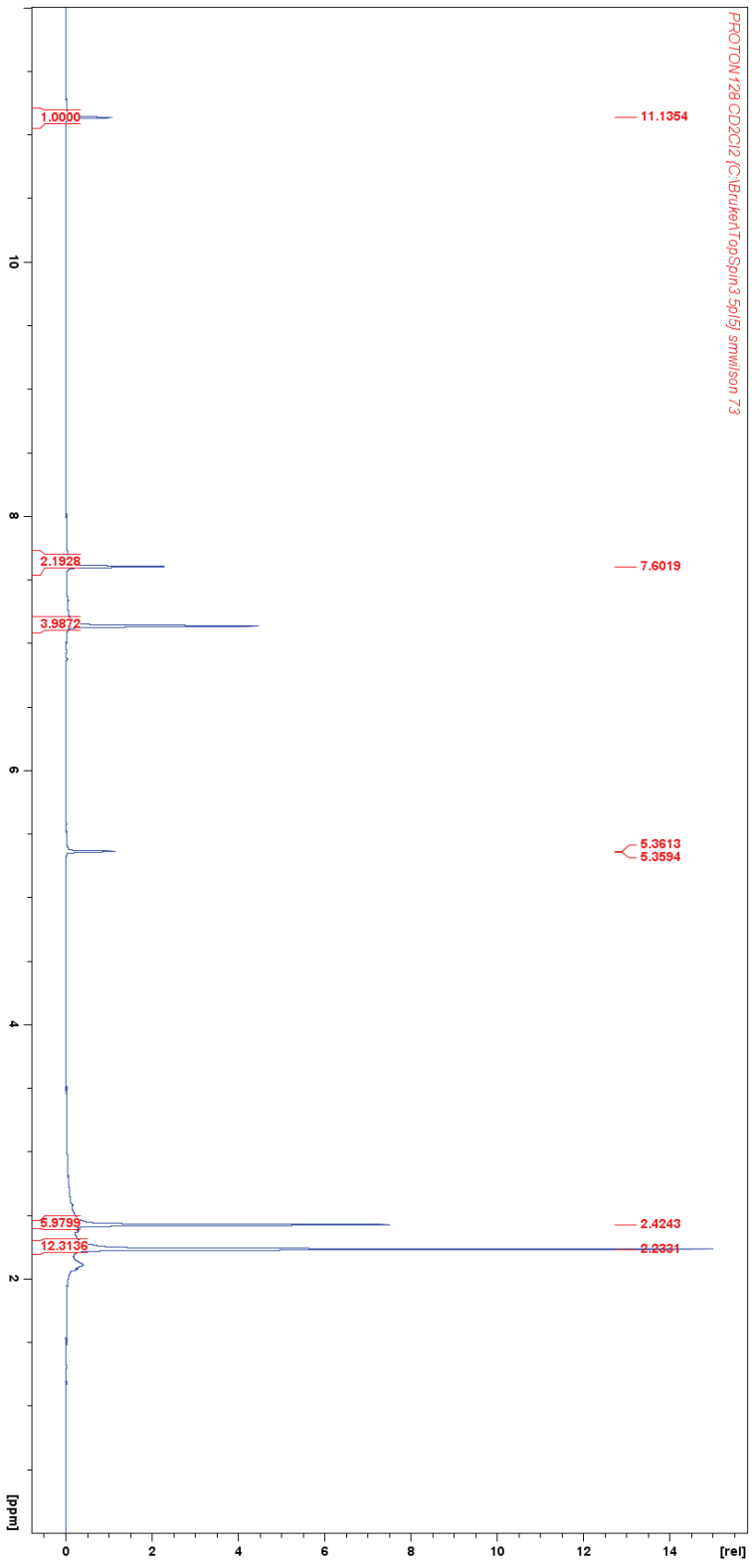

Figure 9: Proton (^{1}H) NMR of bis-mesityl imidazolium chloride.

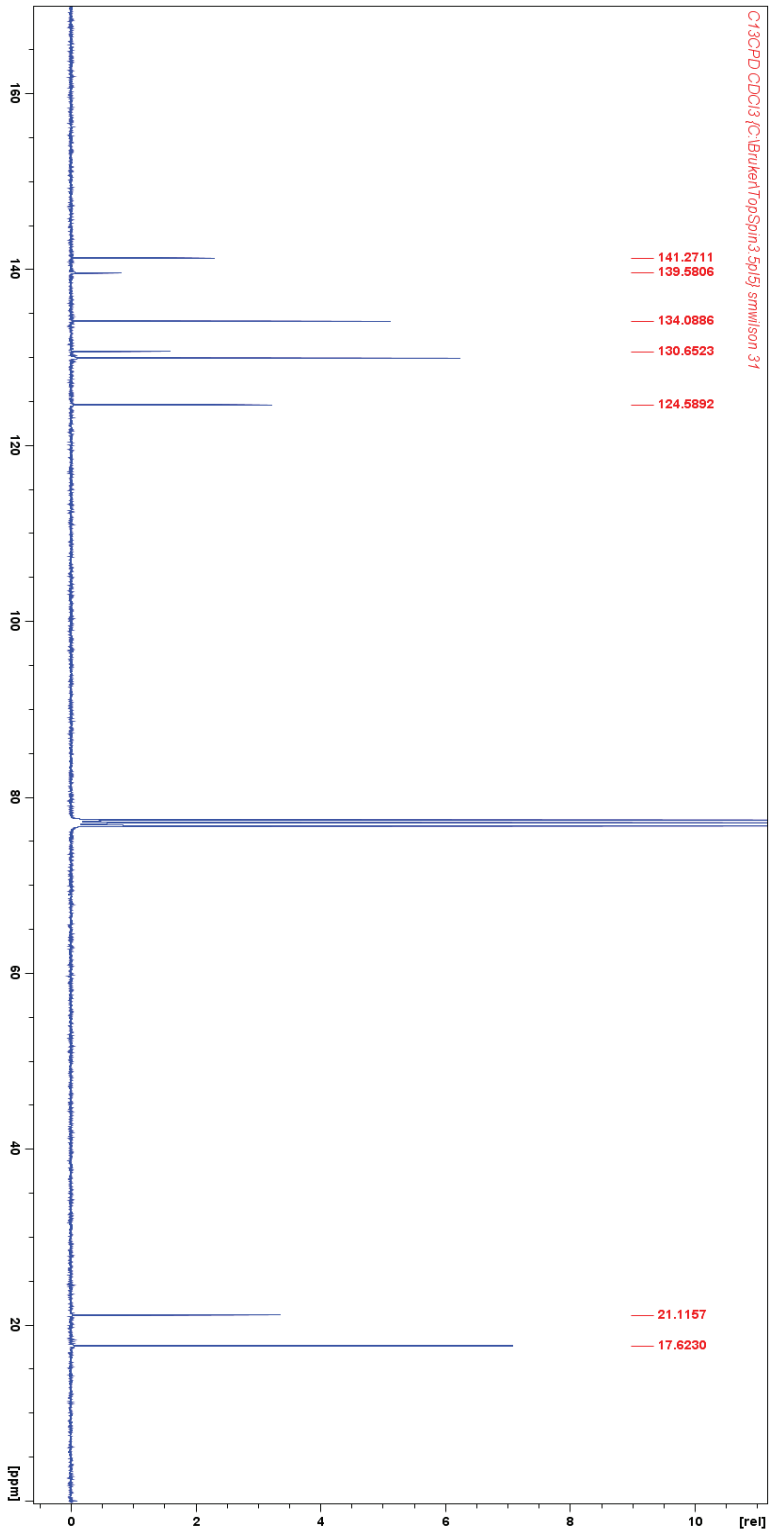

Figure 10: Carbon (^{13}C) NMR of the bis-mesityl imidazolium chloride.

NMR of the $IMesCO_2$:

Bis-Mesityl imidazole chloride (6.8736 g) was dissolved in 100 mL of anhydrous toluene in a round bottom flask while under vacuum. A 50 mL solution of 0.5 M of potassium bis(trimethylsilyl)amide (KHMDS) in toluene was added via an oven-dried syringe to the IMesCl solution. The solution was then stirred for 1 hour and then filtered through Celite while under vacuum. CO_2 was bubbled into the solution via cannula. The reaction was stirred for 2 hours, then washed with diethyl ether. The product was then dried in vacuo overnight and the white powder was weighed. Storage was in a small glass vial that was kept in a desiccator with calcium chloride and Dri-rite. ^{1}H and ^{13}C NMR spectra of the $IMesCO_2$ product in $CDCl_3$ are shown in Figures 11 and 12, respectively

Literature values:

^{1}H NMR for $IMesCO_2$ (DMSO-d_6): δ 7.86 (s, 2H, olefin), 7.08 (s, 4H, aromatic), 2.33 (s, 6H, *para*-Me), 2.09 (s, 12H, *ortho*-Me) ppm [28].

^{13}C NMR for $IMesCO_2$ (DMSO-d_6): δ 152.8 (CO_2), 146.4 (p-C Mes), 139.5 (CH_2 Im), 134.6 (o-C Mes), 131.9 (i-C Mes), 128.8 (m-CH Mes), 121.6 (CH 4, 5 Im), 20.6 (p-CH_3), 16.8 (o-CH_3) ppm [28].

Measured:

^{1}H NMR (400 MHz $CDCl_3$) δ 7.3 (s, 2H, olefin), 7.0 (s, 4H, aromatic), 2.4 (s, 6H, *para*-Me), 2.2 (s, 12H, *ortho*-Me) ppm.Shown in Figure 11.

^{13}C NMR (100 MHz $CDCl_3$) δ 153.4 (CO_2), 147.8 (p-C Mes), 140.6 (CH_2 Im), 134.8 (o-C Mes), 134.7 (i-C Mes), 129.1 (m-CH Mes), 128.4 (CH 4, 5 Im), 20.4 (p-CH_3), 17.6 (o-CH_3) ppm. Reaction yield 50%. Shown in Figure 12. The measured peaks values match the literature for the IMesCO_2.

Both spectra overlaid in Figure 12 illustrate the ^{13}C transition for the IMesCO_2, but to successfully see all the peaks for the compound, thousands of scans would have been needed. The experiment is C13CPD (carbon 13 composite pulse decoupling in red 2000 scans), is overlaid with C13GD (carbon 13 gated decoupling in blue 10,000 scans); however; there are not as many scans for the blue spectra. To account for all the peaks belonging to the IMesCO_2 the spectra were overlaid to show all the expected peaks for the mesityl imidazolium plus a 9^{th} peak showing the CO_2 carbon at 153.4 ppm having a difference due to solvent differences but relating to the literature value of 152.8 ppm. All the other peaks' values for the other carbons match literature values.

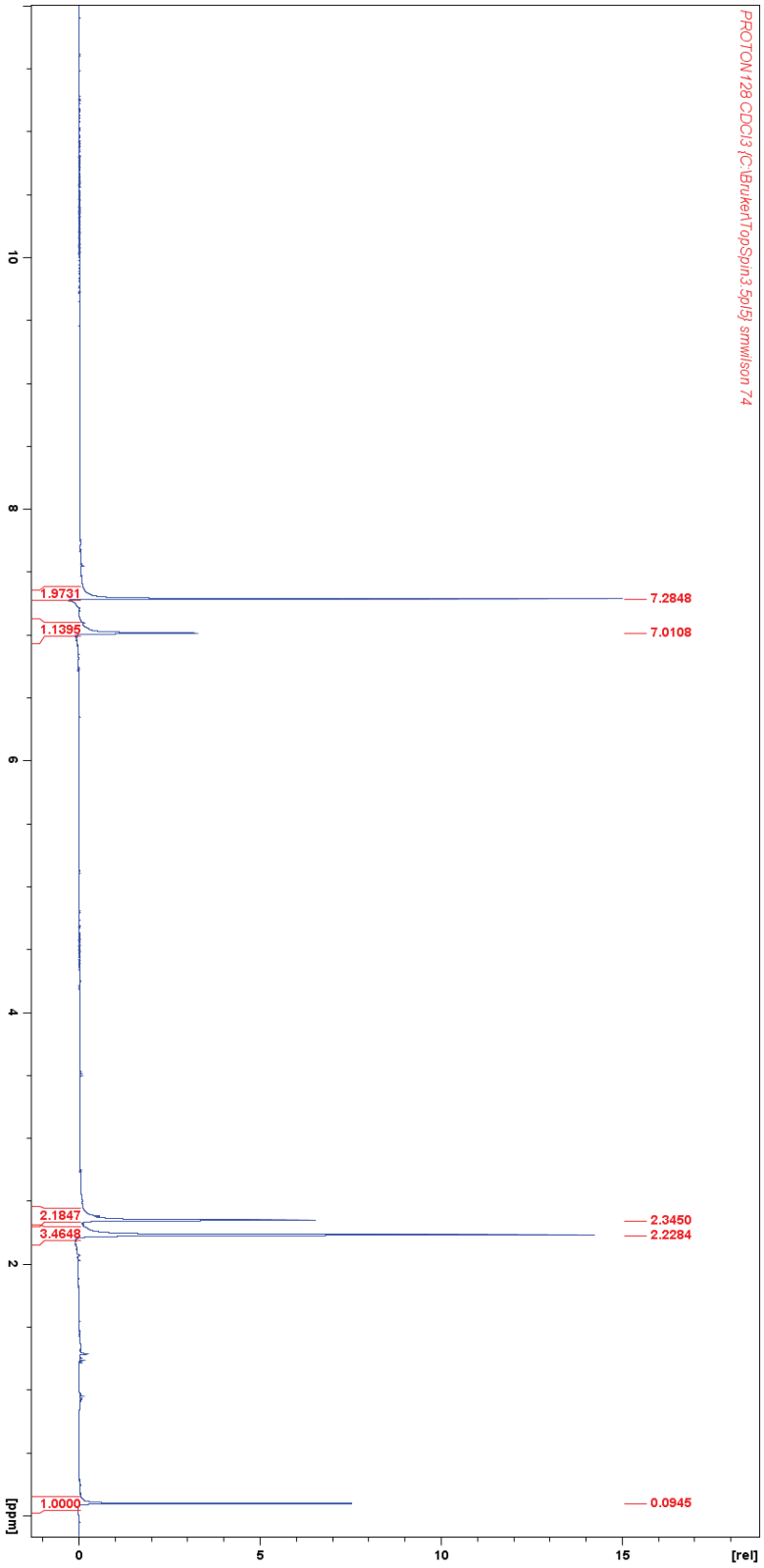

Figure 11: Proton (^{1}H) NMR of the IMesCO$_2$.

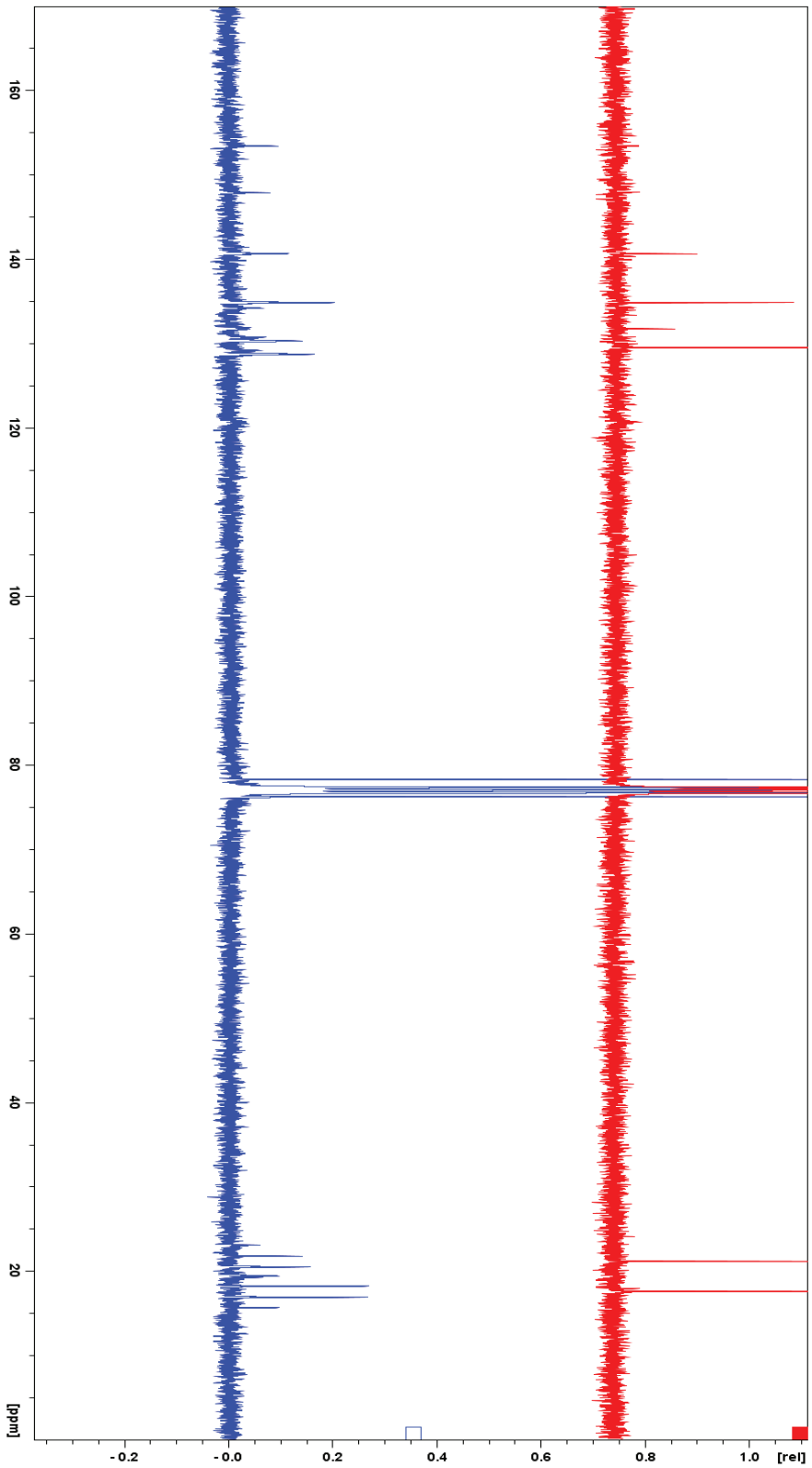

Figure 12: ^{13}C NMR of $IMesCO_2$.

Diagnostic Values for Products:

The anticipated products of $IMesCO_2$ reduction are well known compounds, so there is a large amount of literature references for them involving many different analysis methods. The methods used to detect the presence of these products include IR, NMR, and GC-TCD, and the diagnostic peak values for corresponding wavenumbers, part per million, and retention times, respectively, are referenced for the different methods. The $IMesCO_2$ is reacted using various chemical reduction procedures, and the crude product is analyzed. These different reductions are done in the solvents tetrahydrofuran (THF), dimethyl sulfoxide (DMSO), and acetonitrile (MeCN). The goal is that by having background information and references for the products' characteristic spectral values associated with a given technique they will be easier to detect and identify.

Infrared Diagnostic Peaks:
IR Table General Trends [29].

Table 2: IR peaks of anticipated reduction products.

product	functional group	Absorption (cm^{-1})
methanol	alcohol O-H	3550 - 3200
formic acid	carboxylic acid O-H	3000 - 2500
formic acid	carboxylic acid C=O	1780 - 1710
formaldehyde	aldehyde C=O	1740 - 1690
formaldehyde	aldehyde C-H	2820-2750

Nuclear Magnetic Resonance Diagnostic Peaks:
NMR: Table of Product Shifts [30-33].

Table 3: ^{1}H and ^{13}C shifts for anticipated reduction products.

solvent	^{1}H (ppm) HCOO**H**	^{13}C (ppm)	^{1}H (ppm) H_3CO**H**	^{13}C (ppm)	^{1}H (ppm) H_2CO	^{13}C (ppm)
DMSO-d6	8.14 **11.4**	162.9	3.17 **4.10**	48.6	9.81	84.5
THF-d_8	8.0-8.4 **>10**	160-179	3.27 **3.02**	49.6	9.53	80-85
Methyl-d_3 CN	8.03 **>10**	162.6	3.28 **2.17**	49.9	9.61	80-85

Gas Chromatography Diagnostic Peaks:
GC-TCD Trends.

Preparation of the standards:

Standards representing the various possible reaction products were prepared, to learn where the corresponding signals will be found for product detection via gas chromatography (GC) using a thermal conductivity detector (TCD), details of the instrument are found in Appendix B.

Standard solutions of formic acid, and methanol, were prepared by dissolving 1 µL of the neat liquid into 12.5 mL of dichloromethane (DCM) to make an 80 ppm solution. A formaldehyde solution (37 wt.% in water, containing 14% methanol) was purchased from Sigma Aldrich, and a 1.25 µL aliquot of each solution was injected into the GC. Identical volumes of neat water and dichloromethane were also injected for reference. When methane, CO_2, and hydrogen gas were injected into the GC, 5 mL samples were used. The parameters for the GC were: TCD current at 150 mA, column temperature at 150 ºC, detector temperature at 100 ºC, and injector temperature at 150 ºC. Each standard was injected and allowed 25 minutes to be eluted [34].

GC Table:

Table 4: Concentration and retention times of anticipated reduction products.

standard	concentration	Retention time (min)
methanol	80 ppm	3.15
formic acid	80 ppm	2.02
methane	neat	0.91
water	neat	1.49
hydrogen gas	neat	0.64
carbon dioxide	neat	6.35
DCM	neat	13.38
formaldehyde	37 wt.% in H2O 10-15% methanol	1.85

In the standards chromatograms, the solvent DCM eluted off the column after 10 minutes as described in Figures 13-16. When injected neat, the solvent had a retention time of 13.38 min, shown in Figure 16. All the other tested standards are eluting much earlier at times between 0 and 4 min, as shown in Figures 13-20. This is an advantage because there will not be any interference from the solvent. The dissolved samples contain mostly DCM solvent and if its signal is distinctly separate from the products of interest, the analysis is easier. Figure 13 is the chromatogram of the methanol standard; the major peak at 3.15 min is assigned to methanol; however, there is an extra peak that is most likely water contamination. The methanol standard was taken from a previously opened bottle of methanol, so water contamination is probable (water standard Figure 17).

The formaldehyde used to obtain Figure 20 was an aged solution of 37 wt.% in H_2O containing 10-15% methanol as stabilizer. Considering the bottle was not newly purchased, water contamination may be higher than what was labeled. The chromatogram shows a labeled peak at 1.81 min with an unlabeled shoulder peak and another peak at 3.68 min. The peaks correspond to water 1.49 min and methanol (80 ppm at 3.15 min), so that the shoulder must be formaldehyde.

Standards:

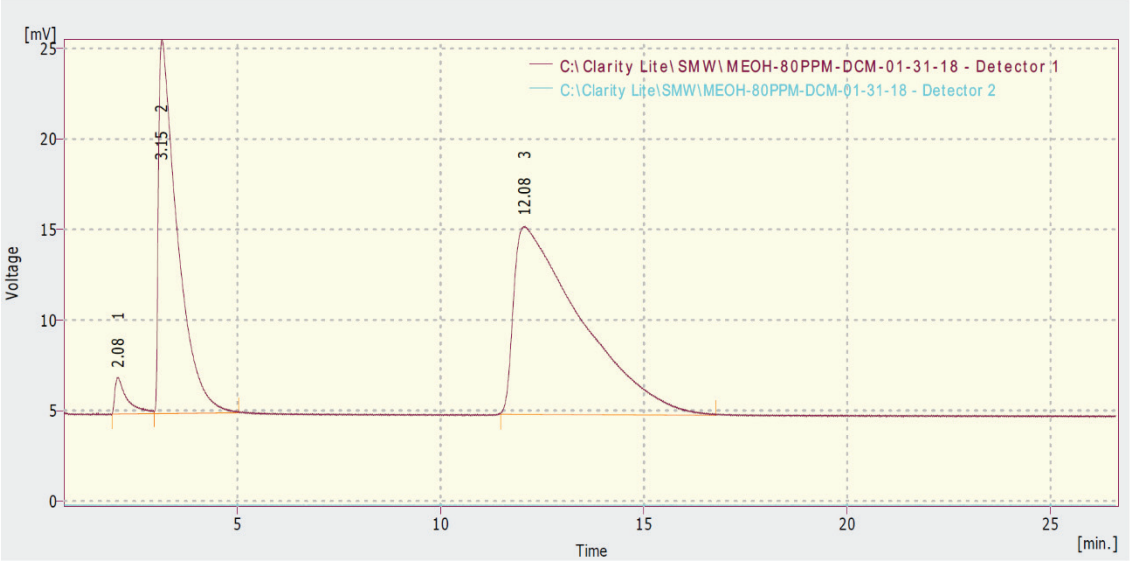

Figure 13: GC Chromatogram of 80 ppm methanol in DCM standard.

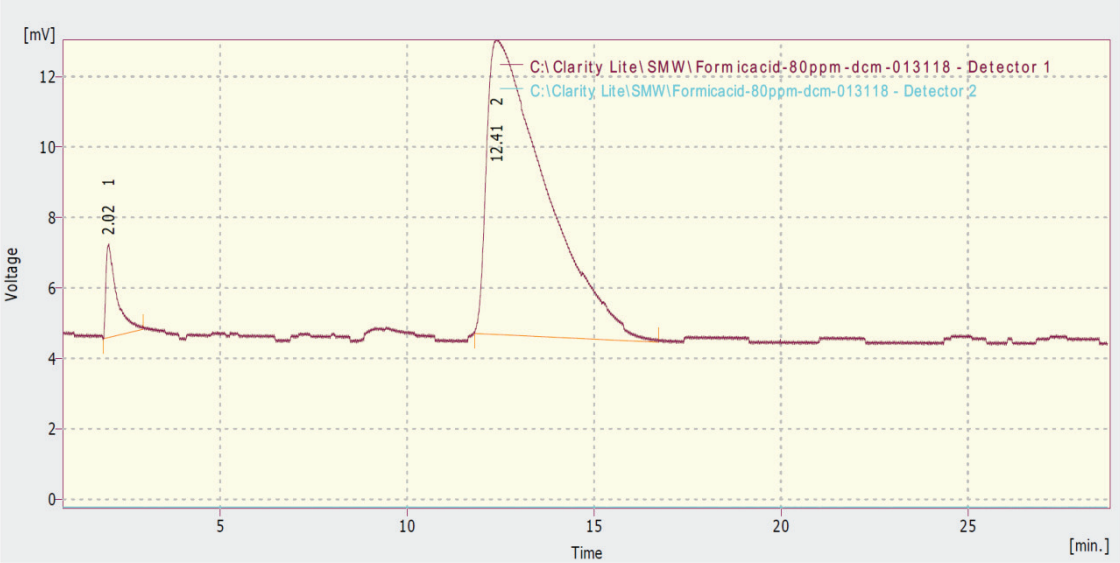

Figure 14: GC Chromatogram of 80 ppm formic acid in DCM standard.

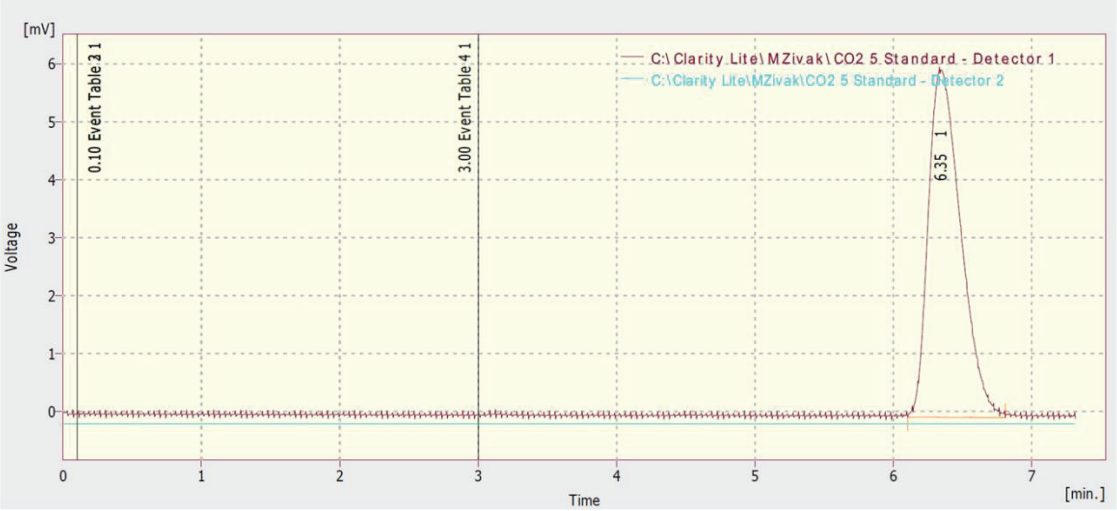

Figure 15: GC Chromatogram of neat carbon dioxide.

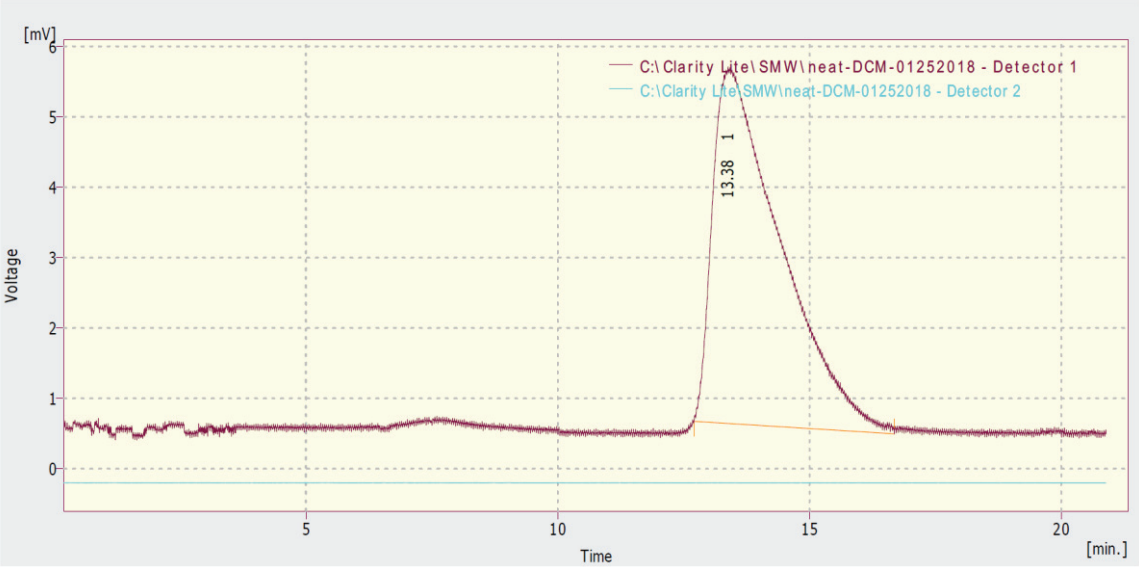

Figure 16: GC Chromatogram of neat DCM standard.

Figure 17: GC Chromatogram of neat water standard.

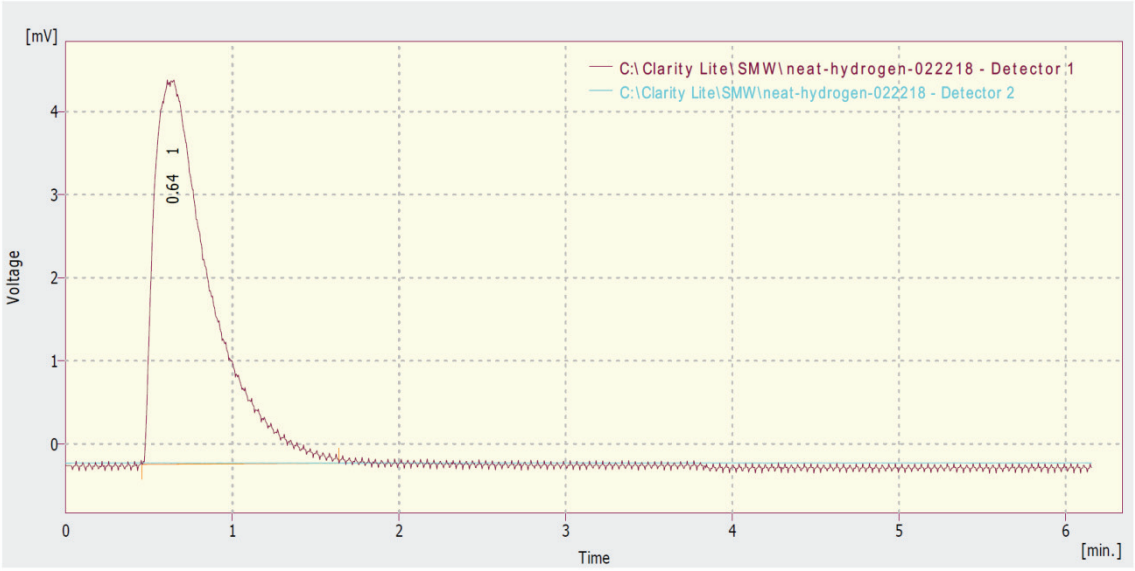

Figure 18: GC Chromatogram of neat hydrogen standard.

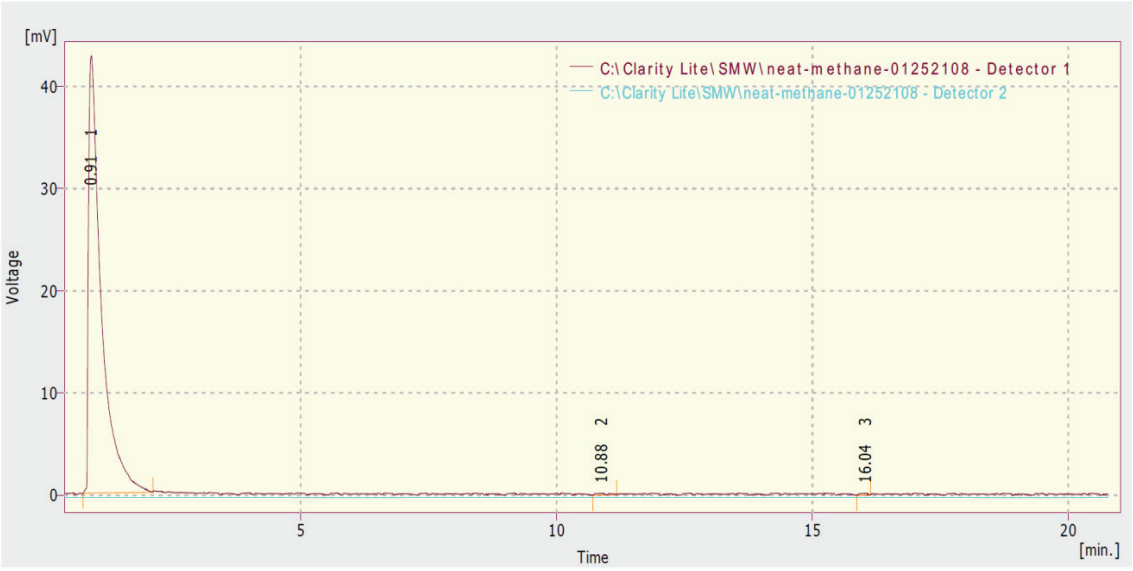

Figure 19: GC Chromatogram of neat methane standard.

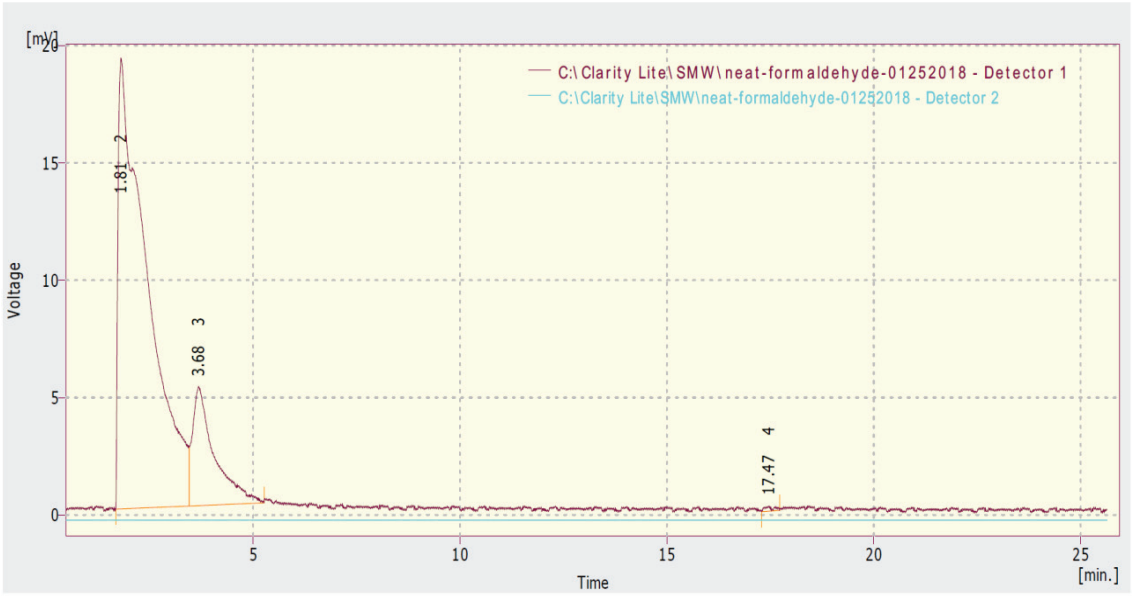

Figure 20: GC Chromatogram of formaldehyde solution standard without DCM.

CHAPTER 3 REDUCTION USING HYDROGEN GAS:

Non-catalyzed Hydrogenation at Atmospheric Pressure (headspace sampling):

Procedure for reaction with hydrogen gas:

A 5 mg amount of $IMesCO_2$ was weighed out and dissolved in 100 mL of DCM in a clean round bottom flask. The setup was purged with nitrogen gas and then 125 mL/min of hydrogen gas was supplied to the system. The gas was bubbled through the solution to promote a reaction. A 5 mL sample of the reaction headspace was injected into the GC. The solution was periodically sampled every 15 minutes.

After allowing the reaction to run 1 hour, Figure 21 was generated. The first peak eluted at 0.74 min, which is closest to hydrogen gas references. DCM should be the peak at 9.99 min. Only the headspace was injected, so IMes would not produce a signal and CO_2 from $IMesCO_2$ would not produce a signal either.

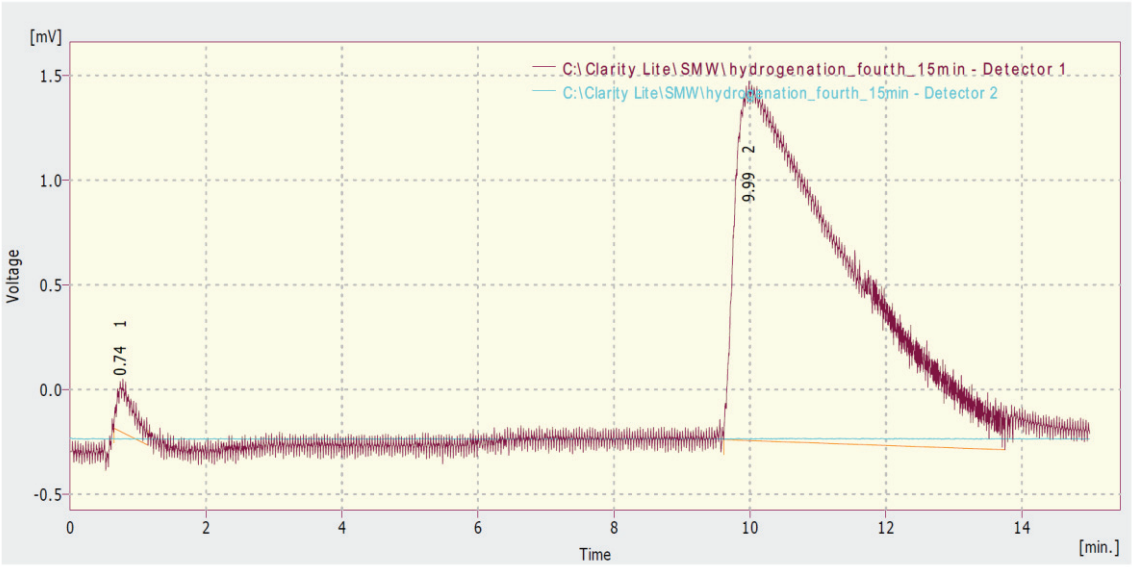

Figure 21: Chromatogram of headspace over $IMesCO_2$ hydrogenation reaction after 1 hour.

Catalyzed Hydrogenation at Atmospheric Pressure (headspace sampling):

Procedure for reaction with hydrogen gas:

A 5 mg amount of $IMesCO_2$ was weighed out and dissolved in 100 mL of DCM in a clean round bottom flask. Then 10 mg of platinum powder was added to the solution. The setup was purged with nitrogen gas and then 125 mL/min of hydrogen gas was supplied to the system. The gas was bubbled through the solution. A 5 mL sample of the solution headspace was injected into the GC. The GC autosampler line was fed to a trap that was submerged in liquid nitrogen. The condensate in the trap was thawed and sampled at the end of the experiment and a 1.25 μL aliquot was injected neat into the GC.

Both chromatograms shown in Figures 22 and 23 are similar, with slight variation of the retention time, but Figure 22 still only indicating hydrogen at 0.46 min and DCM at 9.63 min. There was a catalyst present in this second experiment; however, there was still no detection of products displayed in Figure 23. There were no peaks before 13.91 min, which corresponds to solvent. The hydrogen is not being activated and products are not being formed. To thoroughly sample gases coming from the column, a trap was connected to the system. The contents of the trap were analyzed and found to be just solvent also.

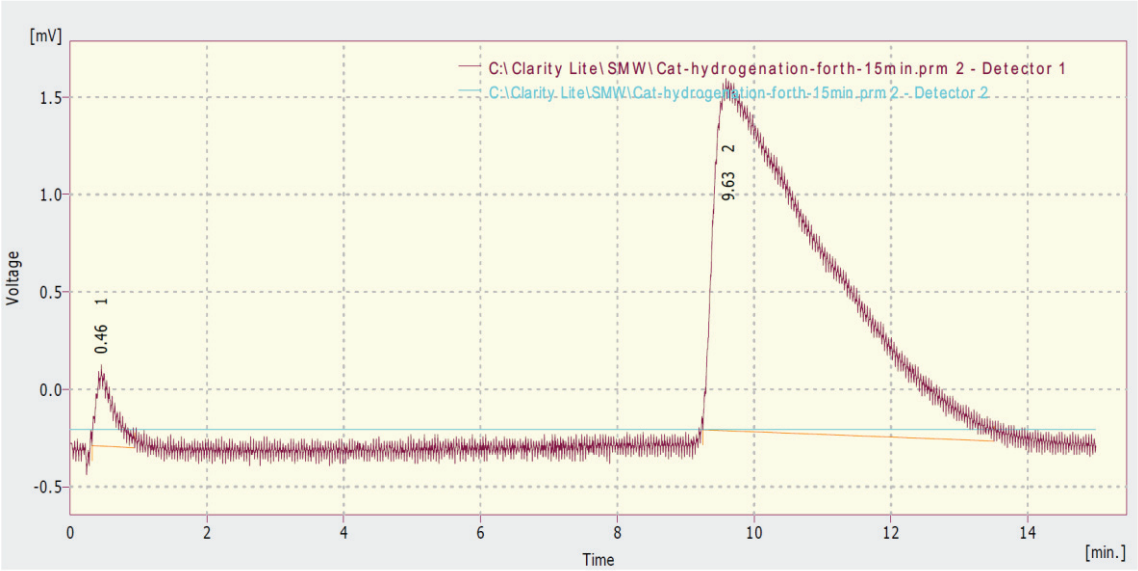

Figure 22: Chromatogram of headspace sample taken from the reaction between $IMesCO_2$ and H_2; 1 hour into Pt black- catalyzed reaction.

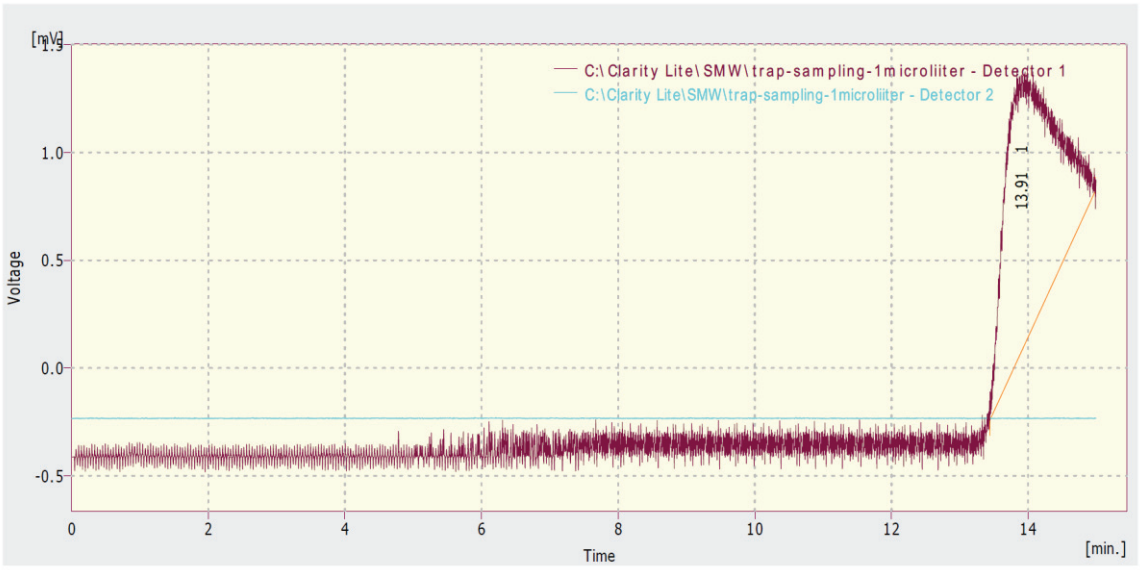

Figure 23: GC Chromatogram of trap contents from Pt Black- catalyzed hydrogenation of $IMesCO_2$.

IMesCO$_2$ Reduction Under High Pressure Hydrogen Gas:

Procedure for hydrogenation with high pressure hydrogen:

1.00 g of IMesCO$_2$ was dissolved in 200 mL of dry DCM in a glass sleeve. The sleeve was placed in a 1-liter pressure vessel and stirred, then a 10 mmol equivalence (0.3075 g) of palladium on carbon (Pd/C) was slowly added to the solution. The vessel was sealed, and each bolt was tightened to 25 ft/lb. The sealed vessel was purged with argon gas and then hydrogen for 10 minutes each. Hydrogen gas was added through stainless steel tubing, and pressurized to 100 atm. The reaction continued to stir for a duration of 19 hours. The pressure was slowly released, and the reaction catalyst was filtered out [35, 36]. The filtrate was subjected to spectroscopic and chromatographic analysis. Reaction displayed in Diagram 16.

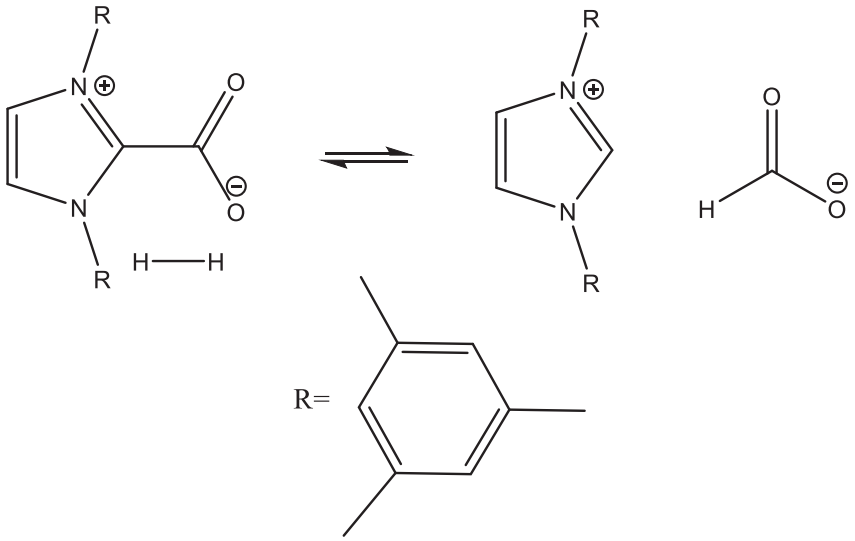

Diagram 13: Mechanism of hydrogen gas and IMesCO$_2$.

There is a broad peak ranging from 2865.5 to 3030.6 cm^{-1}. The C-H and O-H stretches on a formic acid molecule would be in that range; however there needs to be a peak in the 1800-1650 cm^{-1} range as well for the carbonyl functional group on the molecule. That region does show a small peak at 1608.2 cm-1, which is outside the range for the formic acid carbonyl functional group. It could be C=N from the imidazole ring instead. Shown in Figure 24.

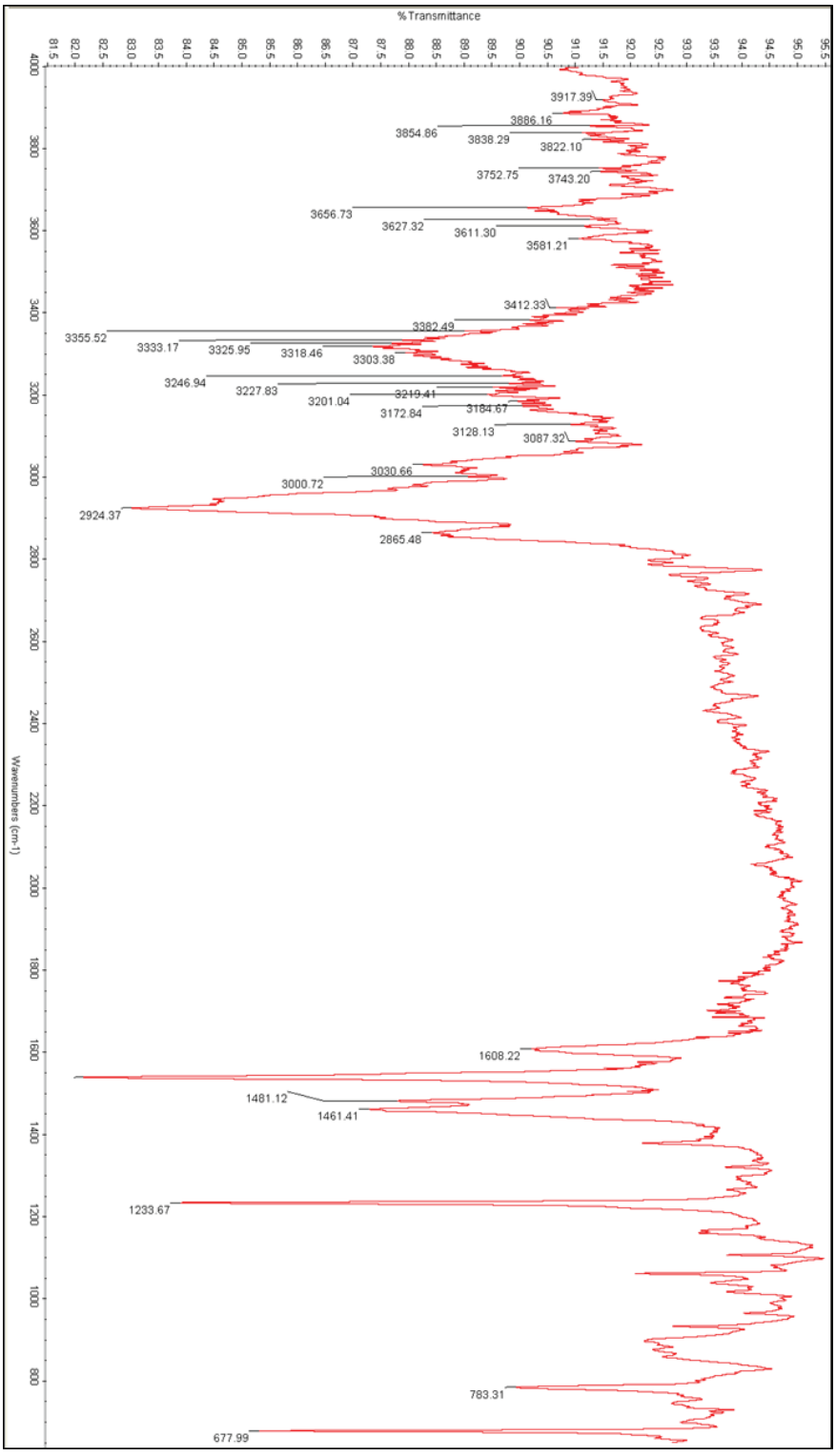

Figure 24: IR spectrum of high pressure reaction between H_2 and $IMesCO_2$.

Figures 25 and 26 show the ^{1}H and the ^{13}C NMR spectra of the high pressure reaction. Evidence of IMes can be found in the spectra, but evidence of the IMesCO_2 has vanished. The proton NMR spectrum shows a small peak at 10.99 ppm. This is the proton on the C2 carbon on the imidazole ring. This peak appeared in the IMesCl starting material at 11.1 ppm, so there is some drift due to the solvent differences, but otherwise it appears that the H2 hydrogen is present. Formic acid would have a peak in this region, but the reaction was not acidified and so that diagnostic proton peak would be unlikely. There is a small peak around 7.7 ppm, this could be a proton on formic acid. Without the acidic proton, the molecule present would be formate. The frequency is low for this species. This could be due to the reaction solvent. The carbon NMR spectrum shows the disappearance of the CO_2 carbon, further supporting the protonation of the C2 carbon. Again, there is a low intensity peak around 169 ppm, which is on the high side of formic acid, and solvent effects may account for this. The reaction solvent was dichloromethane, and the NMR solvent was DMSO. Literature values of formic acid in DMSO show peaks at 8.14 ppm ^{1}H and 162.9 ppm ^{13}C [30-33].

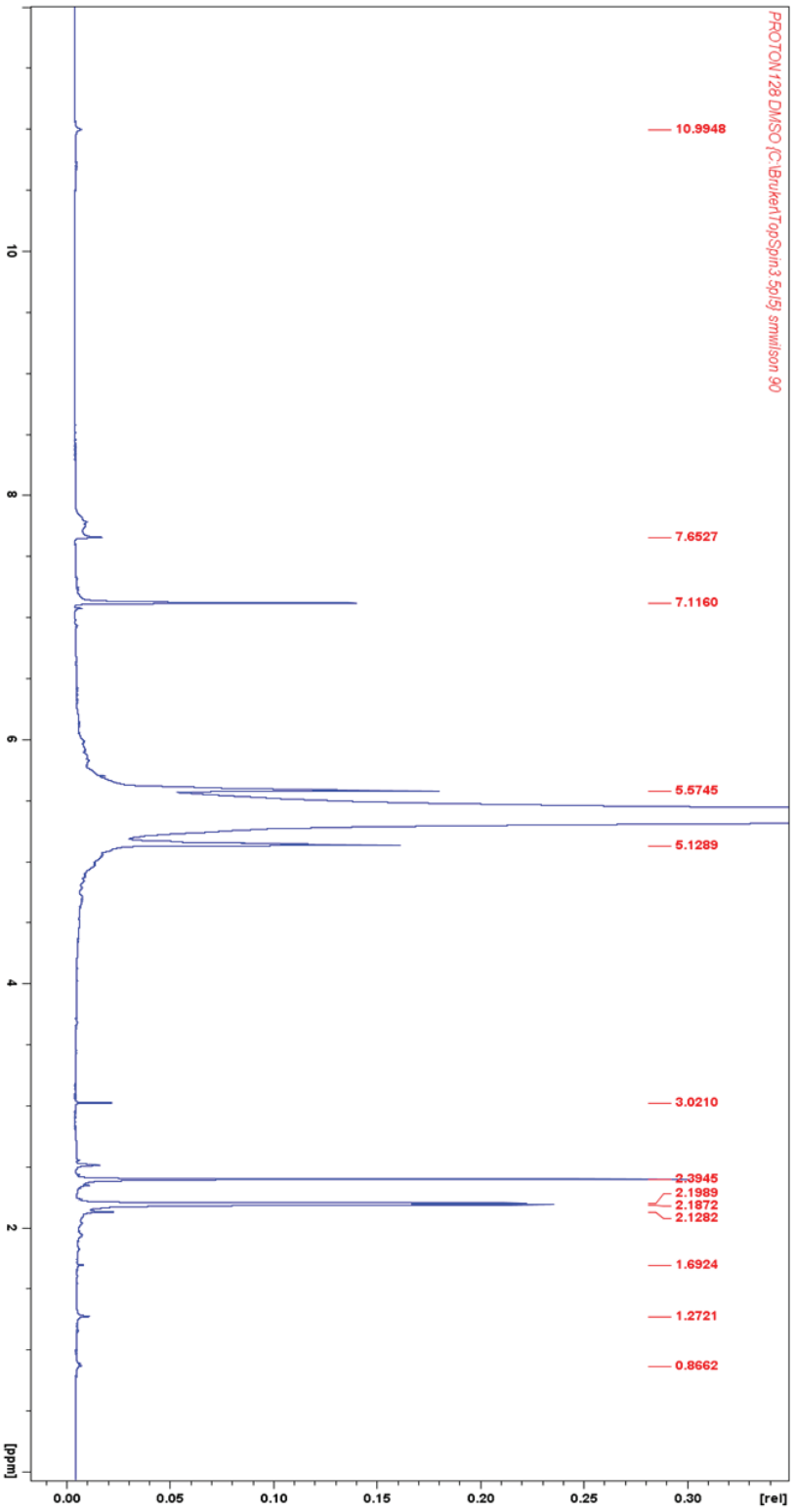

Figure 25: ^{1}H NMR spectrum of high pressure reaction between H_2 and IMesCO$_2$.

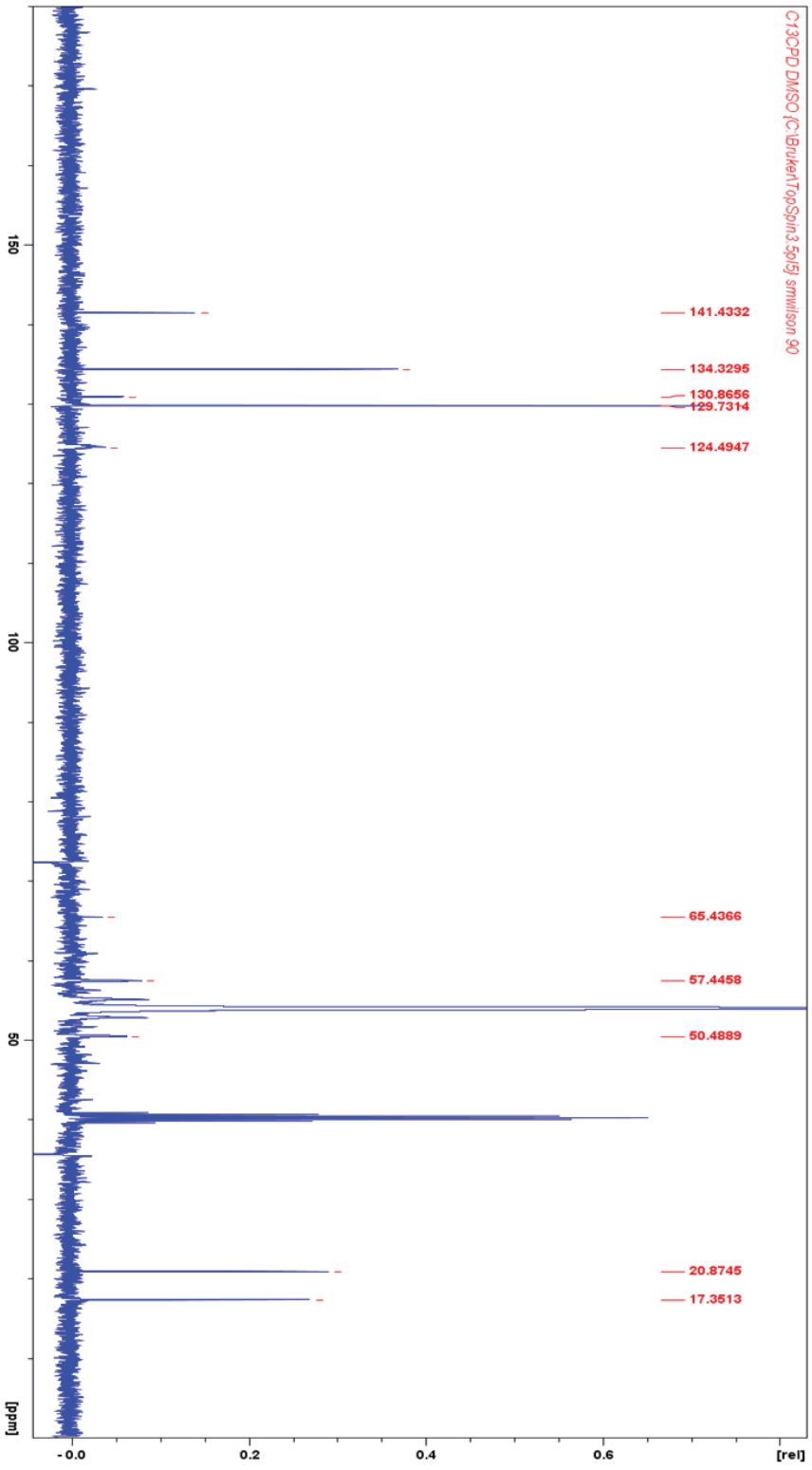

Figure 26: ^{13}C NMR spectrum of high pressure reaction between H_2 and $IMesCO_2$.

There are 3 peaks present on this chromatogram: 0.53, 2.05, and 4.37 min. Hydrogen gas is found at 0.64 min and formic acid was found at 2.02 min. There are slight variations due to systematic error, but there are molecular species present in the chromatograph. The 4.37 min peak does not correspond with any of the reference products. This could be CO_2 and since there is a large abundance of it this could account for the broadness of the peak. However, CO_2 should be coming out closer to 6.35 min. It is also possible that it is air contamination, the sealed vessel was opened to air once the reaction was complete then injected into the instrument. Nevertheless, hydrogen is present in the sample as well as formate. Described in Figure 27.

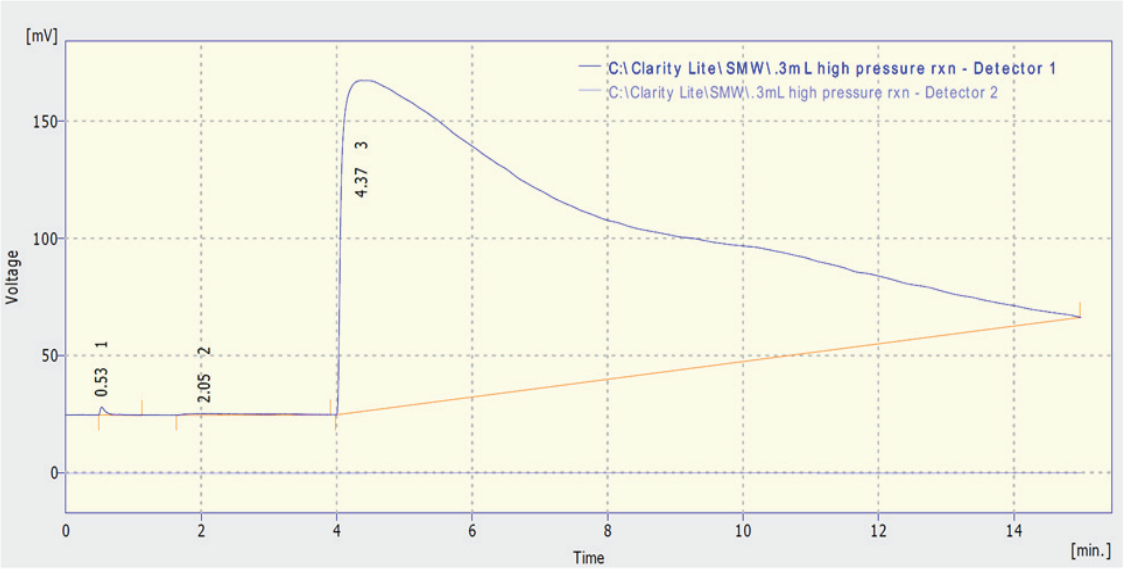

Figure 27: GC chromatogram of the high pressure reaction between H_2 and $IMesCO_2$.

CHAPTER 4 REACTIONS WITH HYDRIDES:

Reduction Using $LiAlH_4$, $LiBH_4$, and $NaBH_4$

0.100 g of $ImesCO_2$ was added to 15 mL of THF in a 25 mL round bottom flask to make a 0.019 M solution and stirred. Then 0.3 mL of 1M $LiAlH_4$ in THF was slowly added to the solution while in an ice bath. After 20 minutes the solution was warmed to room temperature and stirred overnight. The procedure was repeated with MeCN as a reaction solvent and with $LiBH_4$ and $NaBH_4$ as reducing agents. In a clean dry NMR tube, 0.0055 g of $IMesCO_2$ was dissolved in 5 mL of DMSO-d_6 to make 0.003 M solution. 0.1 mL of $LiBH_4$ was added to the solution and then placed in an ice bath overnight. Any precipitated solids were filtered out and analyzed. The NMR tube procedure was repeated in DMSO-d_6 with $NaBH_4$. Solvent and $IMesCO_2$ amounts are summarized in Table 8 below. Reaction mechanism displayed in Diagram 17, 18, and 19.

Table 5: Mass of $IMesCO_2$, solvent, and hydride.

$IMesCO_2$ (g)	solvent	hydride (.3 mL)
0.1033	THF (15 mL)	$LiAlH_4$
0.1017	THF (15 mL)	$LiBH_4$
0.1018	MeCN (15 mL)	$LiBH_4$
0.1015	MeCN (15 mL)	$NaBH_4$
0.0055	DMSO-d_6 (5 mL)	$LiBH_4$
0.0061	DMSO-d_6 (5 mL)	$NaBH_4$

Reaction with Lithium Aluminum Hydride:

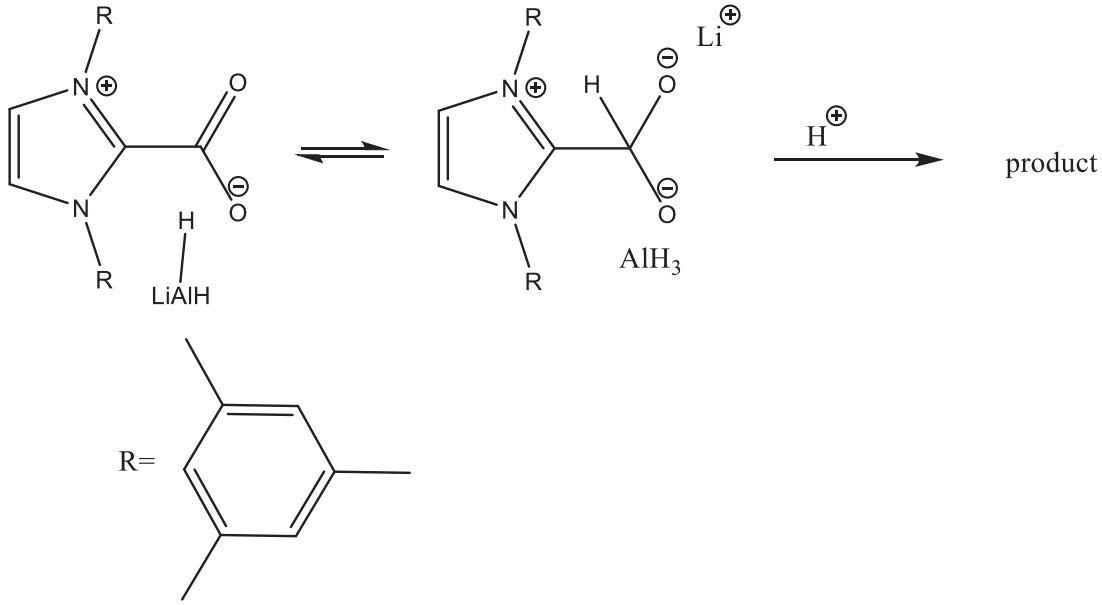

Diagram 14: Mechanism of $LiAlH_4$ reacting with $IMesCO_2$.

There is a broad peak ranging from 3650-3250 cm^{-1}, this is in the range of O-H stretch in methanol with a range of 3550-3200 cm^{-1}. Also, there is 2868 cm^{-1}, which corresponds to the formaldehyde C-H group. There needs to be a peak around 1740-1690 cm^{-1}, and there is a small peak in that range for the carbonyl group of formaldehyde. $LiAlH_4$ is a strong reducing agent. If there is enough hydride present it will not only reduce the ketone, but it will reduce to methanol. Displaying peaks for multiple reduction products is not unexpected for this hydride. Shown in Figure 28.

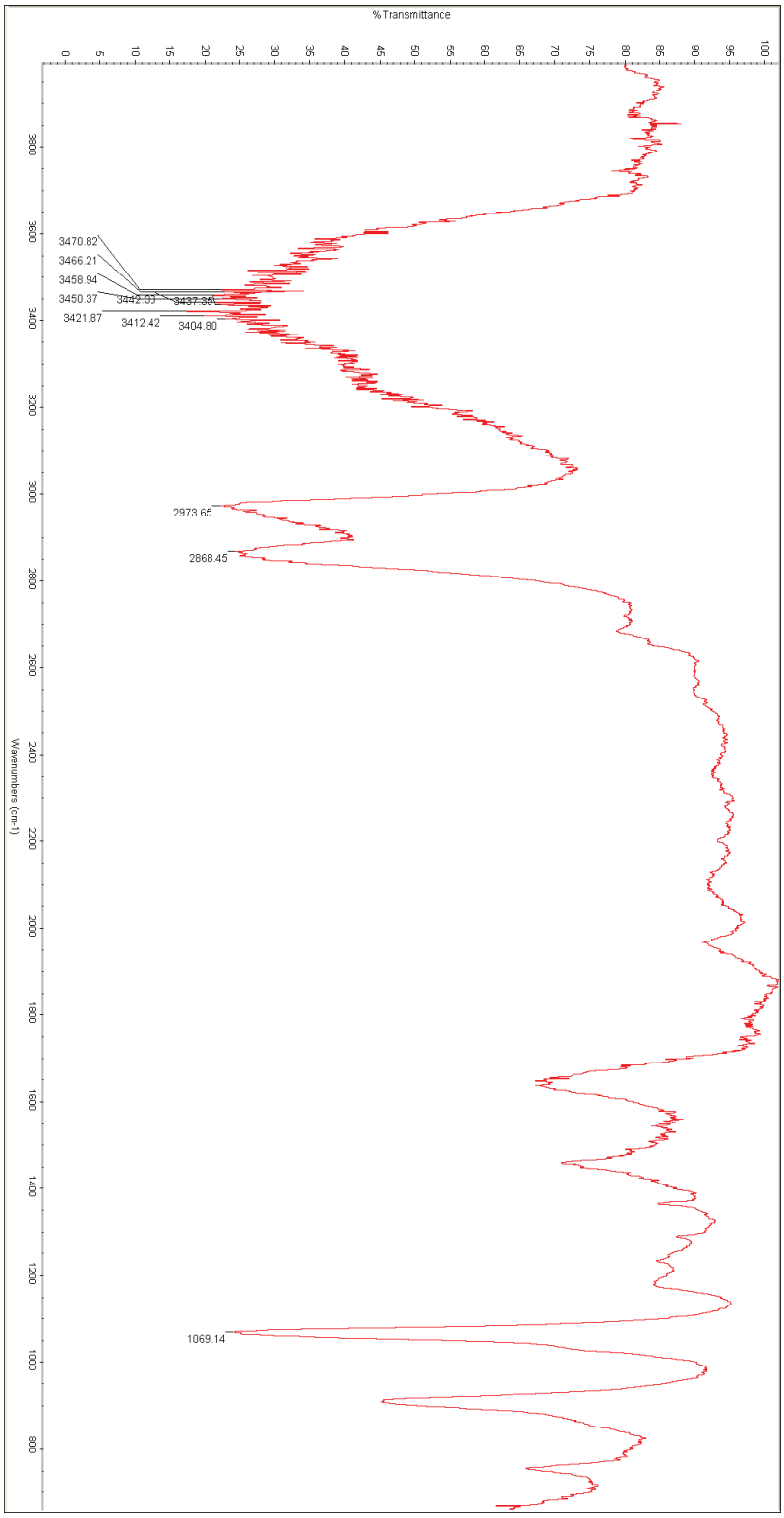

Figure 28: IR spectrum of $IMesCO_2$ in a solution of THF reacted with $LiAlH_4$

The NMR spectrum shown in Figure 29 of the $IMesCO_2$ reacted with $LiAlH_4$ in THF has two large THF peaks in the proton NMR. This weakens the prominence of other peaks. Not to mention, the solubility of the $IMesCO_2$ in THF is low, so if there are products present, they would be from a small amount of the $IMesCO_2$ that dissolved and reacted. Characteristic peaks for IMes are present at low abundance. There are trace peaks corresponding to methanol at 3.25 and 4.20 ppm and formate at 8 ppm on the proton NMR. The carbon NMR displayed in Figure 30 does support this with a peak at 163.5 ppm for formate and peaks close to 50 ppm that are in the range of methanol. There could be other possibilities, but IMes and $LiAlH_4$ would not have peaks in this range. A solvent that $IMesCO_2$ is more soluble and $LiAlH_4$ is unreactive would be ideal for this reaction, but such a solvent remain to be identified.

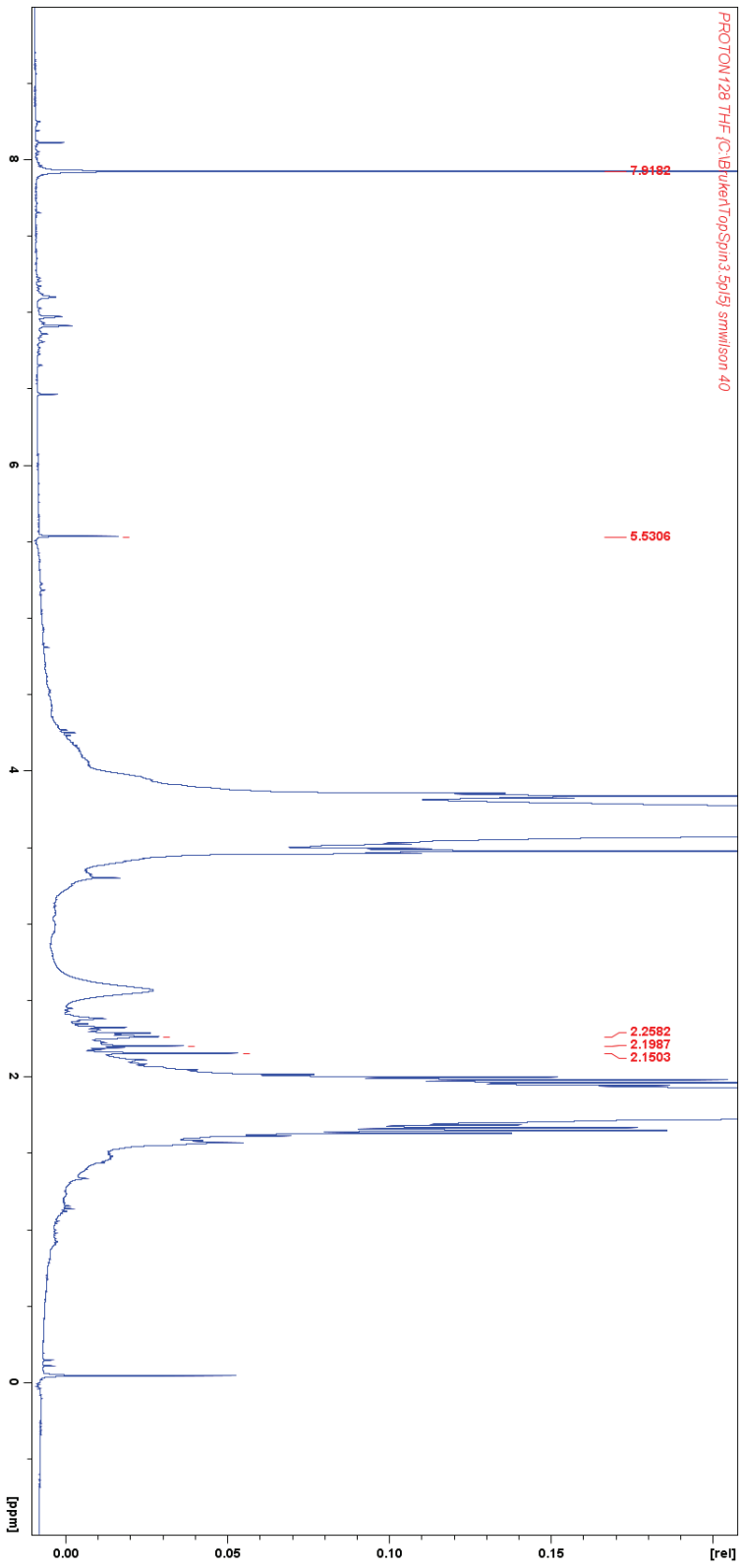

Figure 29: ^{1}H NMR spectrum of $IMesCO_2$ in a solution of THF reacted with $LiAlH_4$.

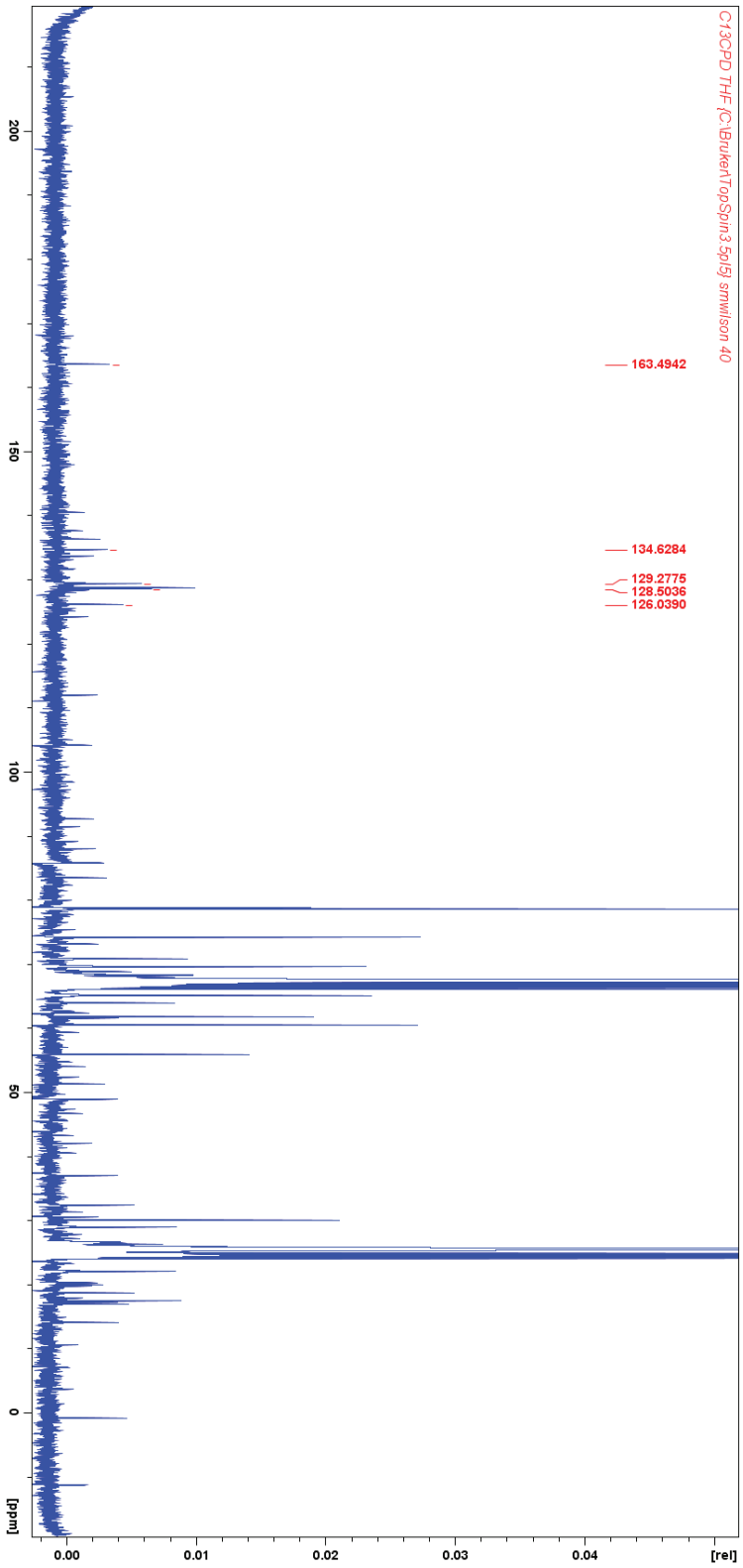

Figure 30: ^{13}C NMR spectrum of $IMesCO_2$ in a solution of THF reacted with $LiAlH_4$.

Reaction with Lithium Borohydride:

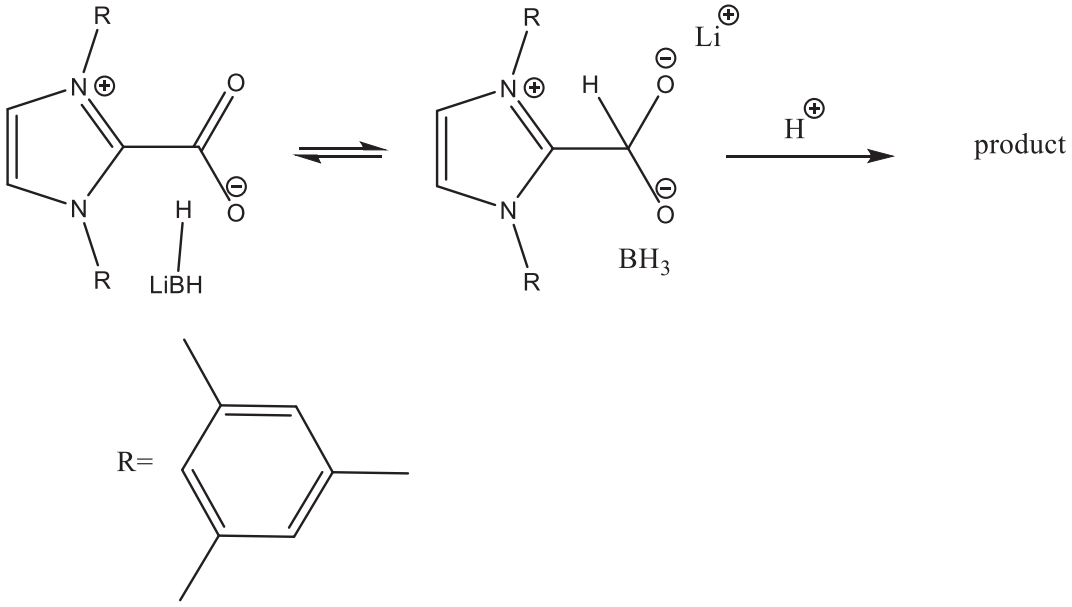

Diagram 15: Mechanism of $LiBH_4$ reacting with $IMesCO_2$.

The IR spectrum in Figure 31 shows broad peaks for the O-H stretching in 3550-3495 cm^{-1} for methanol and 2970 -2850 $cm^{-1}$for aromatic C-H from IMes. This is puzzling for formic acid because there should also be the stretching of the carbonyl bond in the spectrum in the range of 1800-1650 cm^{-1}, there is no such peak. If formate was present in the sample it would not produce a broad peak, but it would have a carbonyl stretch in the same region as formic acid, so formate is not present.

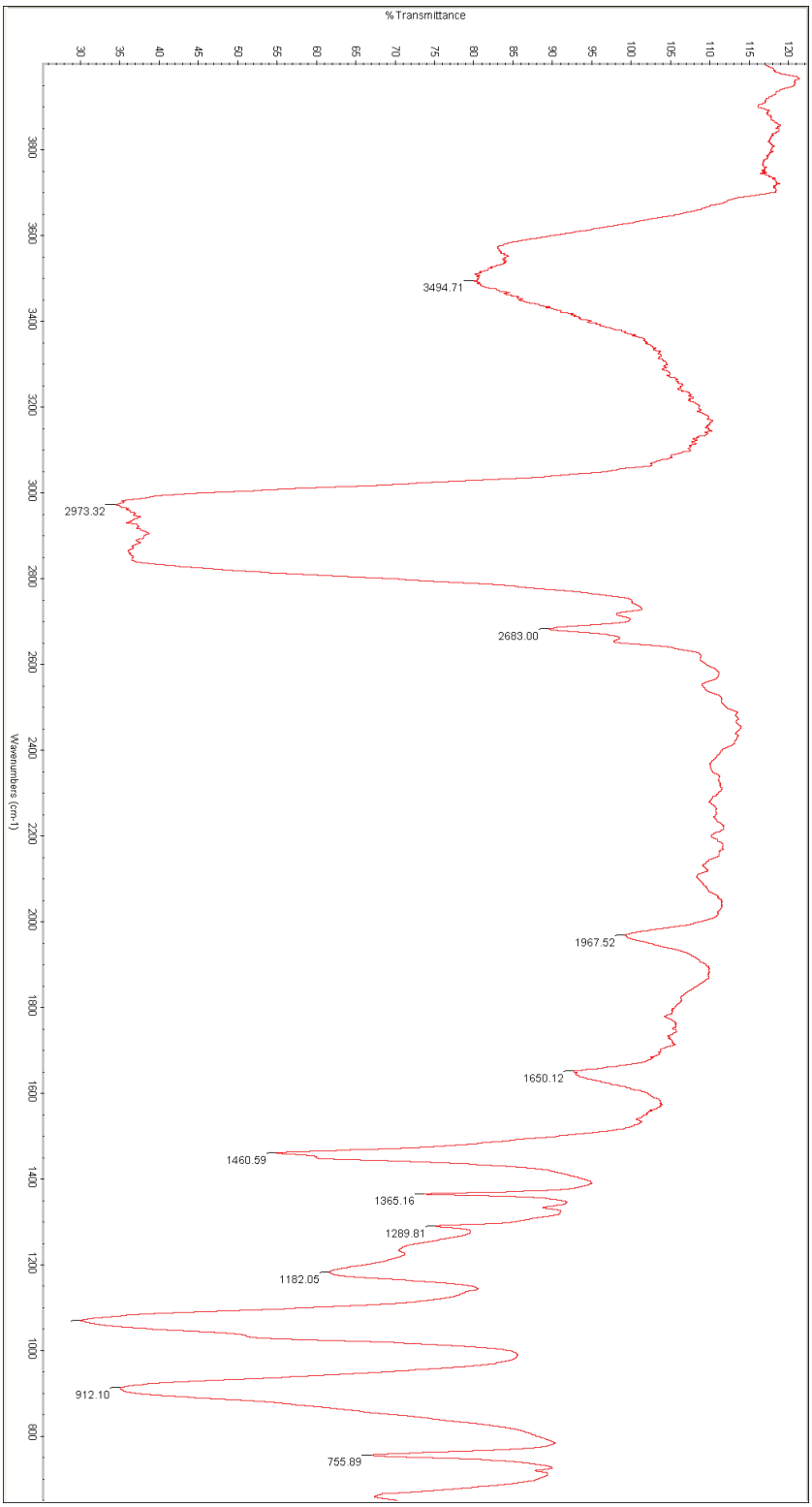

Figure 31: IR of $IMesCO_2$ in a solution of THF reacted with $LiBH_4$.

In the ^{1}H NMR spectrum there are small peaks are around 11 and 8.1 ppm. These peaks could be formic acid; however, a hydrogen on the IMes C2 carbon could also have a signal in the 11 ppm region. It is likely that formate is present instead of formic acid, so the 11 ppm peak would be H2. There are also small peaks close to 3 and 4 ppm, but close to THF solvent peaks that would prove methanol. Also, there are peaks that show that IMes is present in the solution, although peaks at 7.8 and 5.6 ppm are new and not the expected products. The ^{13}C spectrum does not show any peaks for the expected reduction products and the CO_2 peak is not present either. As described in Figure 32 and 33.

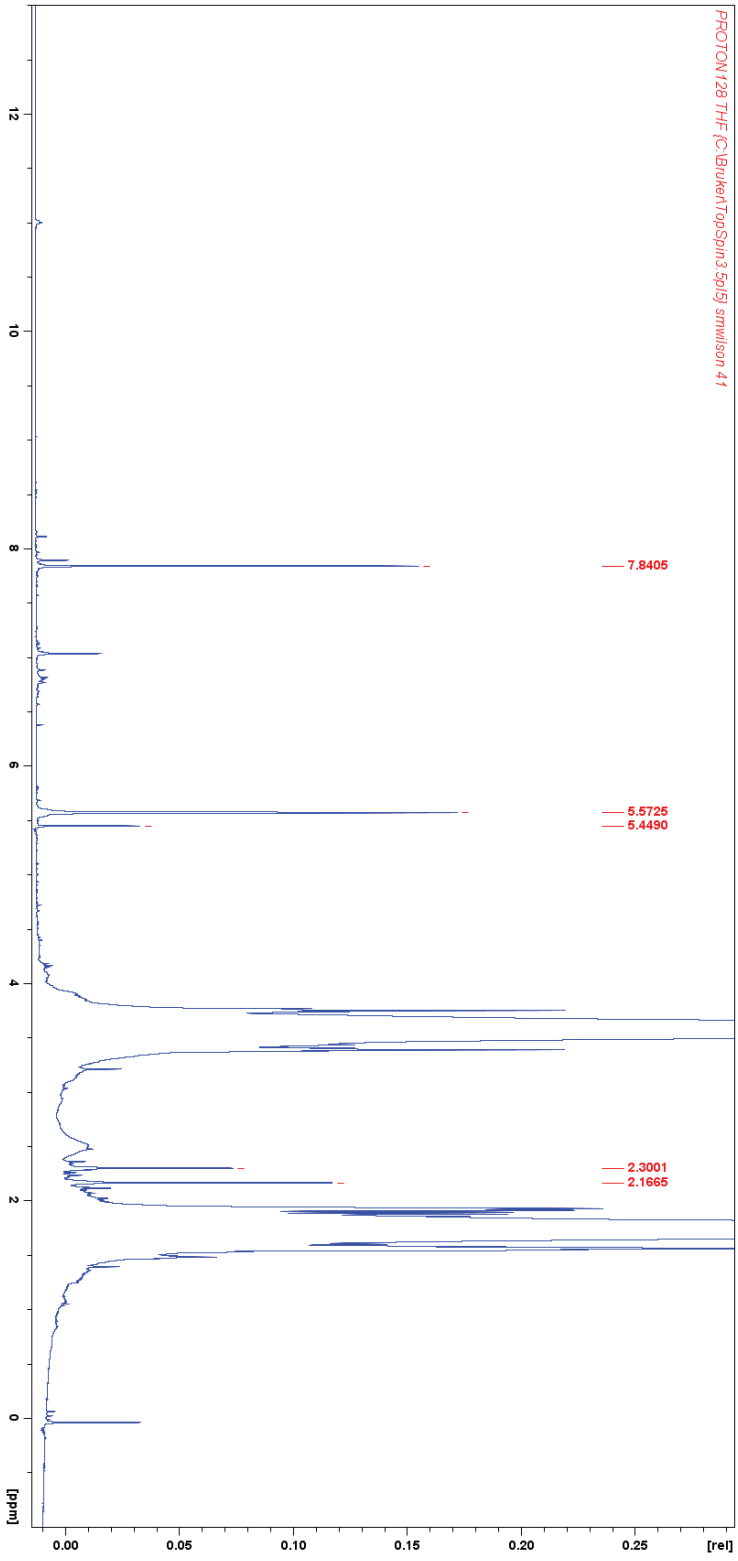

Figure 32: ^{1}H NMR spectrum of IMesCO$_2$ in a solution of THF reacted with LiBH$_4$.

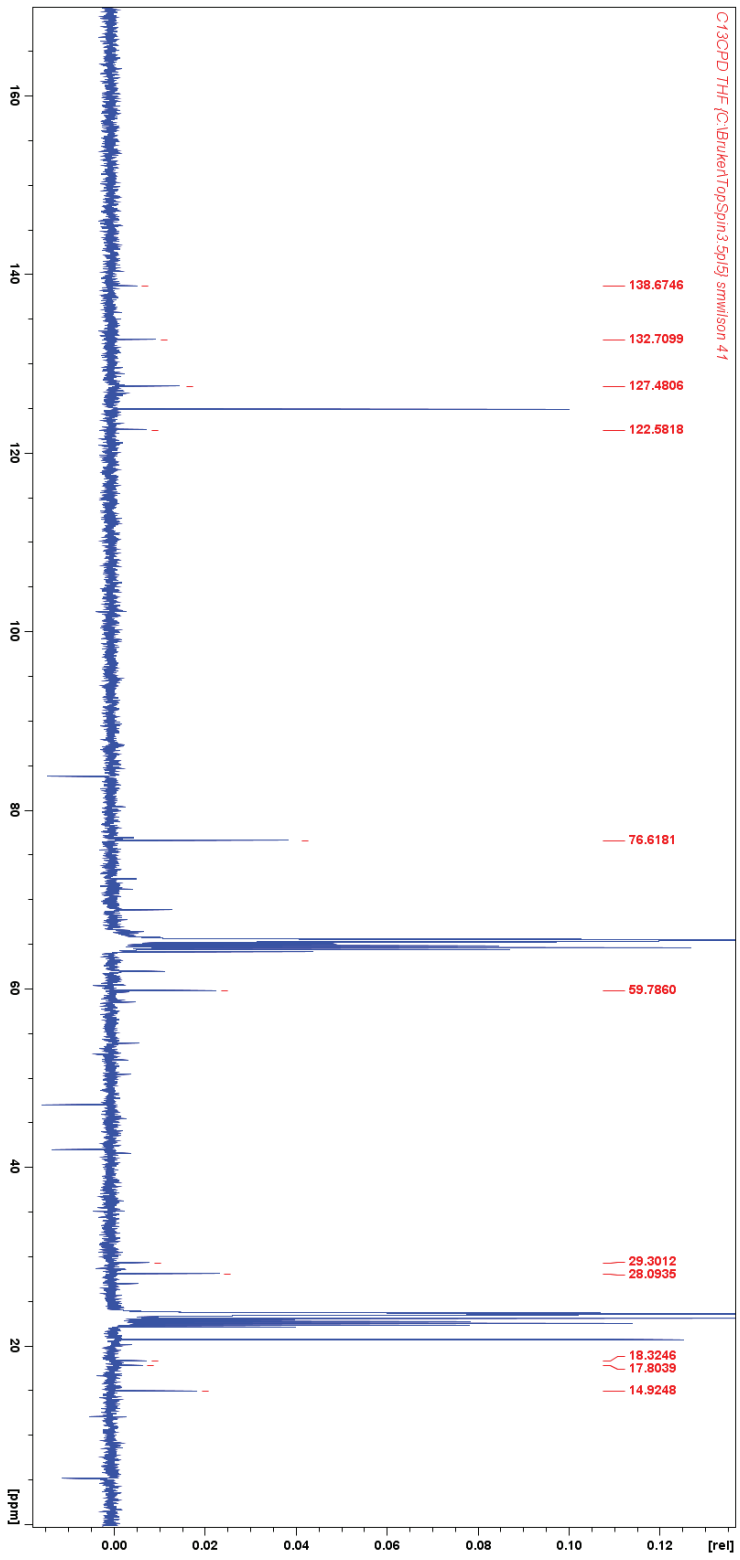

Figure 33: ^{13}C NMR spectrum of $IMesCO_2$ in a solution of THF reacted with $LiBH_4$.

On this IR spectrum the broad peak range 3001- 2874 cm^{-1} is the IMes aromatic C-H stretch, yet again the peak for the carbonyl is missing. There are also other peaks that are more pronounced compared to previous spectrum, but they could be the solvent acetonitrile or IMes in solution. Displayed in Figure 34.

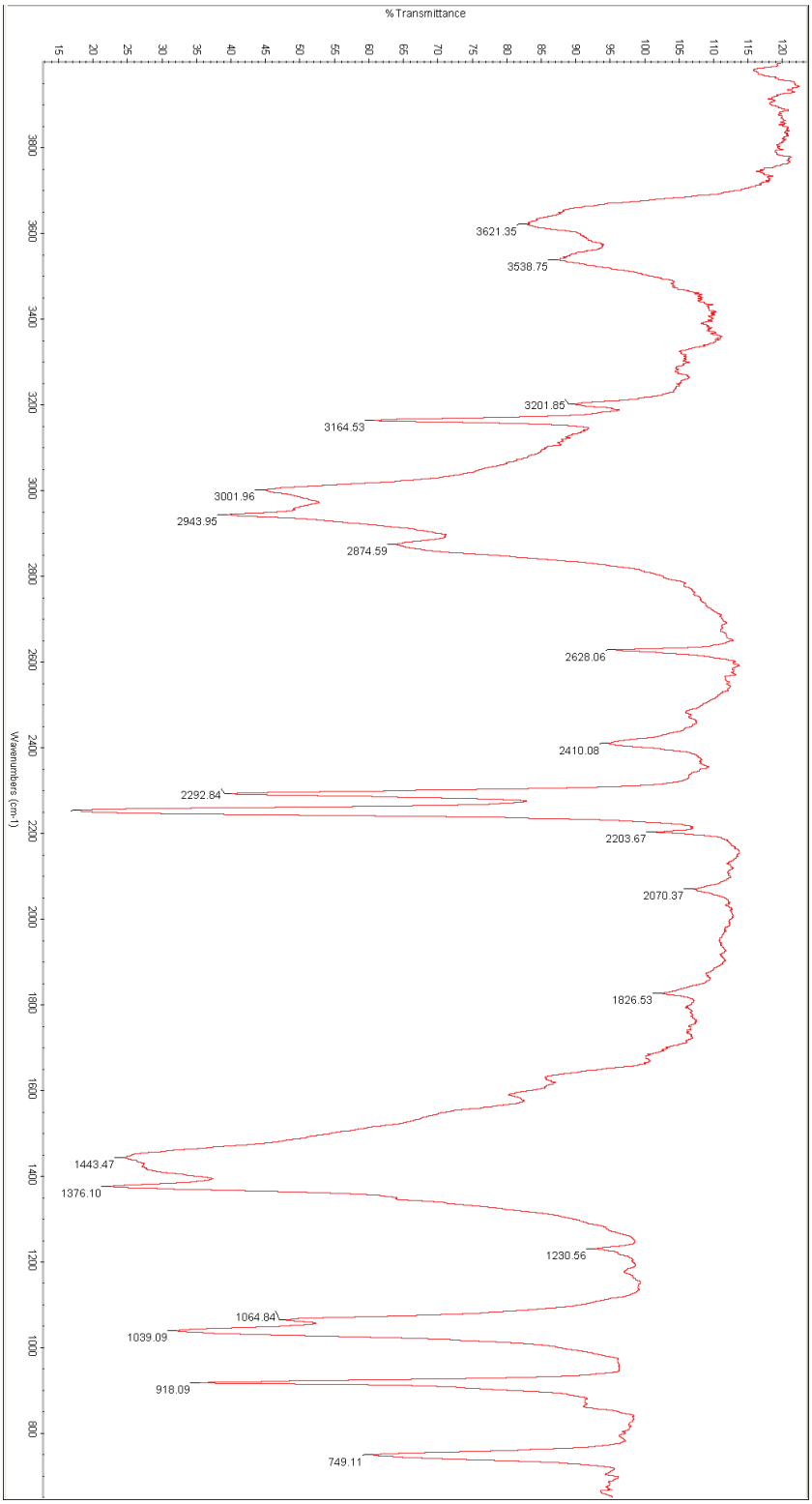

Figure 34: IR spectrum of $IMesCO_2$ in a solution of MeCN reacted with $LiBH_4$.

Formaldehyde and formate are seen in the ^{1}H NMR at 9.6 and 8.1 ppm respectively. There is a peak at 8.5 ppm that is new and the peak at 5.6 ppm is again present. The peak at 8.5 integrates to 0.21 and the peak 5.6 ppm integrated to the 0.7 which is not enough hydrogens for the olefin. The peak at 7.2 ppm is in a better position and integrates to 1.7 which makes it the olefin peak on IMes. The peak is closer to the measured value of the olefin is 7.0 ppm, but the aromatic hydrogens are missing and H2 on C2. There is a peak at 3.2 ppm that is a peak for methanol, yet the peak at 2.2 ppm may be behind the solvent peak. The ^{13}C spectrum helps, showing all the peaks for IMes, but the CO_2 carbon is gone. Instead there is a peak at 54.9 ppm, but the peak should be closer to 49.9 ppm to be methanol. There are no carbon peaks verifying formate and formaldehyde. Shown in Figure 35 and 36.

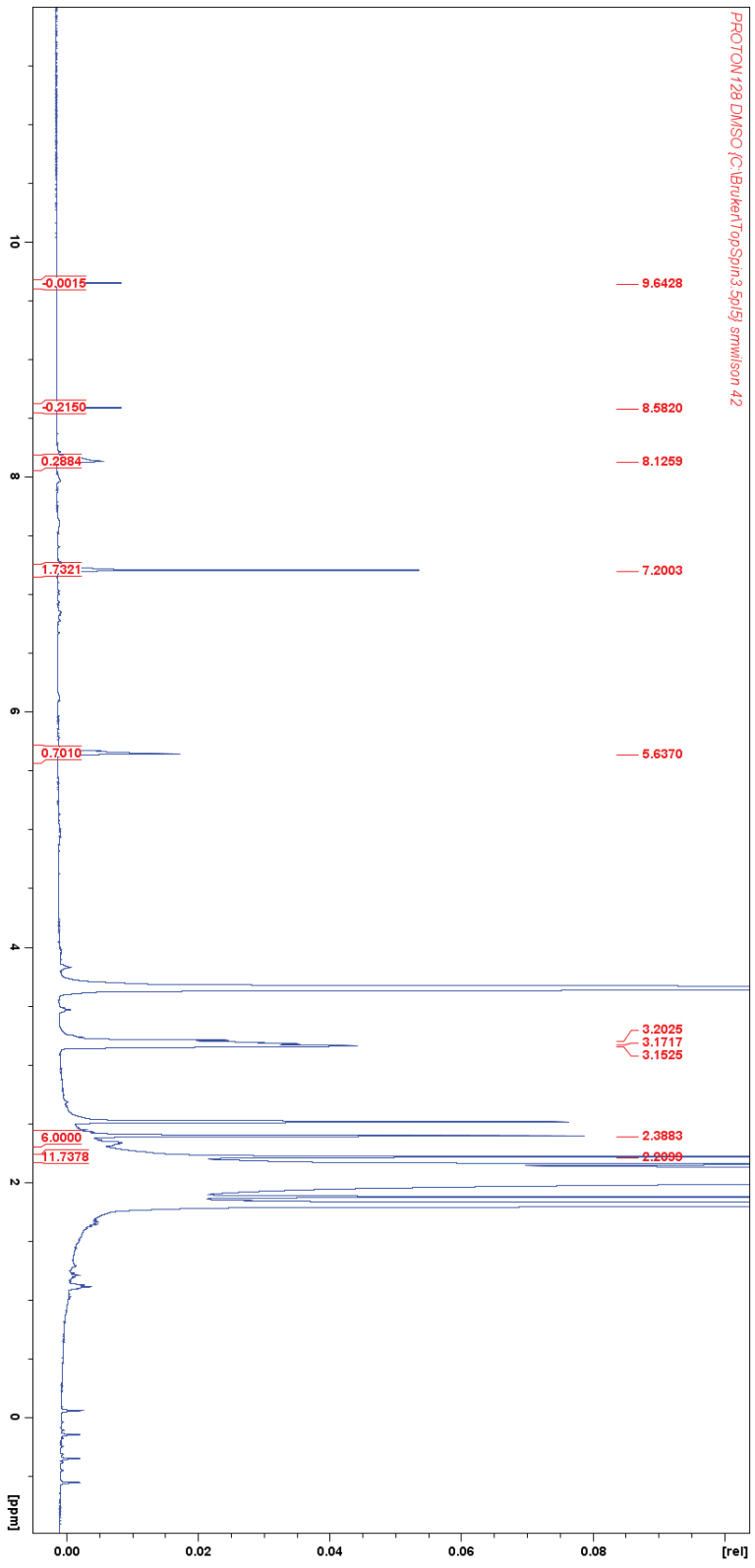

Figure 35: ^{1}H NMR of IMesCO$_2$ in a solution of MeCN reacted with LiBH$_4$ (NMR solvent DMSO).

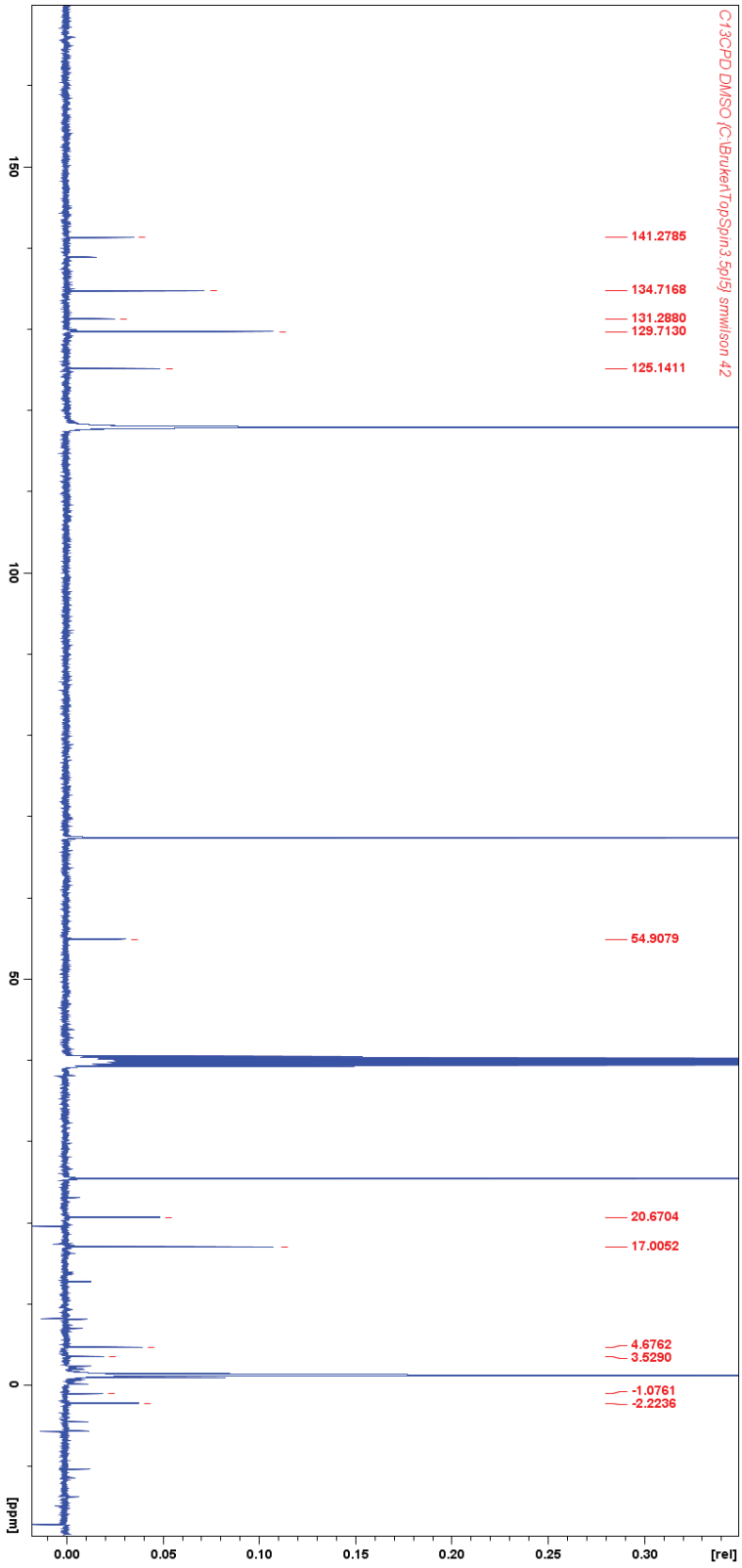

Figure 36: ^{13}C NMR of $IMesCO_2$ in a solution of MeCN reacted with $LiBH_4$ (NMR solvent DMSO).

The NMR spectra from the reaction done in acetonitrile are comparable to the reaction done in DMSO. There are still peaks at 9.6 and 8.2 ppm that correspond to formaldehyde and formate in the ^{1}H NMR spectrum. There is also the 5.75 ppm peak that is unexpected but has been seen before. The signature for IMes can be found in the spectrum, yet the C2 carbon does not have a proton. The ^{13}C NMR spectrum again verifies the presence of IMes. The peak at 55.9 ppm is present as well, but does not fit IMes, products, or solvent. There are two peaks in the 160-170 ppm range in the ^{13}C NMR spectrum. The peak around 162 ppm could be formate carbon, so formate is most likely in this mixture. However, formaldehyde carbon is not present in the spectrum. Displayed in Figure 37 and 38.

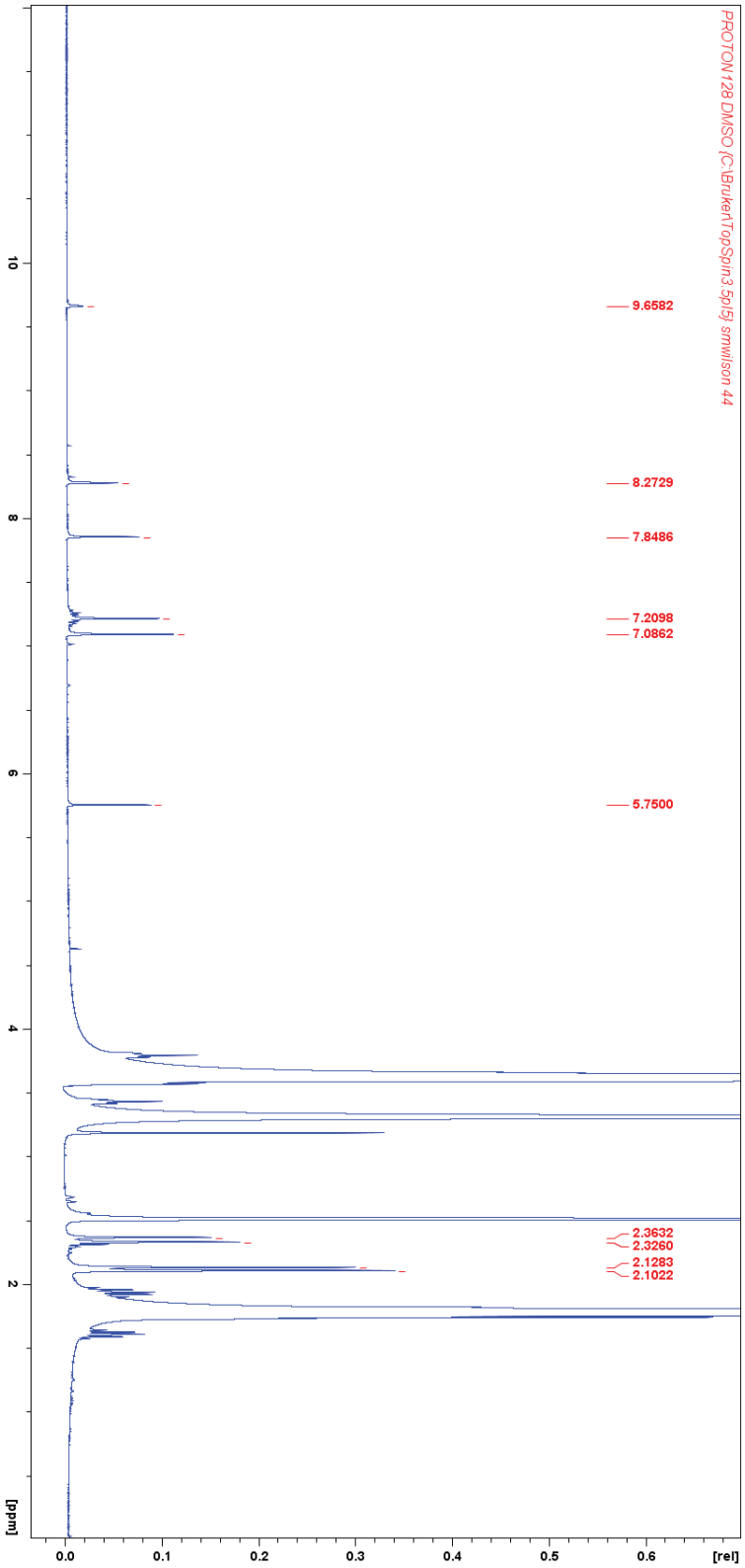

Figure 37: ^{1}H NMR spectrum of IMesCO$_2$ in a solution of d-DMSO reacted with LiBH$_4$.

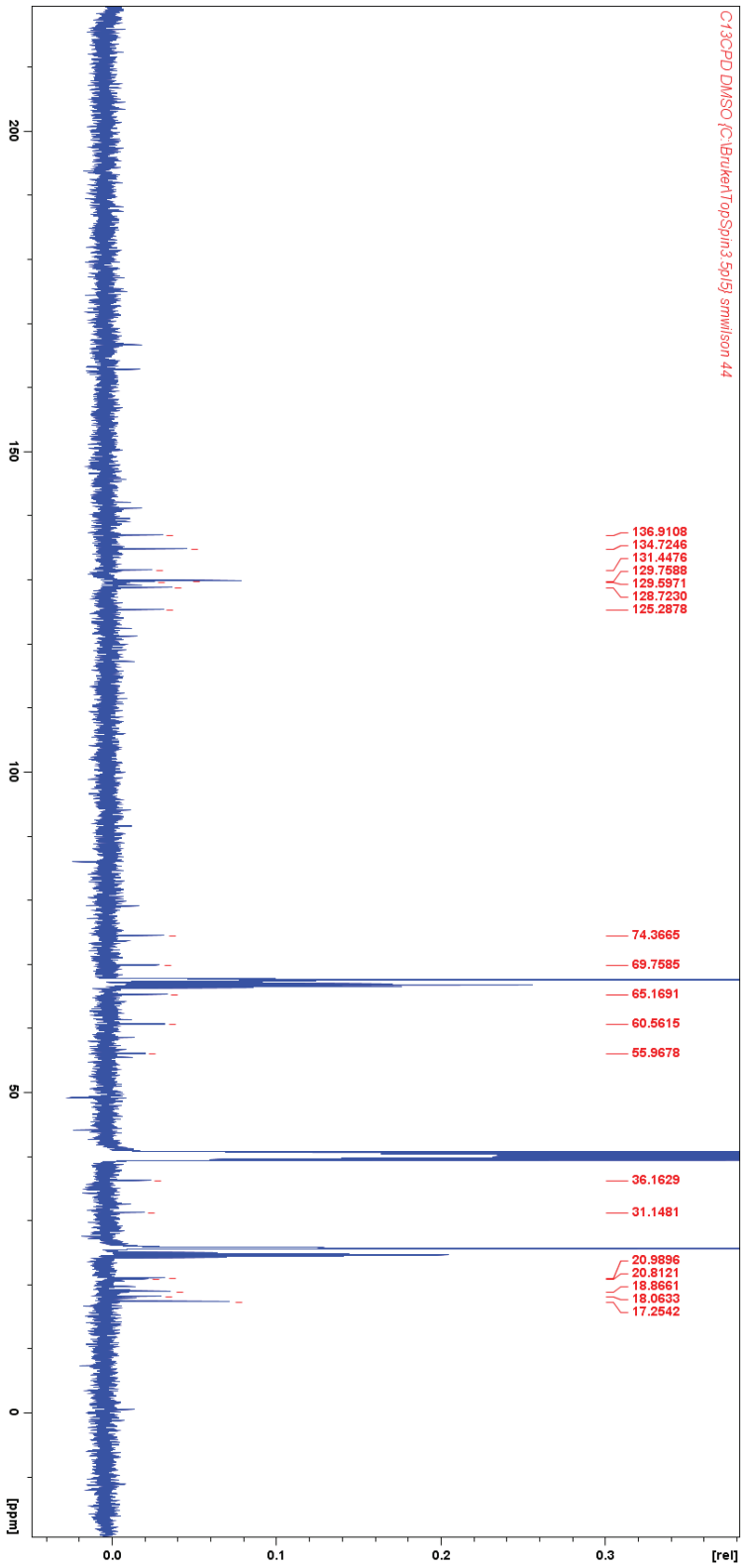

Figure 38: ^{13}C NMR spectrum of $IMesCO_2$ in a solution of d-DMSO reacted with $LiBH_4$.

Reaction with Sodium Borohydride:

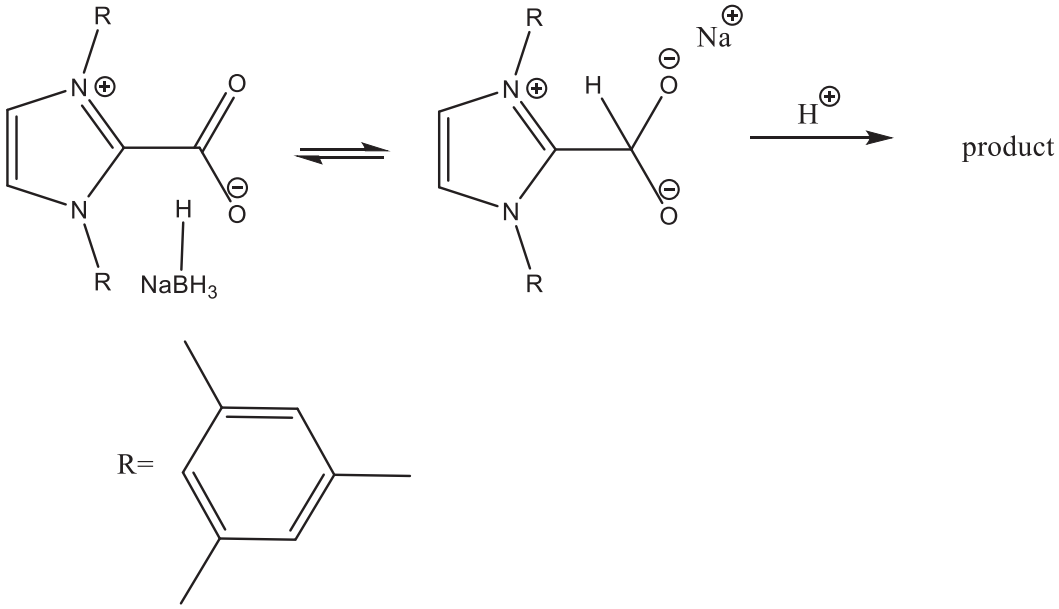

Diagram 16: Mechanism of $LiBH_4$ reacting with $IMesCO_2$.

This IR spectrum for the reaction with $NaBH_4$ is nearly identical to the spectrum from the $LiBH_4$ experiment in the same reaction solvent in Figure 36. The peaks differ by single wavenumbers. There is the presence of a peak at 1677 cm^{-1} that could be formaldehyde and a broad absorption at 3002- 2873 cm^{-1} for the C-H aromatic from IMes stretch. Displayed in Figure 39.

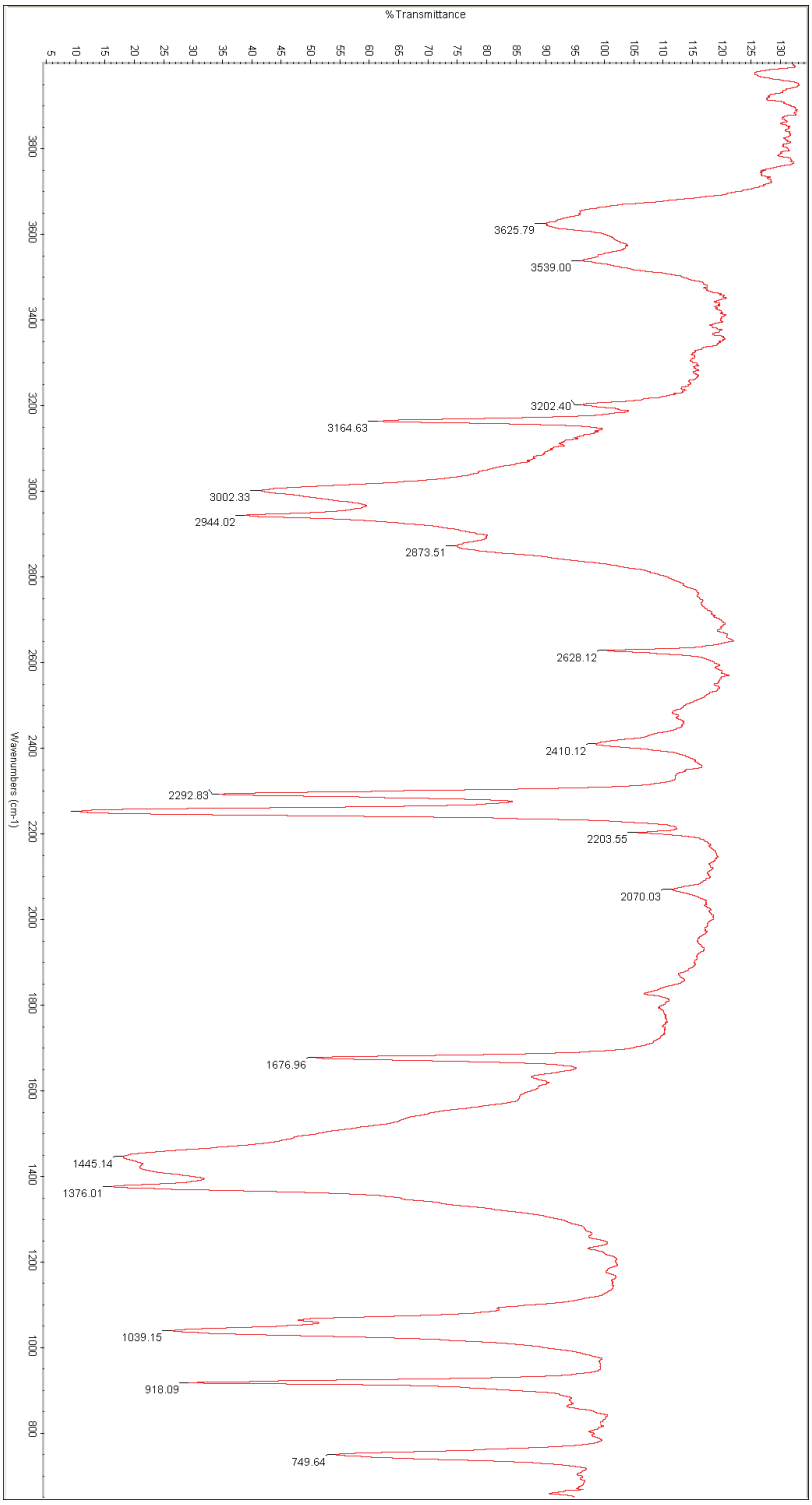

Figure 39: IR spectrum of $IMesCO_2$ in a solution of MeCN reacted with $NaBH_4$.

Formate is present in these reaction conditions. The ^{1}H NMR spectrum in Figure 40 shows a peak at 8.3 ppm that could be formate, but there is no peak above 10 ppm showing the acidic hydrogen on formic acid. Formaldehyde has a peak at 9.65 ppm. As for methanol, there are peaks at 4.6 ppm and near 3 ppm, and in DMSO methanol should appear at 3.17 and 4.10 ppm. The peaks areas near 3 ppm should not be larger than the peak areas for the mesityl methyl groups. Furthermore, the 4.6 ppm shift is higher than the expected 4.1 ppm for the alcohol. The peak at 7.9 ppm is large than expected. It is possible that the aromatic hydrogen peak is overlapping with an imidazole ring fragment peak and increasing the size of the overall found in the spectrum peak. IMes peaks are present, as well a few peaks below 0 ppm from unreacted hydride. The ^{13}C NMR supports formate with a peak at 161.9 ppm. Methanol and formaldehyde are not confirmed by the spectrum. Shown in Figure 40 and 41.

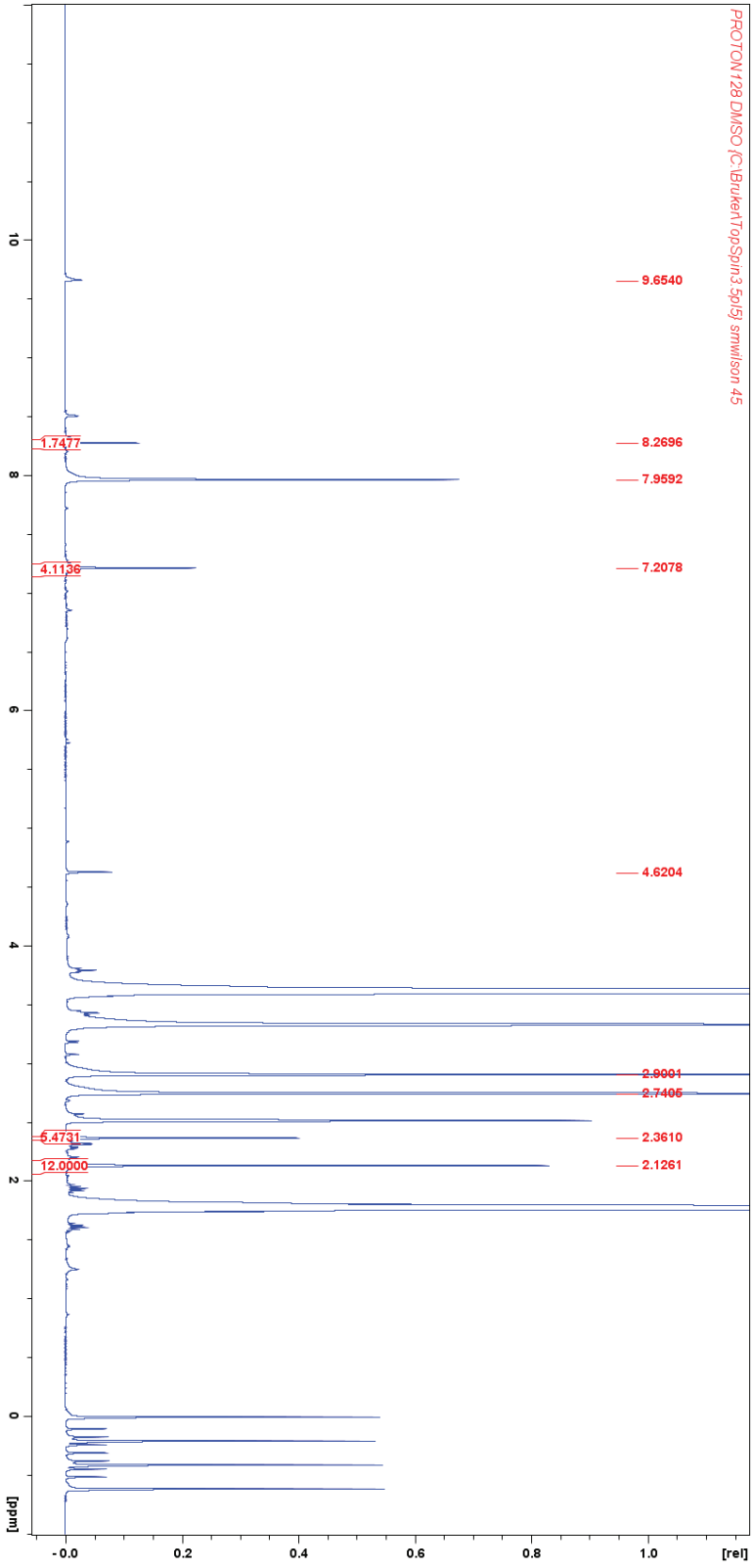

Figure 40: ^{1}H NMR spectrum of $IMesCO_2$ in a solution of DMSO reacted with $NaBH_4$.

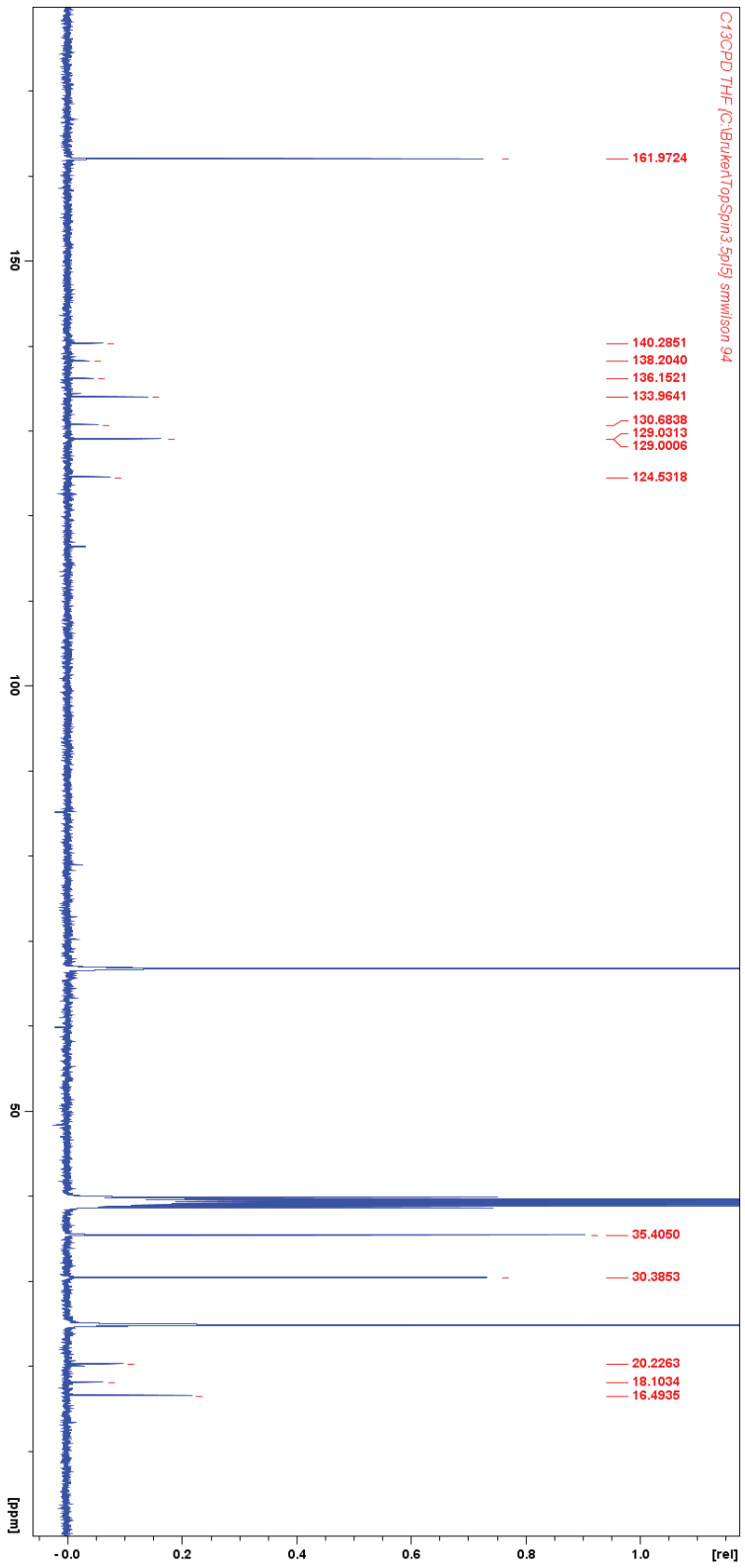

Figure 41: ^{13}C NMR spectrum of $IMesCO_2$ in a solution of DMSO reacted with $NaBH_4$.

Additive:

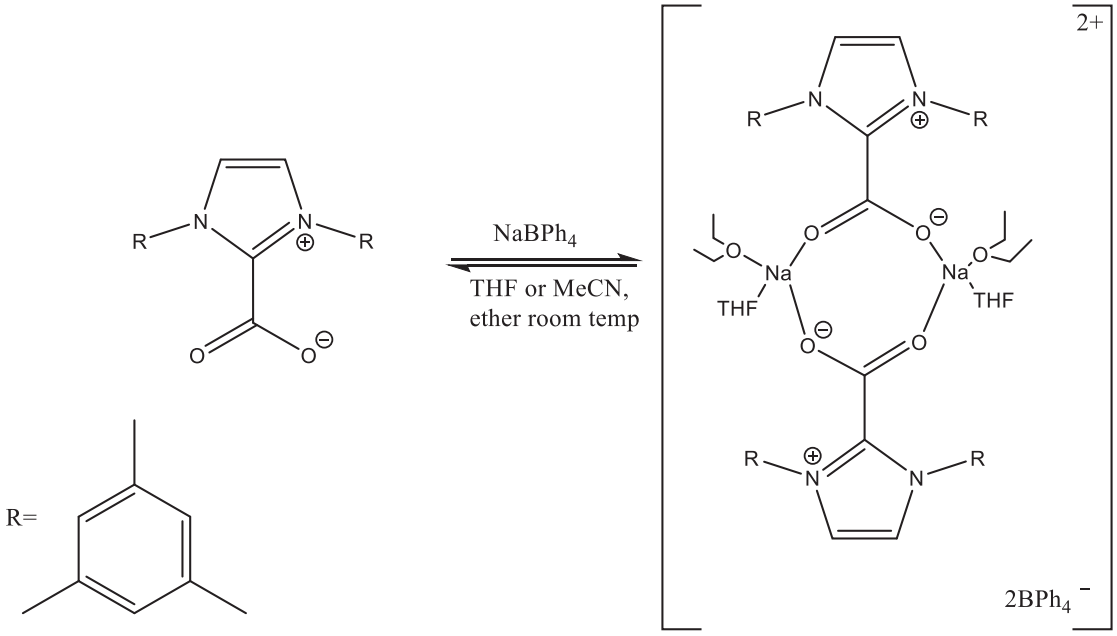

Diagram 17: $IMesCO_2$ additive reaction to form $[(IMesCO_2Na)_2]^{2+}$ $2[BPh_4]^{2-}$ (complex 1).

To help with solubility issues with the limited number of compatible solvents, sodium tetraphenyl borate ($NaBPh_4$) was added to the $IMesCO_2$ to form complex 1, to enable it to be more soluble in ethers, as shown in Diagram 20. $IMesCO_2$ was weighed out in the amount of 48 mg into a vial and dissolved in 5 mL of dry THF or MeCN. In another vial, 50.8 mg of $NaBPh_4$ was weighed out and dissolved in 5 mL of THF. The $IMesCO_2$ solution was added to the $NaBPh_4$ solution, and 5 mL of diethyl ether was added to the solution. The solution sat overnight to allow for diffusion into the ether layer. NMR spectra were taken at this step, then a hydride was added to the solution, then again NMR spectra were taken. Then 0.1 mL of the 0.1 M hydride was added to the solution, and the reaction ran overnight. More NMR spectra were taken. Reagent amounts are in the Tables 9 and 10 below [37].

THF as solvent for $IMesCO_2$.

Table 6: Mass of $IMesCO_2$ and $NaBPH_4$ in a solution of THF.

Hydride (mL)	$LiAlH_4$, 0.1	$LiBH_4$, 0.1	$NaBH_4$, 0.1
$NaBPh_4$ (mg)	50.8	50.7	51.2
$IMesCO_2$ (mg)	48.0	49.7	48.5

MeCN as solvent for $IMesCO_2$.

Table 7: Mass of $IMesCO_2$ and $NaBPh_4$ in a solution of MeCN.

Hydride (mL)	$LiBH_4$ 0.1	$NaBH4_4$ 0.1
$NaBPh_4$ (mg)	50.2	50.5
$IMesCO_2$ (mg)	48.0	50.9

Literature values for $[(IMesCO_2Na)_2]^{2+}$ $2[BPh_4]^{2-}$ in THF ^{1}H NMR: 7.26 multi 8H, 7.07 single 2H, 7.02 single 4H, 6.81 triple 8H, 6.67 triple 4H, 3.61 multi 6H, 3.39 quad 0.8H, 2.32 single 6H, 2.09 single 12H, 1.77 multi 6H, 1.18 triple 1.2H. ^{13}C NMR: 169.6, 165.5, 165.1, 164.7, 164.4, 156.2, 145.9, 142.1, 141.2, 136.9, 135.7, 134.9, 132.6, 131.6, 130.4, 129.7, 126.04, 125.5, 125.4, 122.9, 121.7, 121.5, 68.0, 26.2, 20.9, 20.8, 17.4, 17.2 [37].

Measured values (400 MHz *d*-THF) for $[(IMesCO_2Na)_2]^{2+}$ $2[BPh_4]^{2-}$ in THF ^{1}H NMR: δ 7.20 single, 7.06 single, 6.71 (triple J=4.4 Hz), 6.59 (triple J=4.0 Hz), 3.59 multi, 3.16 (doublet doublet J= 3.84, 10.8 Hz), 2.32 single, 1.93 single, 1.55 multi, 1.22 (triple J= 6.96 Hz), 0.90 (triple J= 6.96 Hz). Shown in Figure 42. ^{13}C NMR: δ 163.1, 162.1, 161.6, 139.5, 135.0, 134.8, 132.3, 128.9, 127.7, 123.3, 122.93, 122.9, 122.88, 122.84, 118.99, 76.8, 74.9, 72.2, 70.4, 68.8, 61.9, 59.99, 58.4, 56.5, 53.8, 51.9, 23.4, 18.6, 17.7, 16.3, 14.6, 10.9 ppm. Shown in Figure 43.

Comparing literature ^{1}H NMR values of the complex $[(IMesCO_2Na)_2]^{2+}$ $2[BPh_4]^{2-}$ to the measured values, there are some differences. The measured values show multiplet peaks at 1.55 ppm and a triplet at 0.90 ppm; these peaks are probably alkyl

contaminants. The other peaks are all accounted for when referencing the literature values. The ^{13}C NMR spectrum has several differences. The measured data has 32 peaks compared to the literature's 28 peaks. The literature spectrum shows peaks at 156 ppm and in the 140 ppm range, but these peaks are not present in the measured values. Also, there are peaks in the 70 and 50 ppm range that were measured but are not in the literature. The peak farthest downfield was 163.1 ppm; the literature value is 169.6 ppm. The peaks furthest upfield were 16.3, 14.6, and 10.9 ppm, but the literature has a peak only as low as 17.2 ppm. There are 3 peaks in the 20 ppm range in the literature spectrum, while there is only one peak in that range for this experiment. The ^{13}C NMR spectrum is not as informative as the ^{1}H spectrum. Complex 1 is not verified, but the solubility of the $IMesCO_2$ did improve in THF and acetonitrile, just as it was mentioned in the literature by Louie *et al.,* so the mixture was still treated with the hydrides. Shown in Figure 42 and 43.

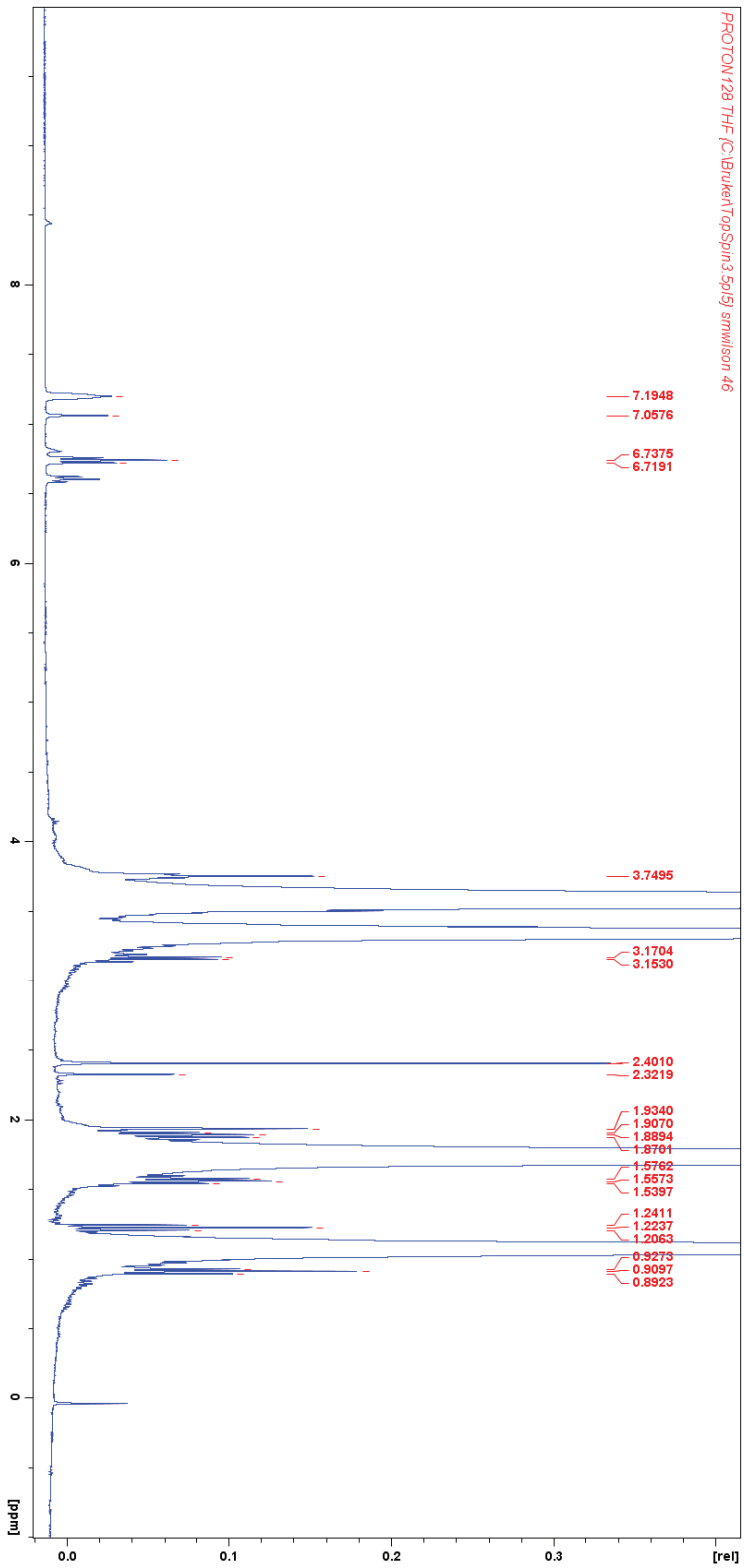

Figure 42: ^{1}H NMR spectrum of $NaBPh_4$ additive complexed with $IMesCO_2$ in a solution of THF.

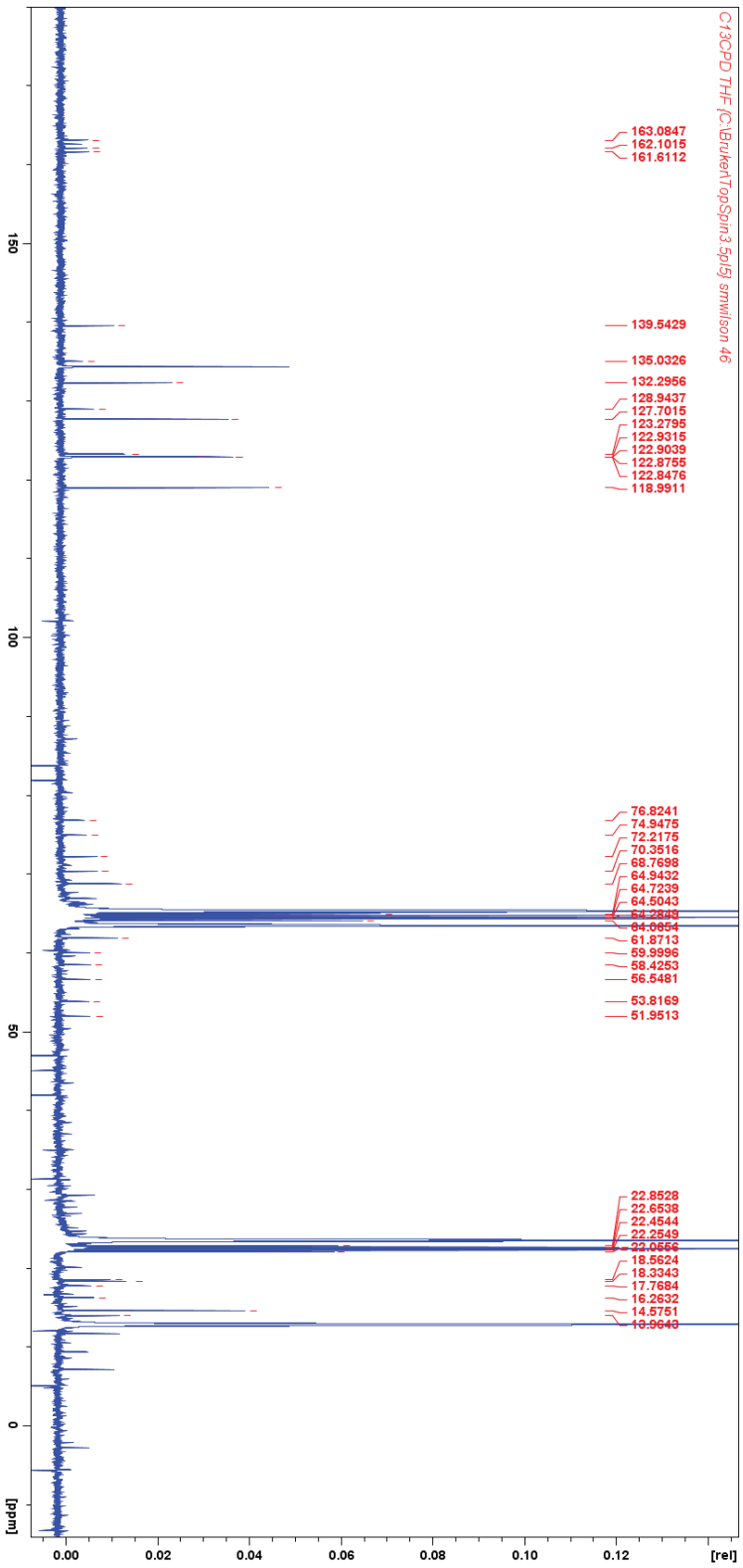

Figure 43: ^{13}C NMR spectrum of $NaBPh_4$ complexed with $IMesCO_2$ in a solution of THF.

Reactions with the Hydrides:

There is evidence of a peak in the ^{1}H NMR for formate at 8.6 ppm. All of the same peaks are present for the complex, including the extra contamination peaks. The ^{13}C NMR shows peaks above 160 ppm; however, there are three of them. The measured ^{13}C NMR spectrum for complex 1 had peaks at 163.1, 162.1, and 161.6 ppm and formate has a ^{13}C NMR peak in the range of 179-160 ppm, so formate may be present in the mixture. The other measured peaks for complex 1 are still present. Shown in Figure 44, 45. General reaction shown in Diagram 21.

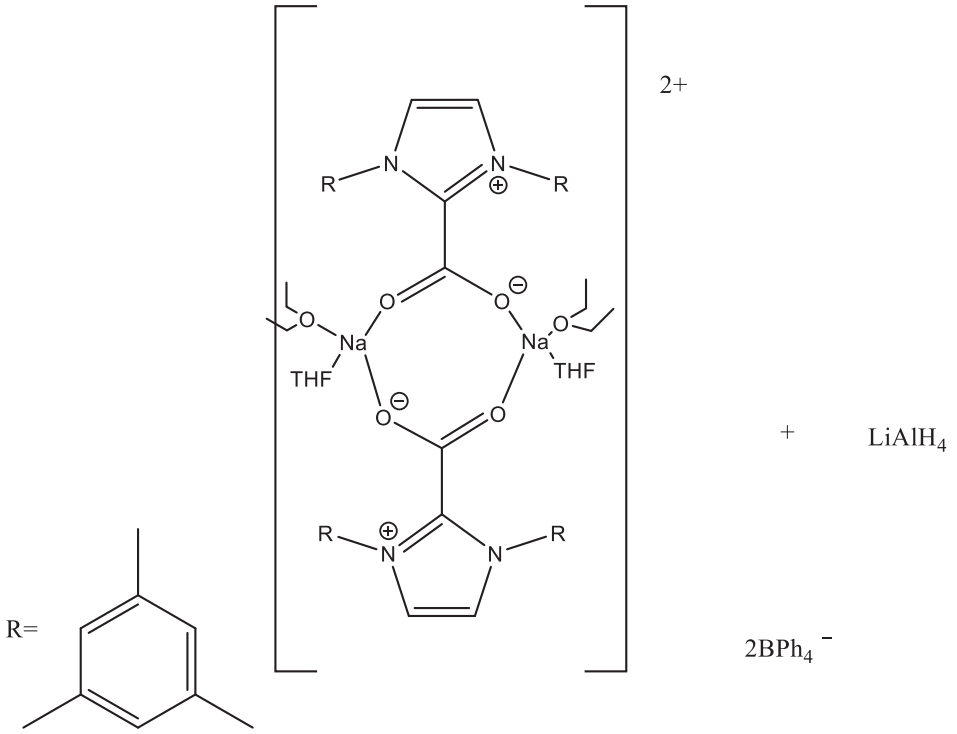

Diagram 18: $[(IMesCO_2Na)_2]^{2+}$ $2[BPh_4]^{2-}$, complex 1, for treatment with $LiAlH_4$.

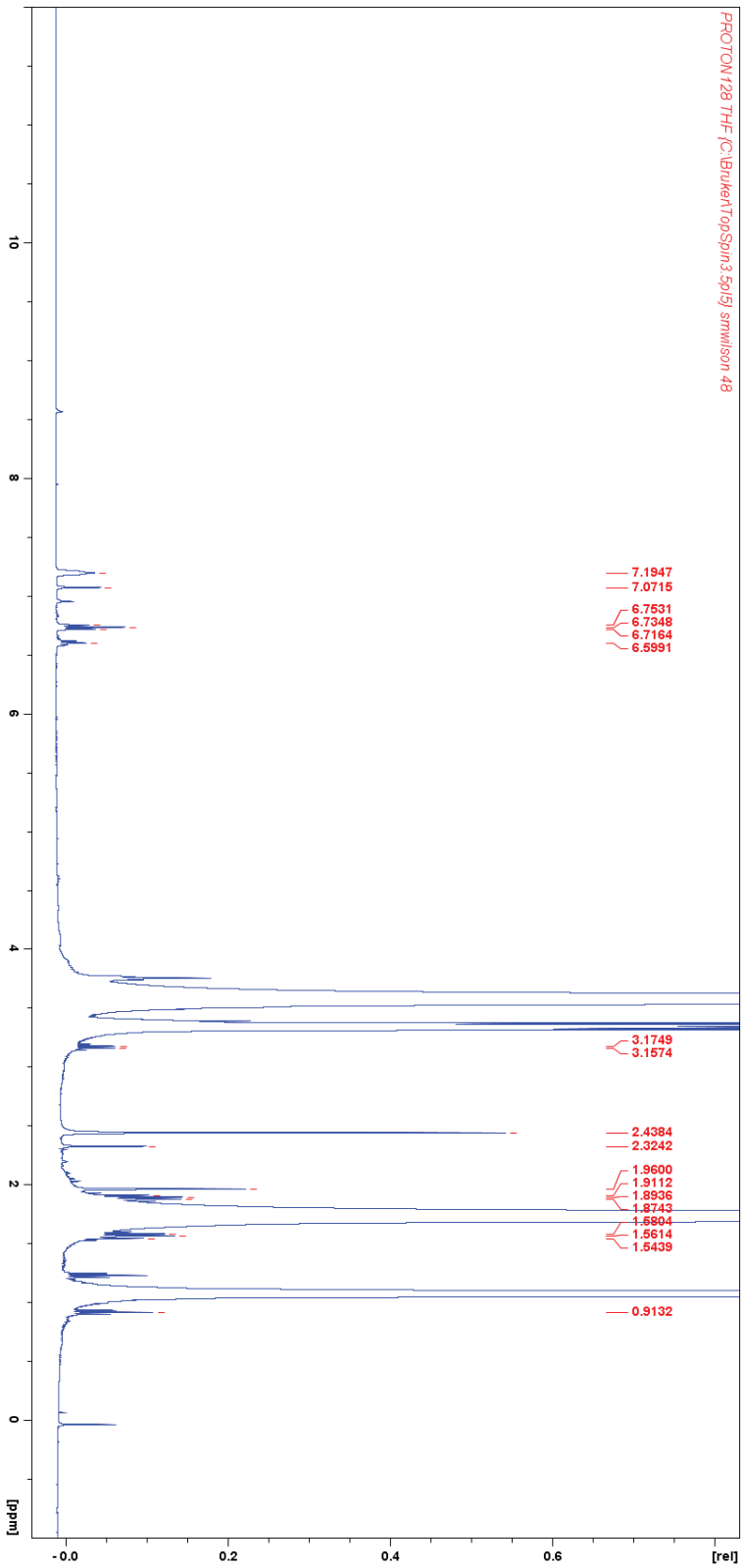

Figure 44: ^{1}H NMR spectrum of IMesCO$_2$ additive reaction in a solution of THF with LiAlH$_4$.

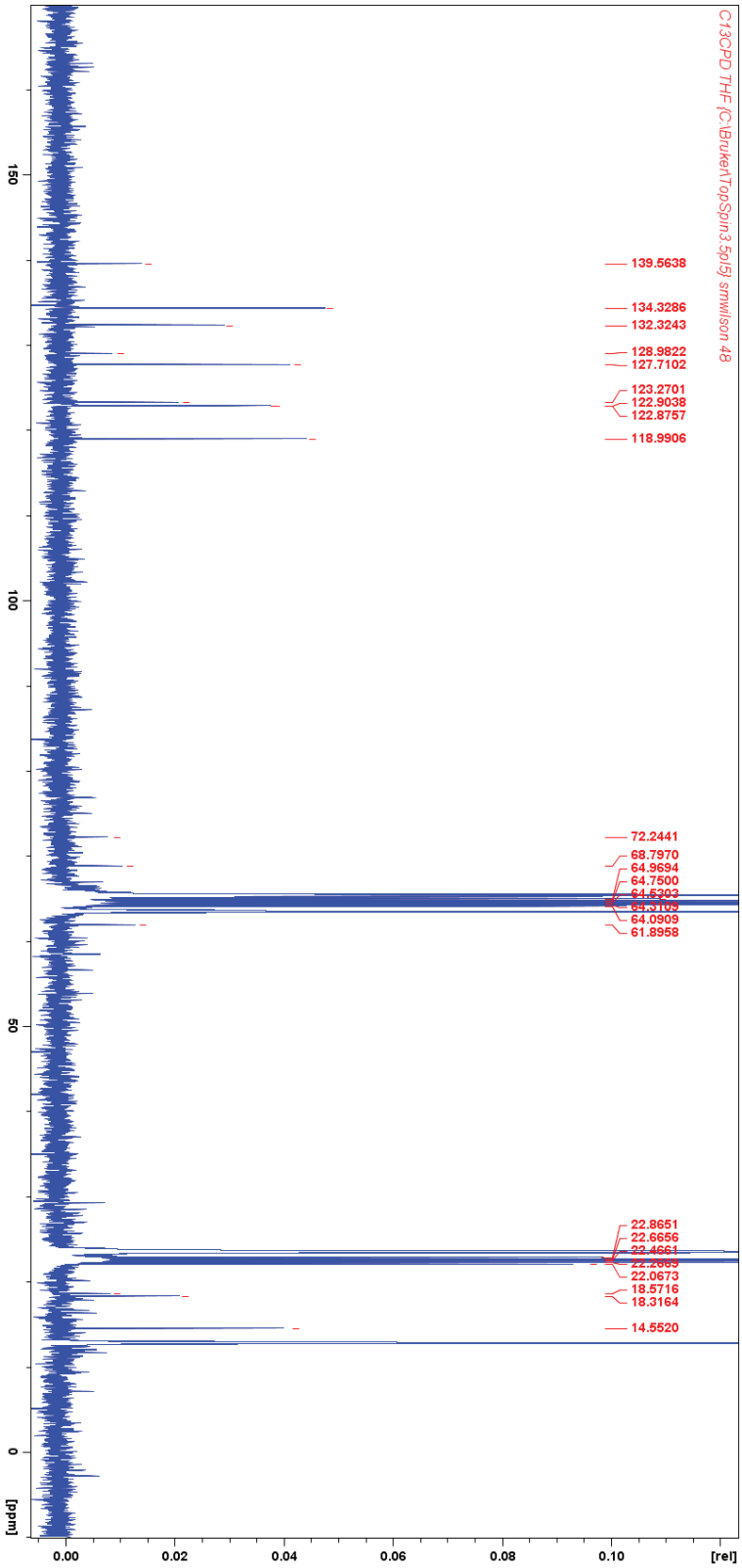

Figure 45: ^{13}C NMR spectrum of $IMesCO_2$ additive reaction in a solution of THF with $LiAlH_4$.

Again, there is a peak for formate in the ^{1}H NMR spectrum. However, there is an observed peak at 5.58 ppm, which is not one of the anticipated products. All the other peaks are still accounted for by the additive complex 1. The ^{13}C NMR still shows the same peaks for the complex, but the three peaks in the 160 ppm range are not pronounced. One of these peaks may be formate. Shown in Figure 46 and 47. General reaction shown in Diagram 22

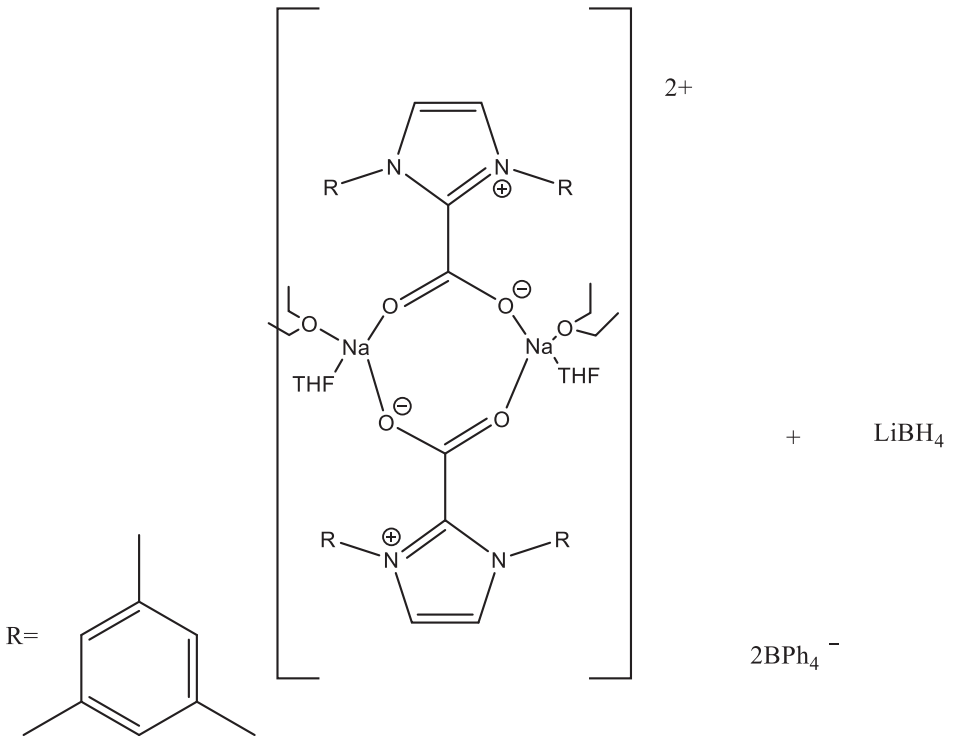

Diagram 19: $[(IMesCO_2Na)_2]^{2+}$ $2[BPh_4]^{2-}$, complex 1, for treatment with $LiBH_4$.

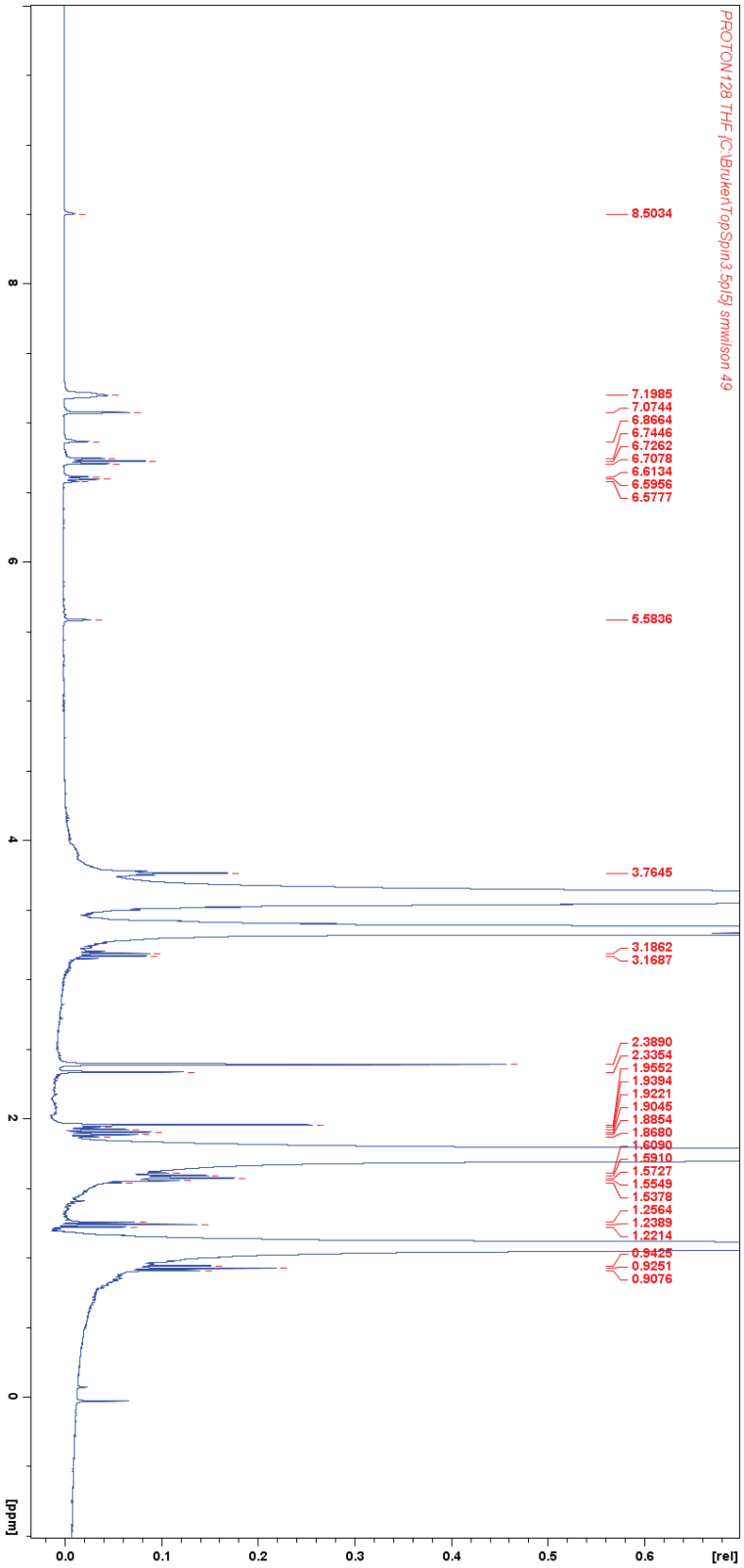

Figure 46: ^{1}H NMR spectrum of IMesCO$_2$ additive reaction in a solution of THF with LiBH$_4$.

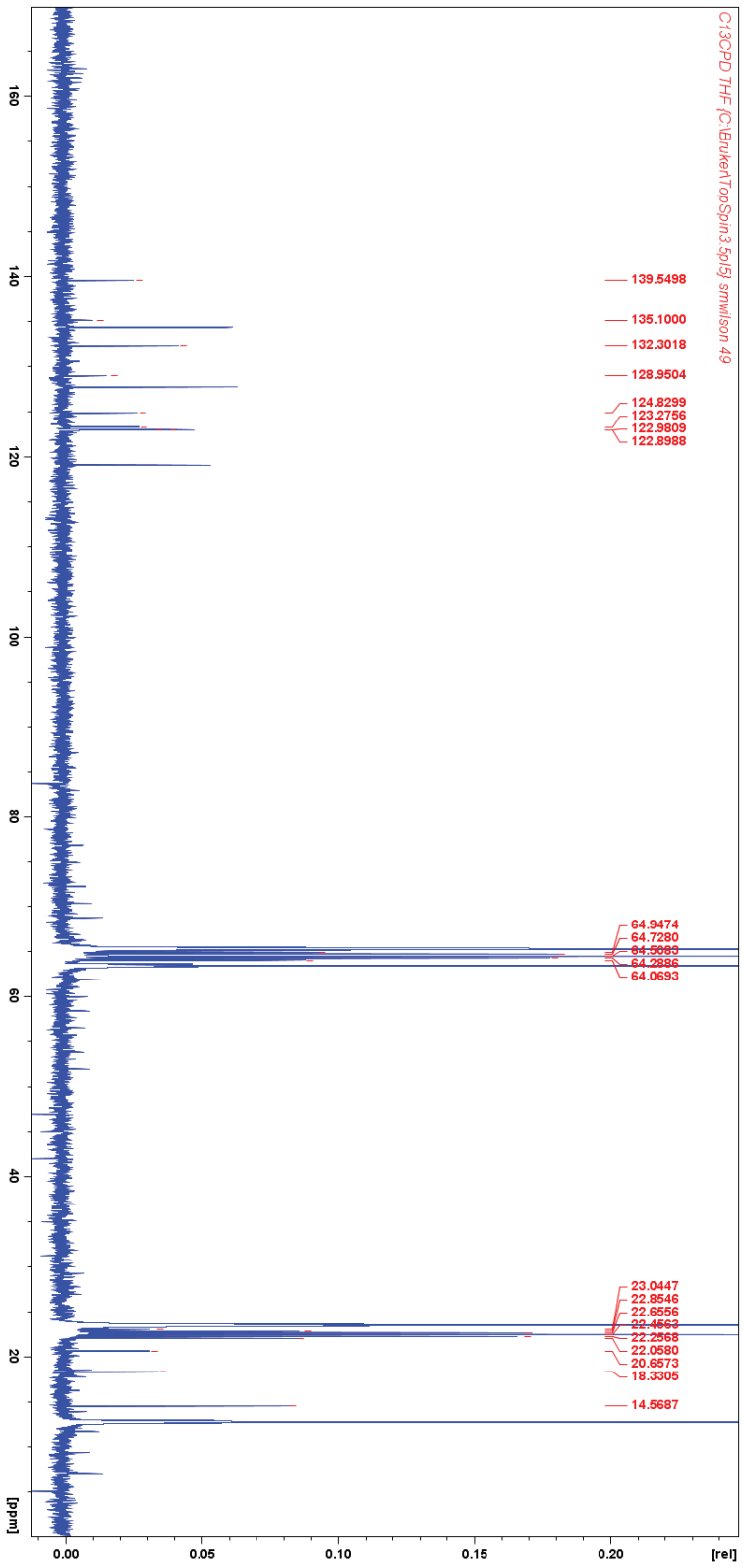

Figure 47: ^{13}C NMR spectrum of $IMesCO_2$ additive reaction in a solution of THF with $LiBH_4$.

The procedure can be done in THF or MeCN as reaction solvent to form the complex. This procedure was done in acetonitrile as the reaction solvent. There was an improvement in solubility in this case as well. The ^{1}H NMR spectrum shows peaks for the complex that agree with the literature values. The peak at 3.6 ppm is overcome by a solvent peak, but all the other peaks are accounted for. There are peaks at 9.5 that is formaldehyde, 8.0 that is formate, and 5.51 ppm. This peak at 5.51 ppm does not belong to either complex 1 or anticipated products. The ^{13}C NMR spectrum contains considerably fewer peaks than before; many of the peaks that belong to complex 1 are missing. The spectrum has 10 peaks that could belong to complex 1, but there should be 29 peaks in the ^{13}C spectrum. There are no carbon peaks for any products in the spectrum. This was not a successful trial. Shown in Figure 48, and 49.

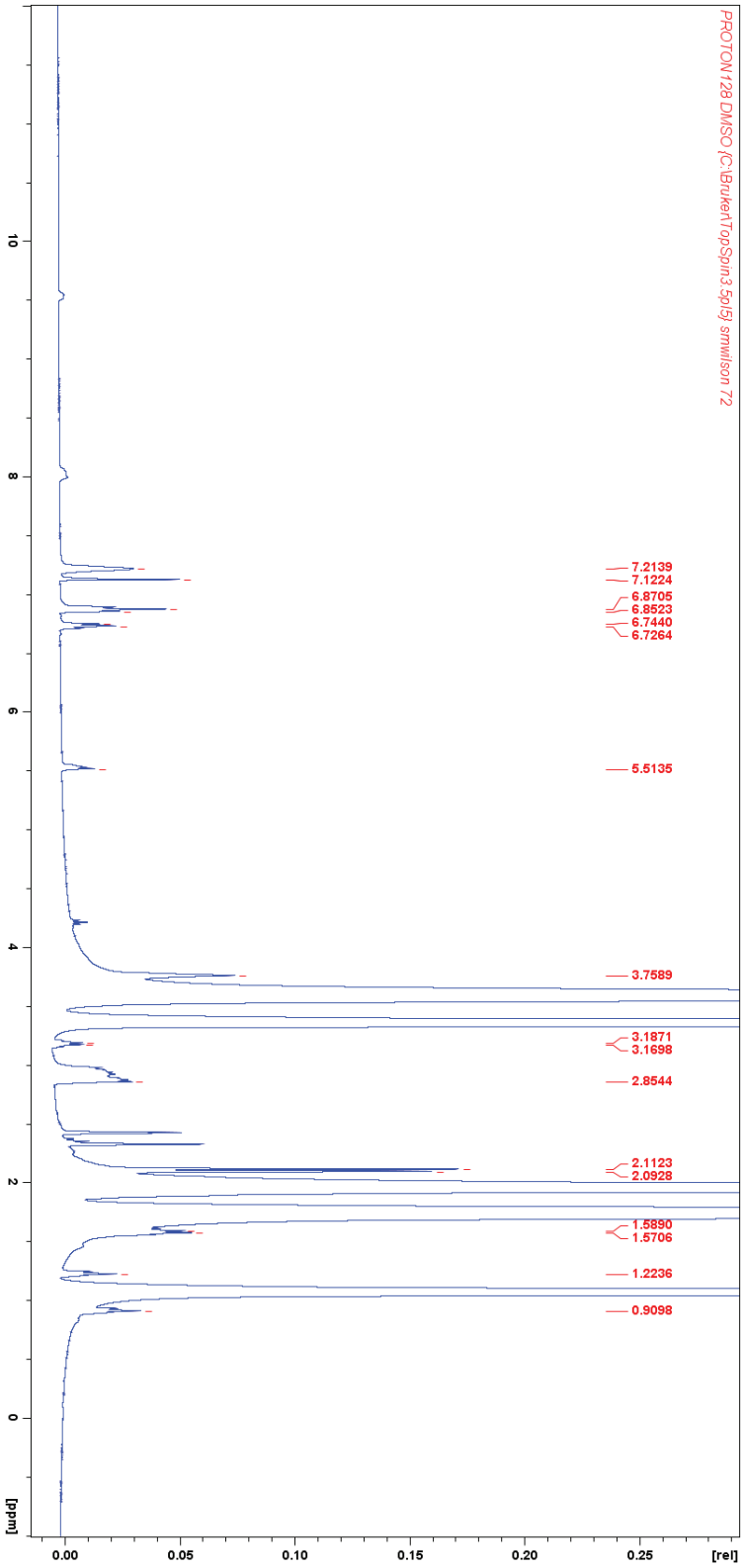

Figure 48: ^{1}H NMR spectrum of IMesCO$_2$ additive reaction in a solution of MeCN with LiBH$_4$.

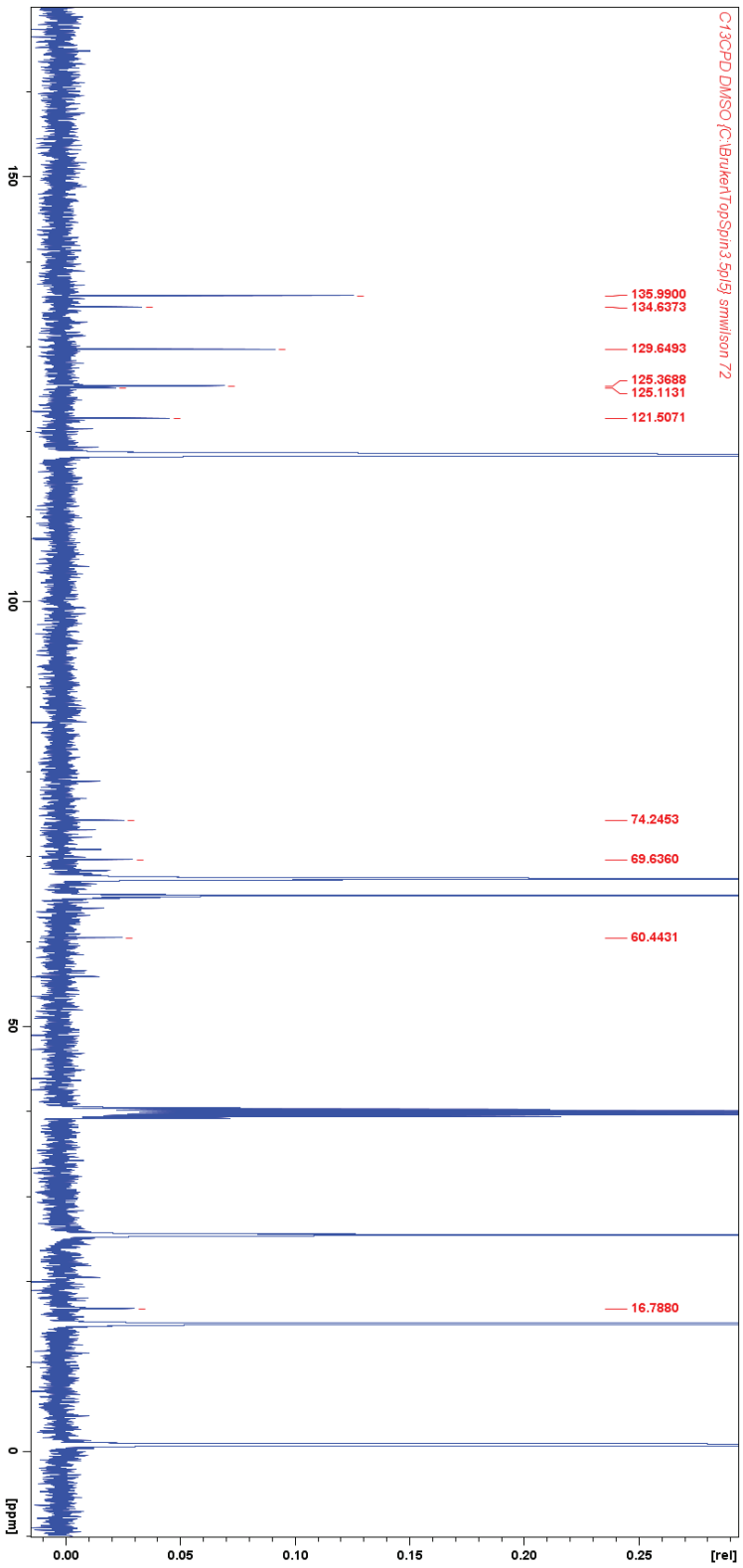

Figure 49: ^{13}C NMR spectrum of $IMesCO_2$ additive reaction in a solution of MeCN with $LiBH_4$.

The presence of complex 1 is confirmed by the ^{1}H NMR spectrum; other than the peak at 5.47 ppm, the peaks agree with the literature values. The 5.47 ppm peak is not from an anticipated product but has been present for most of the hydride reactions. The ^{13}C NMR spectrum again shows a lack of transitions. There are only 14 peaks, which is only half the number of peaks listed for complex 1. Also, there are no carbon peaks for and CO_2 reduction products present in the spectrum. This was once again not a successful trial. Shown in Figures 50 and 51. General reaction shown in Diagram 23

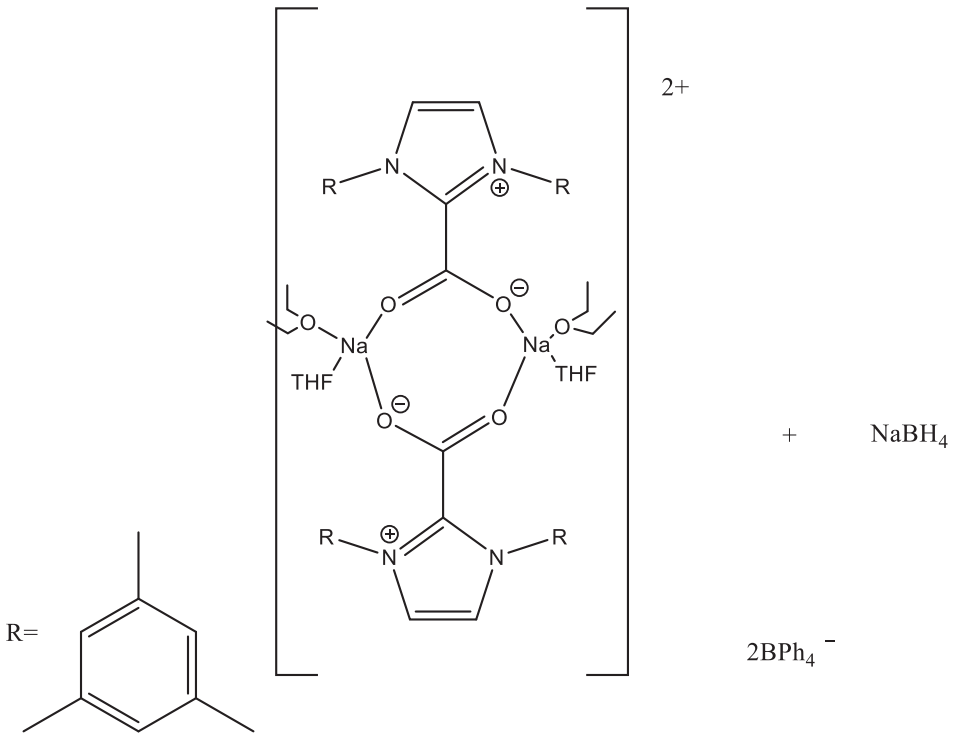

Diagram 20: $[(IMesCO_2Na)_2]^{2+}$ $2[BPh_4]^{2-}$, complex 1, for treatment with $NaBH_4$.

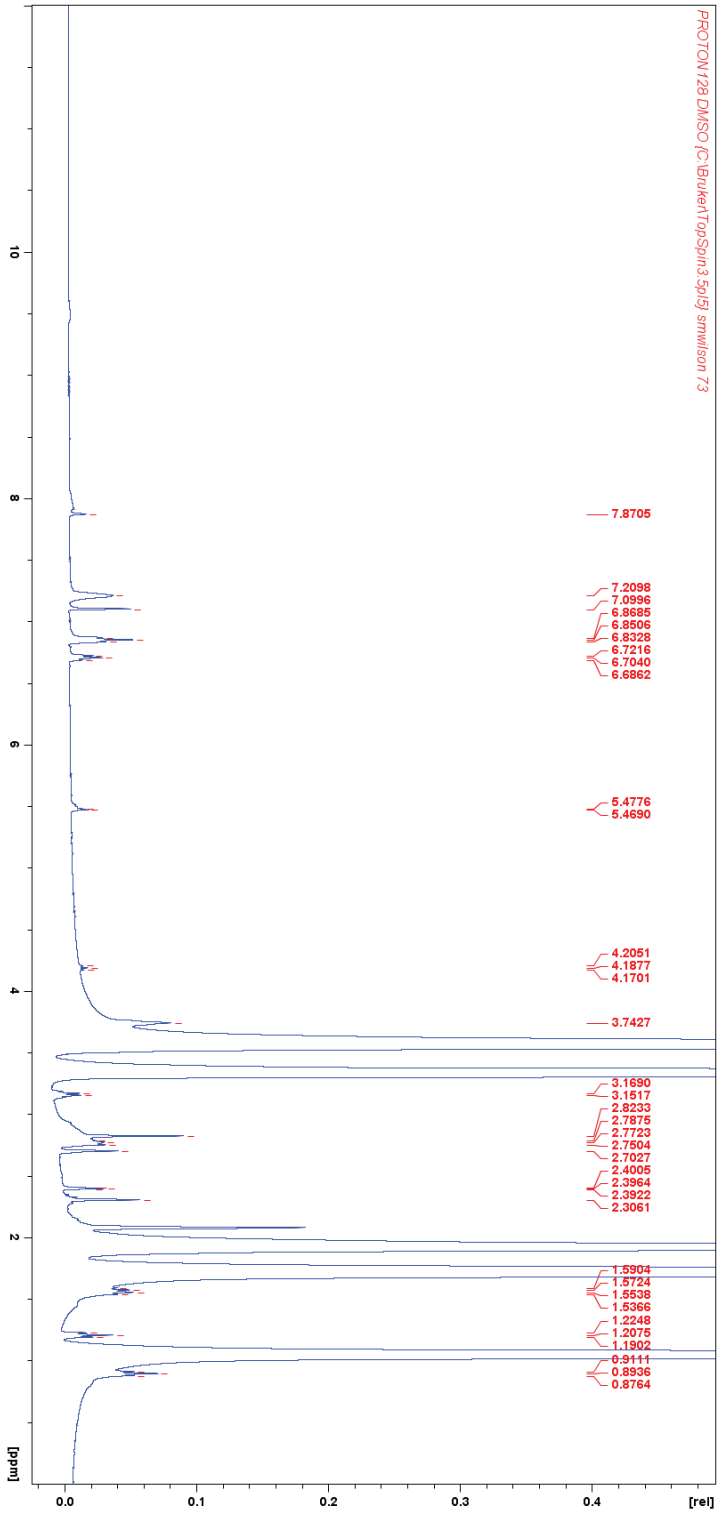

Figure 50: ^{1}H NMR spectrum of IMesCO$_2$ additive reaction in a solution of MeCN with NaBH$_4$.

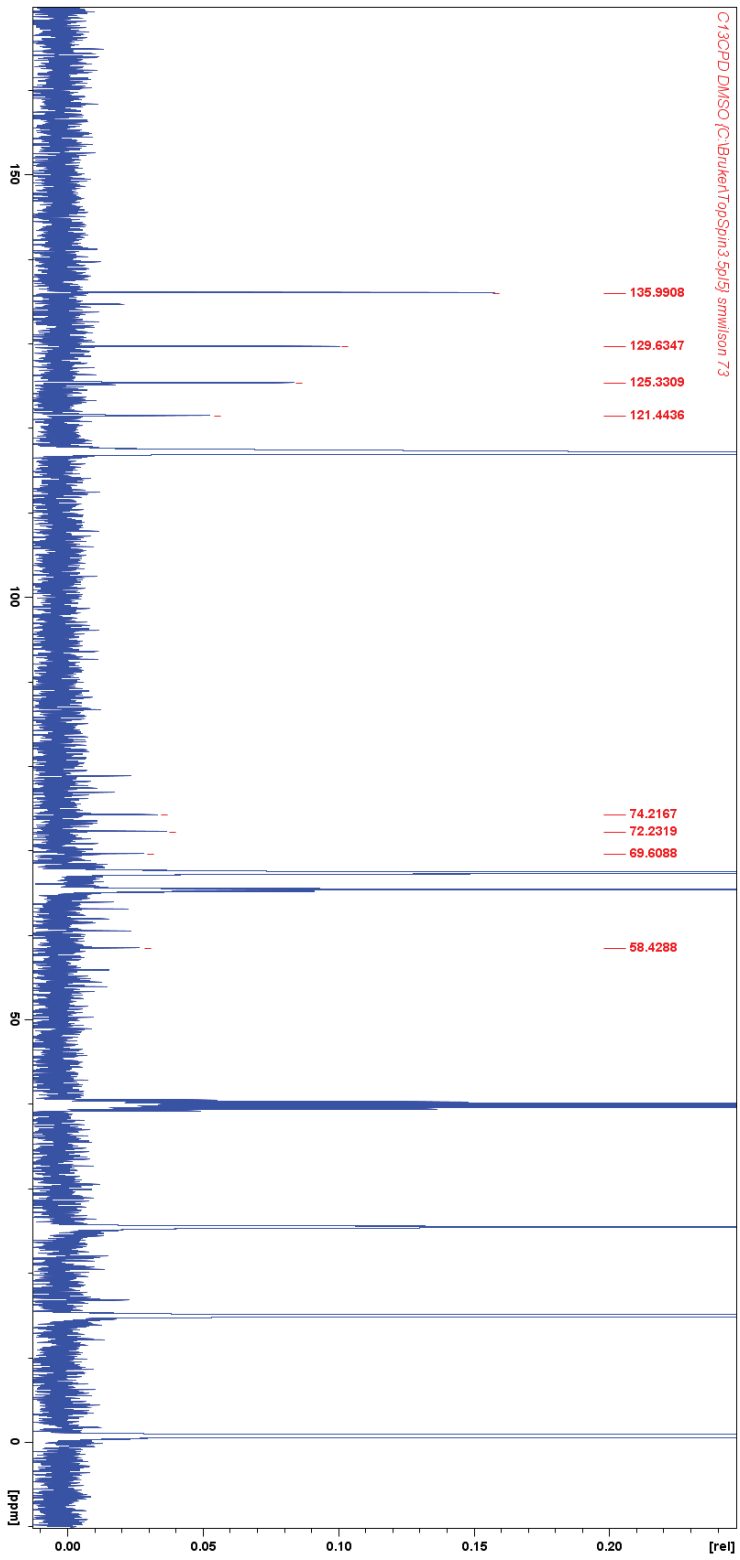

Figure 51: ^{13}C NMR spectrum of $IMesCO_2$ additive reaction in a solution of MeCN with $NaBH_4$.

CHAPTER 5 DISCUSSION:

To avoid the possibility of solvent reactivity with the hydrides, the hydrogenation reactions were only performed in solvents that were inert toward the hydride reagent. Dry THF was the solvent that the hydrides were either bought or stored in, and so they were all reacted with the $IMesCO_2$ while it was in a THF solution. Both $LiAlH_4$ and $LiBH_4$ are soluble in THF; however, $NaBH_4$ had limited solubility in THF and therefore limited reactivity [23]. Reactions involving $NaBH_4$ needed extended amounts of time to react and most reactions did not reach completion in the allotted time. While in the NMR spectrometer, the reaction would continue and precipitate byproducts that would interfere with the function of the instrument. Nevertheless, both borohydrides were brought into reaction with the $IMesCO_2$ in THF. Both borohydrides were also able to react with the $IMesCO_2$ in DMSO and MeCN; these solvents are nonreactive with these borohydrides. Reactions with $LiAlH_4$ were only performed in THF.

The only reactions that gave spectral evidence of protonation of the C2 carbon to regenerate IMes were the high pressure H_2 reaction and the $LiBH_4$ reaction with THF as a reaction solvent. Product peaks were found for most of the other reactions, but H2 on the C2 carbon was not detected for most of them. The high pressure H_2 reaction shows peaks for H2 on ^1H NMR spectrum and evidence for formate via GC. This protonation is needed so that IMes can be the counterion for formate. Moreover, none of the reactions indicated a peak in the ^{13}C NMR spectra for the carbon for CO_2, supporting CO_2 adducts, but not $IMesCO_2$ at 153.4 ppm on a ^{13}C NMR spectrum.

Lithium aluminum hydride shows very small peaks for all the reduction products; however, when the additive reaction was done there was only evidence found for formate. Lithium borohydride proved to be the most successful chemical reduction agent studied. It successfully produced formate for all reaction solvents tested and when the additive reaction was done. Formaldehyde was found when the reaction solvent was acetonitrile, both in the presence of the additive and no additive. Sodium borohydride has the potential to be a successful reducing agent for $IMesCO_2$, but the low solubility of the hydride in THF limited its reactivity. However, in the solvents acetonitrile and DMSO, the solubility of $NaBH_4$ was significantly higher and so its reaction treatment with $IMesCO_2$ did produce formate and formaldehyde.

Another commonality of the $IMesCO_2$ reductions with the hydrides was the appearance of peaks around 5.6 and 7.8 ppm in the ^1H NMR spectra. The 5.8 ppm peak appears in all the spectra except $NaBH_4$ in DMSO and $LiAlH_4$ in THF with the additive. The persistent 5.8 ppm peak might be due to reduction at the C2 carbon while remaining attached to CO_2. A $-CH_2-$ between an ester group and an ammonium group has a resonance at 5.7 ppm [38]. When considering the imidazole ring shown in Diagram 2, an opening for IMes could occur between the nitrogens and carbon 4 or 5 can break forming a carbon chain with an alkene. Alkene ^1H NMR spectral peaks for imidazole ring opening derivatives appear in the 5.9-4.0 ppm range. The regular occurring 5.8 ppm ^1H NMR peak agrees with this. Depending on where the ring breaks, determines what substituents are present. The alkene can separate with a nitrogen ($H_2C=CHNR$) or be separated completely into an ethylene. Carboxylic amines (ROC-NHR) have ^1H NMR peak in the range of 7.9-6.5 ppm and would be a product from an imidazole ring opening

also [39]. The peak at 7.8 ppm only appeared when $LiBH_4$ reacted with $IMesCO_2$ in both DMSO and THF. However, the literature reference in DMSO shows the olefin at 7.8 ppm [27]. The olefin on IMes will shift depending in the reaction solvent, so it is difficult to discriminate a carboxylic amine from the olefin peak.

The products are volatile, and as the reaction proceeds the products may be evaporating away before they can be seen through analysis. This is especially true for the weaker reducing agent because it takes longer to react and produce products; they may be evaporating as they are being produced. This may explain why some spectra show these products, but other spectra of the same sample do not.

Comparing these results to Ying *et al.*, the solvents used were dimethylformamide (DMF), THF, and acetonitrile with the highest yields in DMF. Reactions were also done in situ, while the reactions done for this research were done in stages, so doing the reaction in situ and trying DMF as a solvent could present clearer spectra and a reaction yield may be established. The key to the reduction of $IMesCO_2$ is the solubility of the reducing agent in a solvent that the $IMesCO_2$ is soluble in; this encourages product formation.

CHAPTER 6 CONCLUSION:

In conclusion, $IMesCO_2$ can be reduced through hydrides and through a high pressure hydrogen atmosphere. The high pressure reaction produced formate with IMes counterion that was verified through NMR, IR, and GC. When reducing with a hydride, conclusive results were found with $LiBH_4$ and $NaBH_4$. Both borohydrides produced formate with DMSO as the reaction solvent. Although $LiAlH_4$ is strong enough to reduce the $IMesCO_2$, the low solubility of the $IMesCO_2$ in THF does not allow for extensive formation of products; even so, they were present in small amounts. Detection of methanol was complicated by the fact that peaks were overlapped by peaks for the THF solvent, which is in great excess, so peaks that would correspond to methanol would be hidden. With the $NaBPh_4$ additive, $LiAlH_4$ could better reduce $IMesCO_2$, but the structure of the complex 1 may prevent further reduction, with evidence only showing the formation of formate with IMes as a counterion. The use of the additive did increase the solubility of $IMesCO_2$, but did not produce the expected products when reacted with $LiAlH_4$, $LiBH_4$, or $NaBH_4$. There is spectral evidence that the hydrides are causing the imidazole ring to open. A persistent alkene peak of 5.6 ppm on the ^1H NMR spectrum and a 7.8 ppm peak for a carboxylic amine support the ring-opening hypothesis.

REFERENCES:

1. Saftel, H.; Callery, S. *Earth Science Communication Team* **2013** Retrieved from: https://climate.nasa.gov/400ppmquotes
2. Herrero, M. *The Conversation* **2010** Retrieved from: http://theconversation.com/to-reduce-greenhouse-gases-from-cows-and-sheep-we-need-to-look-at-the-big-picture-56509
3. Kothandaraman, J., Goeppert, A., Czaun, M., Olah, G. A., Prakash, G. K. S. *J. Am. Chem. Soc.* **2016** 138 778-781.
4. Holbrey, J.D.; Reichert, W.M.; Tkatchenko, I.; Bouajila, E.; Walter, O.; Tommasi, I. and, Rogers, R.D. *Chem Commun* **2003**, 28-29.
5. Duong, H.A.; Tekavec, T.N.; Arif, A.M.; and Louie, J. *Chem Commun* **2004**, 112-113.
6. Reed, T. B.; Lerner, R. M.; *American Association for the Advancement of Science* **1973**, 182, 1299-1304
7. Shalini, K.; Sharma, P.K.; Kumar, V.; Pelagia Research Library **2010**, 3, 36-47.
8. Hofmann K.; Part 1 *Imidazole and Its Derivatives*, Interscience Publisher, Inc New York 1953.
9. Hernandez Romero, D.; Heredia Torres, V. E.; Barradas-Garcia, O.; Marque Lopez, M. E.; Sanchez Pavon, E.; Journal of Chemistry and Biochemistry **2014**, 2, 45-83.
10. Eastman, K. J. *N-Heterocyclic Carbenes (NHCs)* Baran Lab Retrieved from: http://www.scripps.edu/baran/images/grpmtgpdf/Eastman_May_07.pdf
11. Arduengo, A.J.; Harlow, R.L.; Kline, M. *J. Am. Chem. Soc.* **1991**, 113, 361.
12. Breslow, R. *Mechanism of Thiamine Action* **1958** 80, 3719-3726.

13. Wanzlick, H.W.; Schonherr H.J. *Angew. Chem* **1968**, 80, 154.

14. Arduengo, A.J.; Rasika Diaz, H.V.; Harlow, R.L.; Kline, M *J. Am. Chem. Soc.* **1992**, 114, 5530-5534.

15. Kuhn, N.; Kratz, T. *Synthesis* **1993**, 561-562.

16. Amyes, T. L.: Diver, S. T.; Richard, J. P.; Rivas, F. M.; Toth, K.; *J. Am. Chem. Soc.* **2004,** 126, 4366-4374.

17. Van Ausdall, B.R.; Glass, J.L.; Wiggins, K.M.; Arif, A.M., Louie, J. *J.Org. Chem.* **2009**, 74, 7935-7942.

18. Madej Lachowska, M.; Kasprzyk-Mrzyk, A.; Moroz, H.; Lachowski, A. I.; Wyzgol, H.; *Chmeik* **2014**, 1 61-68.

19. Kortlever, R., Shen, J., Schouten, K. J. P., Calle-Vallejo, F., Koper, M. T. M.. *J. Phys. Chem. Lett.* **2015** 6 4073-4082.

20. Riduan, S. N.; Zhang, Y.; Ying, J. Y.; *Angew. Chem. Int. Ed.* **2009**, 48 3322-3325.

21. Trassati,S.; J. *Electroanal. Chem*., **1980** 111 125--131

22. Reduction of Aldehydes and Ketones using NaBH4 or LiAlH4 Retrieved from: https://home.cc.umanitoba.ca/~hultin/chem2220/Support/Reduction_of_Carbonyl_Compounds_using_NaBH4_or_LiAlH4.pdf

23. Brown, H. C.; Narasimhan, S.; Choi, Y. M.; *J. Org. Chem.* **1982,** 47, 4702-4708.

24. Brown, H. C.; Mead, E. J.; Subba Roa, B. C.; Organic and Biological Chemistry **1955,** 77 6209-6213.

25. Oomens J. Steill J. D.; *J. Phys. Chem. A*, **2008**, 112 (15), pp 3281–3283

26. Hans, M.; Lorkowski, J.; Demonceau, A.; Delaude, L.; Beilstein *J. Org. Chem.* **2015**, 11, 2318–2325. doi:10.3762/bjoc.11.252

27. Tudose, A.; Demonceau, A.; Delaude L.; *J. Organomet. Chem.* **2006**, 691, 5356-5365.

28. Academics Wellesly Retrieved on September 12 2018 http://academics.wellesley.edu/Chemistry/chem211lab/Orgo_Lab_Manual/Appendix/Instruments/InfraredSpec/Chem211%20IR%20Lit%20Value%20Table.pdf

29. Dahn, H.; Pechy, P.; *Magnetic Resonance in Chemistry* **1996**, 34, 723-724

30. Fulmer, G. R.; Miller, A. J. M.; Sherden, N. H.; Gottlieb, H. E.; Nudelman, A.; Stoltz, B. M.; Bercaw, J. E.; Goldberg, K. I. *Organometallics* **2010**, 29, 2176–2179.

31. National Center for Biotechnology Information, U.S. National Library of Medicine Retrieved on: July 28 2018 https://pubchem.ncbi.nlm.nih.gov/compound/formaldehyde#section=1D-NMR-Spectra.

32. Babij, N. R.; McCusker, E. O.; Whiteker, G. T.; Canturk, B.; Choy, N.; Creemer, L. C.; De Amicis, C. V.; Hewlett, N. M.; Johnson, P. L.; Knobelsdorf, J. A.; Li, F.; Lorsbach, B. A.; Nugent, B. M.; Ryan, S. J.; Smith, M. R.; Yang, Q.; *Org. Process Res. Dev*. **2016**, 20, 661−667.

33. Operating Manual **2001** Series 580 TCD Isothermal Gas Chromatograph. GOW-MAC.

34. Diez-Ramirez, J.; Valerde, J.L.; Sanchez P.; Dorado, F.; *Catal Lett* **2016**, 1 61-68.

35. Huff, C. A.; Sanford, M. S.; *J. Am. Chem. Soc.* **2011**, 133, 18122-18125.

36. Van Ausdall, B. R.; Poth; N. F.; Kincaid, A. M. A.; Louie, J. J. *Org. Chem*. **2011**, 76 8413-8421.

37. Kos, I.; Weitner, T.; Biruš, M.; *Research Gate* **2003** Impurity Control by NMR Spectroscopy in Betainhydroxamic Acid Chloride Synthesis.
38. Nystrom, R. F.; Yanko, W. H.; Brown, W. G.; Communication to the Editor **1948**, 441.
39. Reich, H. J.; Structural determination using NMR, University of Wisconsin 2018**,** Accessed on April 21 2019. https://www.chem.wisc.edu/areas/reich/nmr/h-data/hdata.htm
40. Technical Handbook **2006** Ecotec E3000 Multi-Gas Leak detector. Inficon.
41. Chem Draw 1998 PerkinElmer Inc.

Figure 1

Illustration of CO_2 radiation admission. Retrieved from: https://www.skepticalscience.com/empirical-evidence-for-co2-enhanced-greenhouse-effect-intermediate.htm

Figure 2

Volcano curves. The strength of metal-hydrogen bonds was derived from the heat of formation of the corresponding hydrides (after Calle-Vallejo). Original data are adapted from Trasatti [21].

Appendix A:

Product gas sampling via mass spectrometry.

The Inficon Ecotec 3000 is a single quadrupole mass spectrometer shown in

Figure A1: The Inficon Ecotec 3000

Schematic 1. It has a "sniffer" line for sampling. The instrument is designed to test for gas leaks. Gases are drawn into the instrument with a turbo molecular pump. The pressure of the internal system must be between four to ten millibars for measurements. The main instrument should not be moved during operation, for this will interfere with the pumps and possibly disrupt the vacuum. If the system exceeds the ten mbar range the turbo molecular pump will not be able to maintain the vacuum. The system can be set to detect four gases at one time. The sample is drawn in to the system and flows through a

particle filter in the sniffer probe, then continues to the main system through the sniffer line. In the system there are two flow dividers, one is direction is sent directly to the Transpector mass spectrometer or to the other flow divider. The second flow divider flows to the turbo pump or the backup pumps, both paths then lead to the mass spec detector. The mass spectrometer is made of an ion source, a separator, and an ion collector. The ion source charges the particles from the sampled gas. The charged particles are then sent through the quadrupole field and separated. The particles are separated by their respective charge to mass ratio. The single quadrupole is selective; the voltage can be adjusted to only allow certain ions to flow through the quadrupole to the detectors while others will collide with the rods of the quadrupole. The ion collector measures the current of the ions. This signal is used to measure the leak rate of the detected gas. The system is able to report both the presence of a selected gas, but also a concentration of the detected gas at a given sampling location. The molecular weight of the gas of interest can be programmed into the system. The mass spectrometer will detect the ions with the programmed masses. However, this can be a source of error. Some compounds have similar molecular weights. The system cannot distinguish between them. For example, oxygen gas with a molecular weight of 32 can be detected as methanol with a molecular weight of 32 because the system cannot distinguish the two.

The system needs to be go through a run-up for approximately 20 minutes before any sampling can begin. The system will automatically start its run-up when the system is switched on. The on switch is located on the back of the instrument. When the system is turned on, one will notice that the sniffer nozzle will almost instantaneously start to draw any surrounding gas. However, data will not be shown until the system has gone through

the run up process when first switched on for the day. The display screens on both the sniffer line and the main system will light up. The alarm and LED lights will also be triggered when the system is first turned on.

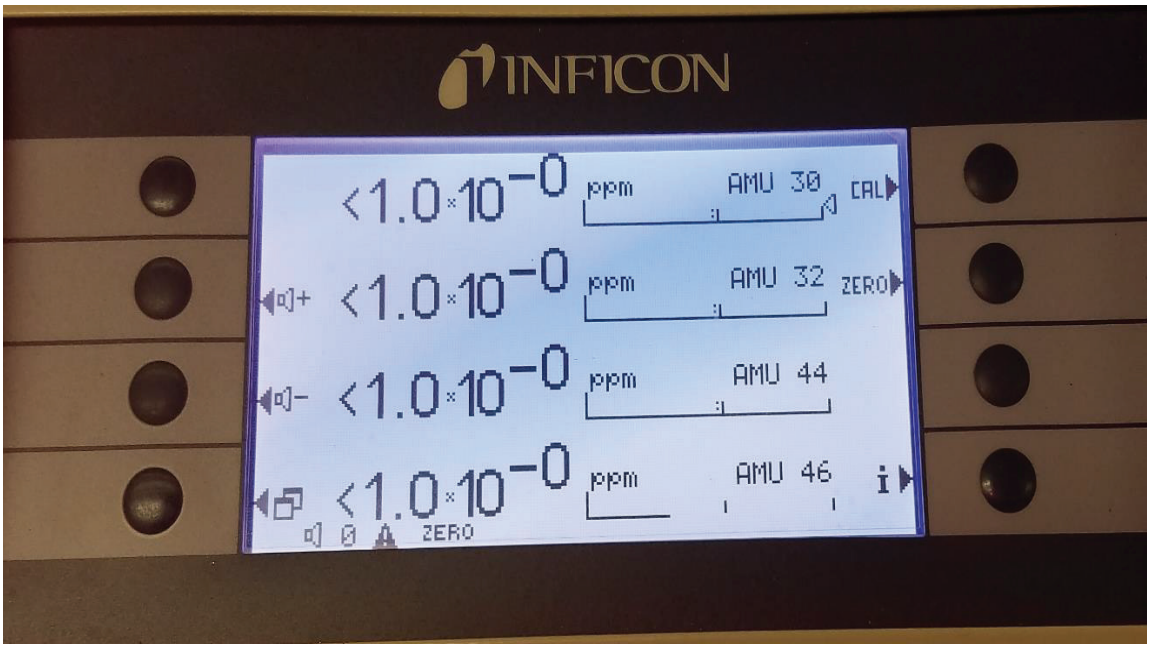

Figure A2: Main unit display

Once the run-up process has completed, the main display screen on the system will exhibit the concentrations of the selected gas or gases (Schematic 2). The sampling is continuous. The display on the instrument will show nearly real time concentrations. There is a phase lag of perhaps a few seconds between a volume of gas entering the probe and appearing on the display screen. The concentrations can be displayed in a variety of units, but the units used were parts per million. The system is sensitive enough to reliably detect single digit ppm. The gases selected were CO_2, methanol, formaldehyde, and formic acid. The formula weights of the gases of interest were programmed in to the detection software.

To program the gas of interest, start at the main display on side 1(left hand side) the last button on the bottom will display the main menu. Selecting gas trigger will take the display to the four gases that are currently programmed for detection. The software is always programmed with four gases, but they can be temporarily disabled for current detecting. The gas trigger menu allows one to change the trigger gas one at a time, enable and disable detection, program a user gas and return back to the main menu or the main display. When programming a new gas for detection, one must select gas 1, gas 2, gas 3, or gas 4 (basing the decision on which gas is of no relevance to the current experiment.) The gas that is selected will be changed to the new gas programmed. Once a gas is selected to be changed, the button coordinating to the gas number must be selected. This new display is the Edit User Gas menu displayed in Schematic 3. The gas

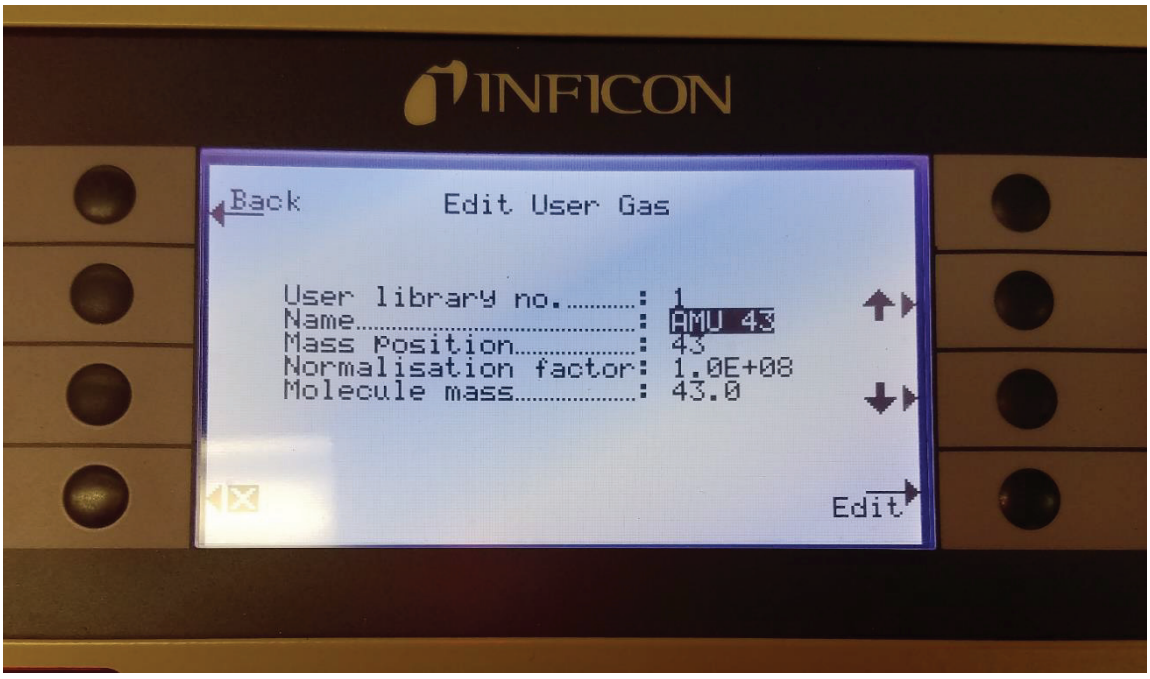

Figure A3: Edit User Gas display

name, mode, trigger unit, search limit, internal calibration, mass, calibration factor, last calibration, and calibration mode can be edited from here. Simply scroll down to the item that is to be changed by pressing the button that displays a downward arrow, and

then select the button next to Edit. From there, the system displays all options that can be changed, and by scrolling to the desired option then pressing the button next to "OK," the system is programmed. However, Gas Name has a library with many options, so just highlighting the gas and selecting "OK" will program it. Most of the options are preprogrammed, however the system can be programmed to detect other gases that are not listed in the library. To add a gas to the library, the Gas Trigger menu must be on display shown in Schematic 4. Selecting User Gas, which is the second button from the

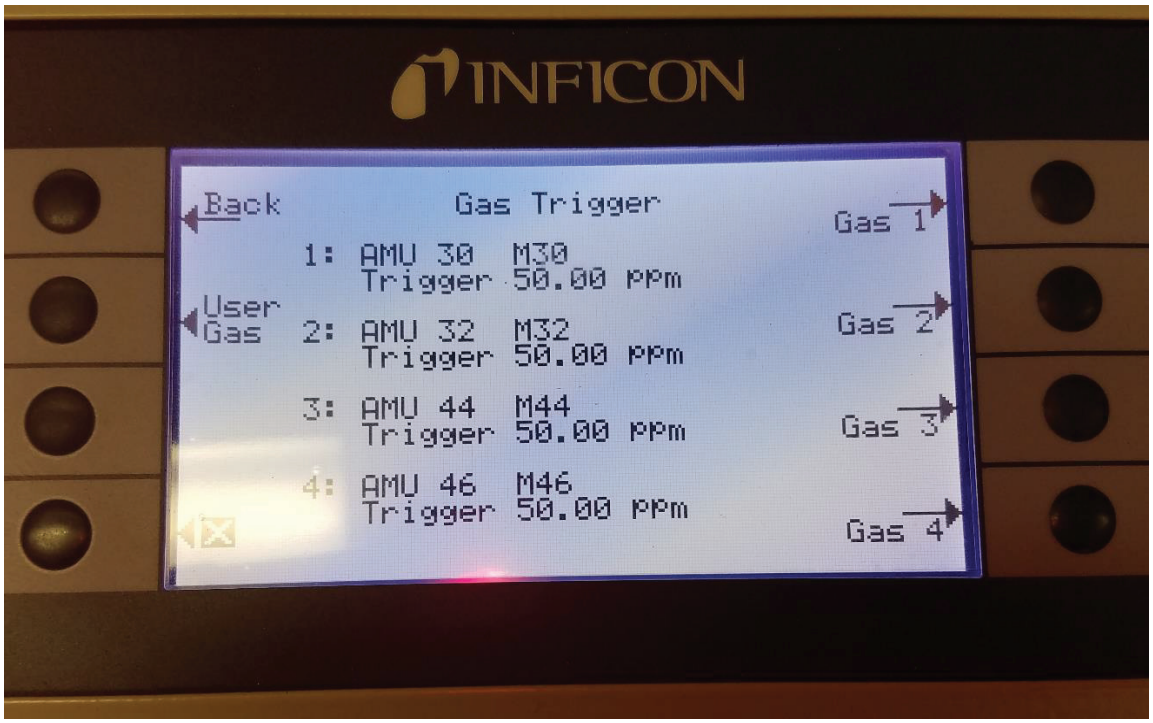

Figure A4: Gas Trigger display

top right side will display select user gas menu. The library will hold up to six user gases that are programmed, and they will stay programmed until changed. The user gas to be changed is highlighted with the scrolling buttons; then Edit is selected. Now the name, mass position, normalization factor, and molecule mass can be selected and edited. Schematic 5. Once these factors are edited and saved the gas is now in the library and can be selected for detection.

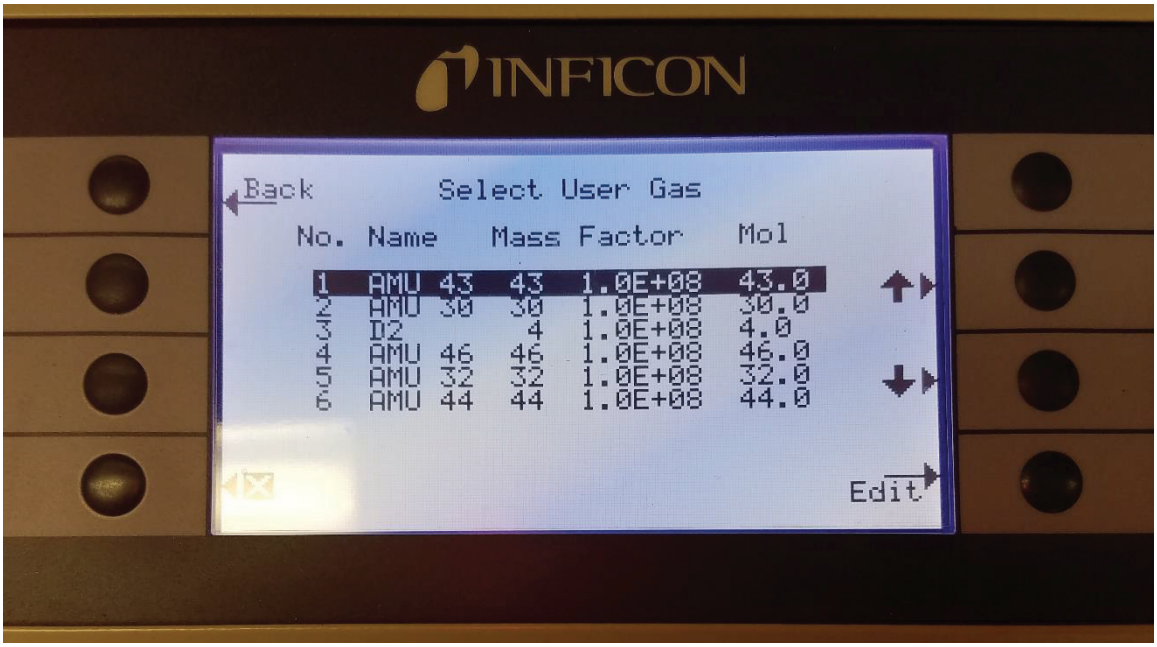

Figure A5: Select User Gas display

Once the instrument is warmed up and the desired gases are programmed for detection, the instrument will be taking real time measurements continuously. To allow the instrument to only detect gases from the experiment, an apparatus was set up to allow the reaction to take place without the concern for air leaks and contamination. Three round bottom flasks were used: one single neck 250 mL, one three neck 250 mL, and one three neck 100 mL. The single neck round bottom contained dichloromethane solvent, the small three neck contained the IMesCO_2 product, and the large three neck was a gas chamber. The single round bottom containing solvent was connected to the smaller three neck via a cannula. The small round bottom had a cannula that connected it to the large three neck. This large three neck had a cannula that vented out to mineral oil, a sealed neck and the last neck was connected to the sniffer probe. The probe was sealed with a rubber septum to discourage air contamination. The sniffer probe cannot directly contact fluids, or else the probe will draw up the fluid and the instrument will be damaged, so the

probe is kept in a separate chamber to detect gases only. The system was purged using nitrogen and the solvent was pushed through the cannula to dissolve the product in the small three neck round bottom. The system was switched to hydrogen gas, which was hooked up to a mass flow controller to control flow rate. This part of the experiment needed quantitative values for reagents. The hydrogen was set to enter the system at the small three neck round bottom to proceed with a hydrogenation reaction. The gas was allowed to bubble through the solution to create an agitation that encouraged a reaction. All gas phase reagents traveled through a cannula to the large three neck round bottom for sampling by the sniffer probe. Excess gas was vented through mineral oil to control pressure. Once the systems use is done for the day, the off switch can be switched on the back of the system. [40]

Appendix B:

Product gas sampling via gas chromatography with a thermal conductivity detector.

Figure A6: Gow-Mac Series 580 Thermal Conductivity Isothermal Gas Chromatograph

Gas chromatography, shown in Schematic 6, is used to detect products in the gas phase. Formaldehyde, methane, and CO_2 are possible products that the GC can detect. The temperature of the GC is kept high enough so that all sample components can be detected in the vapor phase. The GC used has a thermal conductivity detector. The detector measures a current imbalance across a bridge circuit due to the differential thermal conductivity of sample versus carrier gas. This information, along with an elution time that a reagent requires to exit from the column, produces a chromatogram. The plot shows bridge current as a proportional voltage versus time. The GC is a Series 580 TCD Isothermal Gas Chromatograph made by GOW-MAC Instruments. Carrier gas must purge the column and detector for five to ten minutes at 40 psi before power is applied to the system. The carrier gas used is helium because of its inert nature and its

high thermal conductivity. Once the purging is complete, the system can be switched on using the switch located on the rear right of the instrument. The modes and settings can now be adjusted. The GC has manual control knobs located on the instrument. The knobs on the front right hand side of the instrument are clearly labeled as to what parameter is adjusted, but there is only a single digital display, so that only one parameter at a time may be observed. There is also an "actual/set" switch, which determines whether the actual value or set point value for a given parameter is displayed. The parameters that can be alternately shown on the display are injector temperature (degrees Celsius), column temperature, detector temperature, and bridge current (in milliamperes). A push bush button switch corresponding the desired parameter must be pressed in order for the display screen to display the proper value. To adjust the parameter, the e knob on the front panel is dialed up or down to the desired value by pushing in the lock ring on the knob and turning it clock-wise or counter clock wise. Once the temperatures and current are set, the system needs time to heat to the desired temperatures. To check the progress of heating, release the actual/set switch and press the switch corresponding to the value to be checked. Other knobs and switches on the right front panel include: polarity, zero, attenuator, and fan. The polarity switch reverses the sign of the bridge current signal, which is dependent on the thermal conductivity of what is being sampled versus the carrier gas. The switch ensure that a positive deviation from the baseline for any sample component will occur. The zero knob adjusts the chromatogram, so that the zero concentration line can be adjusted to line up with the time axis base-line or adjusted otherwise. The fan switch turns on a fan and heater that is used to ensure uniform temperature inside the column oven cavity, and to cool the detector when the system will

be shut down for the day. The attenuator knob amplifies the output of the bridge current, which is usually set to a sensitivity of approximately six. The A and B knobs on the lower middle of the font panel are needle values adjusting the gas flow out of the A and B outlets. There is a left hand front panel related to the autosampler feature of the chromatograph, whose controls include, Exit line A, Exit line B, purge/inject solenoid switch, restrictor needle valve, and series/bypass solenoid switch. The autosampler enables sampling and injecting a fixed volume of gas from a continuously flowing gas stream by opening and closing valves that mix carrier gas with the contents of a "sampling loop," a coil of stainless steel tubing of precise length and internal volume. The sampling loop used in this work is 2.00 mL. The purge/inject switch controls when to inject the contents of the sample loop into the chromatograph column(s). The oven cavity has sufficient gas fittings to assemble two chromatographic columns in series. The series/bypass switch allows for the system to bypass column 2 and use column 1 only, or use them both. A restrictor valve compensates for the reduced gas flow impedance when only one column is employed in the chromatographic analysis.

The arrangement of columns in the oven cavity must be configured differently, depending on whether the system will be operated in autosampling mode or manual injection mode, where a sample is injected via syringe through a septum-sealed portal. Currently the system is configured for manual injection into column 1 only, so that as soon as the sample is injected into the system, the sample will go straight through the first column. The column's original position in the oven cavity was switched with a jumper tube (hallow connection tube), so that column 2 can be avoided. Column 2 is packed with a molecular sieve absorbent that binds very strongly with CO_2, so the column was

avoided. Column 1 contains 7’ x 1/8” Porapak Q, 80/100 mesh, which is inert enough for this experiment. Once a sample is injected into the GC, the sample goes through the column and then straight to the thermal conductivity detector. The carrier gas bifurcates, flowing through the gas sampling valve (G.S.V.). When set in bypass mode, the gas will go through the G.S.V. and then through the jumper to a restrictor and then to the detector. These are the settings that served best for this experiment.

The output signal from the TCD is connected to a laptop with Clarity Lite software. The user must be logged onto the laptop and then the Clarity Lite software can be opened from the desktop. Once the software is opened the program will prompt for the user name that was used to log on to the laptop. The menu displayed is used to program a method, display saved chromatograms, and acquire data. To program a method, select method at the top of the display at the middle tab, then select event table on the drop down box. The method setup box will appear and under the measurement tab located on the bottom left, manually import settings for measurements. The setup will prompt for method description, column, mobile phase, flow rate, detection, temperature, notes, enable auto stop, run time, and enable start/stop. Once settings are filled out, select “OK” and the main menu will reappear. Select the Data Acquisition icon to have the data acquisition screen appear. Here the base line and the zero line can be adjusted with the knobs on the instrument. When ready, select the Analysis tab at the top right hand corner of the screen, and select “run single” to start an analysis. Immediately inject sample into injection port B. The syringe should penetrate the septum and reach into the instrument for a thorough injection. If a gas is being injected, up to 5 ml was used, but for fluids only a few microliters are used. When the run time ends the chromatogram is displayed

and saved. Once done for the day, all the temperatures and currents must be reduced down to the lowest setting, and the detector fan can now be switched to “fan only” to cool the column, note that the detector temperature will not reach higher temperatures if the “fan only” is on throughout the experiment. Once the detector temperature is less than 80 degrees Celsius, the system can be turned off and the carrier gas turned off. [33]